

January 2015

Methods Of Analysis For Fermentation Science Products Using Various Analytical Techniques

Casey Jay Howdieshell
Eastern Kentucky University

Follow this and additional works at: <https://encompass.eku.edu/etd>

 Part of the [Organic Chemistry Commons](#)

Recommended Citation

Howdieshell, Casey Jay, "Methods Of Analysis For Fermentation Science Products Using Various Analytical Techniques" (2015).
Online Theses and Dissertations. 277.
<https://encompass.eku.edu/etd/277>

This Open Access Thesis is brought to you for free and open access by the Student Scholarship at Encompass. It has been accepted for inclusion in Online Theses and Dissertations by an authorized administrator of Encompass. For more information, please contact Linda.Sizemore@eku.edu.

**METHODS OF ANALYSIS FOR FERMENTATION SCIENCE
PRODUCTS USING VARIOUS ANALYTICAL TECHNIQUES**

By

Casey Jay Howdieshell

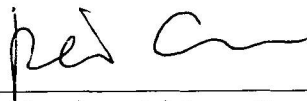
Thesis Approved:



Chair, Advisory Committee



Member, Advisory Committee



Member, Advisory Committee

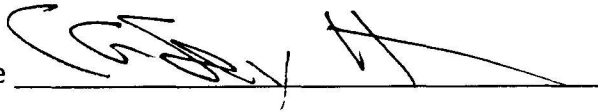


Dean, Graduate School

STATEMENT OF PERMISSION TO USE

In presenting this thesis, in partial fulfillment of the requirements for a Master's degree at Eastern Kentucky University, I agree that the Library shall make it available to borrowers under rules of the Library. Brief quotations from this thesis are allowable without special permission, provided that accurate acknowledgment of the source is made. Permission for extensive quotation from or reproduction of this thesis may be granted by my major professor, or in [his/her] absence, by the Head of Interlibrary Services when, in the opinion of either, the proposed use of the material is for scholarly purposes. Any copying or use of the material in this thesis for financial gain shall not be allowed without my written permission.

Signature

A handwritten signature in black ink, appearing to be "G. H. H.", written over a horizontal line.

Date

5/18/2015

METHODS OF ANALYSIS FOR FERMENTATION SCIENCE
PRODUCTS USING VARIOUS ANALYTICAL TECHNIQUES

By

CASEY JAY HOWDIESHELL

Bachelor of Arts
Eastern Kentucky University
Richmond, Kentucky
2015

Submitted to the Faculty of the Graduate School of

Eastern Kentucky University

in partial fulfillment of the requirements

for the degree of

MASTER OF SCIENCE

August, 2015

Copyright © Casey Jay Howdieshell, 2015
All rights reserved

DEDICATION

This thesis is dedicated to my parents Tim and Kathy Howdieshell for their unwavering support. To my two obnoxious roommates Joshua “the D” Lang and “Master” Kyle Francis who have done an excellent job at keeping me on track while writing this thesis. To all of my friends, both fellow students and faculty who help me achieve this great milestone in my life. To my mentor Dr. Darrin Smith who was as much a friend as a teacher. Without all of your support and guidance I would have never made it this far, and we all still have quite a ways to travel together.

ACKNOWLEDGMENTS

I would firstly like to thank my research mentor, Dr. Darrin Smith, for his guidance, patience, and dedication to my pursuit of knowledge. I would secondly like to thank Dr. Bruce Pratt, the agricultural collaborator for these projects, without whom the research presented in this body of work would have been impossible to achieve. Through Dr. Pratt I would also like to thank Eastern Kentucky University's Center for Renewable Alternative Fuel Technologies (CRAFT) department who supplied the sampled needed for this analysis. The Defense Logistics Agency (DLA) who provided funding for this research also have my deepest thanks. Finally, I would like to thank the previous students of Dr. Smith's research group studies laid the groundwork for these experiments, namely Joseph Johnson, Michael Mazzotta and Daudi Saang'onyo. Without these students/faculty/organizations, the research that is presented would not have been made possible, and as such, they have my sincerest gratitude.

ABSTRACT

Fermentation science, the study of microorganisms as they digest food sources to produce usable products for consumption, has been around since the dawn of modern civilization. Historically, the fermentation process has been utilized for the production of alcoholic beverages. More recently, however, the production of bioethanol and biodiesel as a fuel source alternative to classical fossil fuels has gained increased popularity. As with any synthetic process, derivations and optimizations for ideal production are needed. As such, analytical techniques must be implemented to ensure quality control and pinnacle efficiency. This body of work describes analytical techniques providing key qualitative and quantitative information about various steps in the fermentation process. Experiences and conclusions drawn about biofuel production are described in two quantitative projects: Storage Analysis of Sugar Saccharification using Ultrahigh Performance Liquid Chromatography using Corona Charged Aerosol Detection (UPLC-CAD), and Thermal Energy Quantitation of Residual Biomass Using Oxygen Bomb Calorimetry (OBC).

The first major technique employs liquid chromatography to separate and quantitate major sugars (xylose and glucose) in the saccharification of biomass (switchgrass). Storage conditions can determine the economic viability of switchgrass as an alternative fuel source. As such, the extent of degradation of switchgrass over a course of one year, and limitations of useable sugars produced needed to be assessed. Results showed no significant loss in sugar production over the course of one year from three distinct storage conditions. From an industrial perspective, this provides low cost storage with minimal to no loss in bioethanol and biodiesel. In addition to biofuels, biomass, switchgrass for example, can be used directly as a combustion source to produce thermal energy. The energy produced (BTU/lb.) can be used mainly to power boiler systems or residential stoves to provide heat, and electricity through a steam turbine. Using OBC, the amount of thermal energy produced by biomass, was obtained and similar degradation

studies were accessed. As with the sugar production, the extent of degradation was found to be insignificant.

An additional preliminary study explored as an alternative to the pretreatment phase: Ionic Liquid (IL) pretreatment of lignin, characterized by Direct Analysis in Real Time Mass Spectrometry (DART-MS). The goal of these projects was the development of methods to characterize and quantitate specific products during major stages of biofuel production applied which can be easily to many fermentation studies. These methods can then be used as a template for further fermentation studies, both in biofuel and alcoholic beverage production.

TABLE OF CONTENTS

CHAPTER		PAGE
CHAPTER 1: INTRODUCTION AND BACKGROUND		
1.1	Research Objectives.....	1
1.2	The Energy Crisis: Global Energy Use.....	3
1.2.1	Non-Renewable Fuel Sources	5
1.2.1.1	Diminishing Fossil Fuel Sources	5
1.2.1.2	Consequences of Fossil Fuels.....	6
1.2.2	Renewable Fuel Sources	8
1.2.2.1	The Need for Renewable Energy	8
1.2.2.2	Alternative Energy Options.....	9
1.3	Biomass to Biofuel	12
1.3.1	Biomass as a Fuel Energy	12
1.3.2	Biomass Components	14
1.3.2.1	Lignin	15
1.3.2.2	Cellulose and Hemicellulose	16
1.3.3	Switchgrass	17
1.3.4	Biofuel	17
1.3.4.1	Types of Biofuels	18
1.3.4.4	Current Conversion Processes for Lignocellulose Biofuel Production	20
1.3.4.4.1	Pretreatment	20
1.3.4.4.2	Enzymatic Hydrolysis	22
1.3.4.5	General Fermentation Process for Ethanol Production	24
1.3.4.2	Drawbacks of Biofuel	26
CHAPTER 2: EXPERIMENTAL METHODS AND INSTRUMENTAL THEORY		
2.1	Current Method of Analysis for Fermentation Products.....	29
2.1.1	Traditional Methods of Analysis for carbohydrates	29
2.2	Novel Method of Analysis for Fermentation Products.....	32
2.2.1	Liquid Chromatography	32
2.2.1.1	Separation Theory.....	33
2.2.1.2	Types of Liquid Chromatography.....	37
2.2.1.3	The Van Deemter Equation.....	40
2.2.1.4	Ultrahigh Performance Liquid Chromatography	46
2.2.1.5	Detection Sources	50
2.2.1.6	Charged Corona Aerosol Detection	52
2.2.2	Oxygen Bomb Calorimetry	55

CHAPTER		PAGE
CHAPTER 3: SACCHARIFICATION STUDY USING UPLC-CAD		
3.1	Introduction	58
3.2.1	Sample Preparation	59
3.2.2	Reagents.....	60
3.2.3	Standard Preparation.....	61
3.2.4	Instrumentation	61
3.3	Standard Results	63
3.4	Sample Results	67
3.5	Data Discussion	72
3.6	Saccharification Study Conclusion	73
CHAPTER 4: BIOMASS THERMAL ENERGY ASSESSMENT		
4.1	Introduction	75
4.2.1	Sample Preparation	76
4.2.2	Standard Preparation.....	76
4.2.3	Instrumentation	77
4.2.4	Experimental Procedure	78
4.3	Standard Results	79
4.4	Sample Results	80
4.5	Data Discussion	83
4.6	Thermal Energy Assessment Conclusion	84
CHAPTER 5: LIGNIN DISSOCIATION USING IONIC LIQUIDS		
5.1	Introduction	86
5.2	Instrumentation	87
5.3	Experimental Procedure	89
5.3.1	Microscopic Analysis of Lignin Extract Dissolution	91
5.3.2	DART-MS Analysis of Dissolved Lignin in Ionic Liquids	91
5.4	Preliminary Results	92
5.5	Project Discussion	95
5.6	Future Directions for Lignin Study using Microscopy and DART-MS Methods.....	96
CHAPTER 6: CONCLUSIONS AND FUTURE DIRECTIONS		
6.1	Introduction	98

CHAPTER	PAGE
6.2	Saccharification Study Conclusions..... 99
6.3	Calorimetric Study Conclusions 100
6.4	Lignin Dissociation Conclusions 101
6.5	Closing Remarks 102
	List of References.....104
	Appendices.....110
A.	Calibration curves generated from xylose and glucose standards prepared for saccharification study..... 110
B.	Mass spectra of switchgrass lignin extracted by formic acid at 50 °C dissolved in various ionic liquids..... 117

LIST OF TABLES

TABLE	PAGE
3.1. Standard R ² values for standard calibration curves.....	64
3.2. Saccharification concentration based on month.....	69
3.3. Saccharification concentration based on structure.....	69
3.4. Saccharification concentration based on sample position with total concentrations for all samples.	69
4.1. Benzoic acid standard raw and corrected values.	80
4.2. Thermal energy values (in British Thermal Units per pound) for switchgrass samples monthly statistics.....	81
4.3. Thermal energy values (in British Thermal Units per pound) for switchgrass samples structure statistics with total for all samples.	82
5.1. Chemical formulas, names, and structures of ionic liquids used in lignin dissolution project.....	90
5.2. Categorization of each IL's capacity fo dissolve lignin extract.....	93

LIST OF FIGURES

FIGURE	PAGE
1.1. Total global energy consumption from years 1980 to 2012 in quadrillion British Thermal Units (BTU).....	4
1.2. Annual ethanol production volumes (in billions of gallons) in the United States.	13
1.3. Component percentages of common agricultural residues and wastes.....	14
1.4. Structure of several lignin monomers and dimers.	16
1.5. Transesterification reaction of triglyceride with methanol to produce glycerol and biodiesels (methyl esters).....	19
1.6. Conversion of crystalline cellulose to glucose through cellulase enzymes.....	23
1.7. Hexose catabolism of <i>Saccharomyces cerevisiae</i>	25
1.8. Structures (from left to right): glucose-6-phosphate, fructose-6-phosphate, pyruvate, thiamine phosphate, and NADH.....	26
2.1. Structures of glucose (left) and xylose (right) are shown.....	35
2.2. Structure of BEH amide column (left) and acetonitrile (right) are shown.	36
2.3. Theoretical illustration of band broadening via multiple flow paths (eddy diffusion) on a solute peak.....	42
2.4. Visual representation of mass transfer in a chromatographic system.....	44
2.5. Graph of theoretical plate height versus flow rate of helium GC system.	46
2.6. van Deemter plots for acetophenone on Acquity and XBridge column C ₁₈ at three particle diameters: 5 μm, 3.5 μm, and 1.7 μm.	48
2.7. Schematic of Charged Corona Aerosol Detector is presented.	53
2.8. Sample schematic of bomb calorimeter.....	57
3.1. Storage conditions for switchgrass samples: hooped (left) uncovered (middle), and tarped (right).....	59
3.2. Dionex Ultimate 3000 RS UHPLC system (left) and block diagram (right).	63

FIGURE	PAGE
3.3. Representative xylose calibration curve for saccharification analysis where concentration (μg) is plotted against peak area.	65
3.4. Representative glucose calibration curve for saccharification analysis with concentration (μg) plotted against peak area.	65
3.5. Example chromatogram of standards sugars is shown with the elution order of xylose (left) and then glucose (right).	66
3.6. Example chromatogram of sample 5UW3 is shown with the elution order of xylose (left) and then glucose (right).	68
3.7. Monosaccharide concentration (g/L) versus time for saccharification study.	70
3.8. Monosaccharide concentration versus structure for saccharification study.	71
3.9. Monosaccharide concentration versus sampling position for saccharification study.	71
4.1. Structure of benzoic acid.	77
4.2. Parr 1341 Plain Jacket Bomb Calorimeter.	78
4.3. Thermal energy (in BTU/lb) produced by untreated switchgrass over 12 months.	82
4.4. Thermal energy (in BTU/lb.) produced by untreated switchgrass of three different storage structures.	83
5.1. Leica DM EP Polarized Light Microscoped used to visually observe lignin-IL interactions.	88
5.2. Thermo Scientific LTQ XL with DART ion source used to characterize lignin-IL interactions.	88
5.3. Cartoon illustration (left) and photo close-up of DART ion source used (right). .	89
5.4. Dissolution of lignin extract in [BMIM][Cl] at t = 0 min (left), t = 30 min (middle), and t = 24 hr.	93

FIGURE	PAGE
5.5. DART positive (+) ion mode spectrum with lignin extract (FA 50 °C) after dissolution with [BMIM][Cl].....	94
A.1. Xylose and glucose calibration curves for 08142013 data sets.....	111
A.2. Xylose and glucose calibration curves for 08162013 data sets.....	112
A.3. Xylose and glucose calibration curves for 08212013 data sets.....	113
A.4. Xylose and glucose calibration curves for 08302013 data sets.....	114
A.5. Xylose and glucose calibration curves for 09052013 data sets.....	115
A.6. Xylose and glucose calibration curves for 10092013 data sets.....	116
B.1. Mass spectrum of lignin (FA 50 °C) dissolved in 1-allyl-3-methylimidazolium chloride ([AMIM][Cl]).....	118
B.2. Mass spectrum of lignin (FA 50 °C) dissolved in 1-allyl-3-methylimidazolium xylene sulfonate ([AMIM][XS]).....	118
B.3. Mass spectrum of lignin (FA 50 °C) dissolved in 1-butyl-3-methylimidazolium chloride ([BMIM][Cl]).....	118
B.4. Mass spectrum of lignin (FA 50 °C) dissolved in 1-butyl-3-methylimidazolium xylene sulfonate ([BMIM][XS]).....	119
B.5. Mass spectrum of lignin (FA 50 °C) dissolved in 1-pentyl-3-methylimidazolium bromide ([PMIM][Br]).....	119
B.6. Mass spectrum of lignin (FA 50 °C) dissolved in 1-pentyl-3-methylimidazolium nitrate ([PMIM][NO ₃]).....	119
B.7. Mass spectrum of lignin (FA 50 °C) dissolved in trihexyltetradecylphosphonium bromide ([THTDP][Br]).....	120
B.8. Mass spectrum of lignin (FA 50 °C) dissolved in trihexyltetradecylphosphonium nitrate ([THTDP][NO ₃]).....	120

LIST OF ABBREVIATIONS

Energy Information Administration	EIA
Organization for Economic Cooperation and Development	OECD
British Thermal Units	BTU
Hydrocarbon	C_xH_y
Carbon Dioxide.....	CO_2
Sulfur Dioxide.....	SO_2
Nitric Oxides.....	NO_x
Alkoxy Groups	RO-
Glucose-6-Phosphate.....	G-6-P
Fructose-6-Phosphate.....	F-6-P
Nicotinamide Adenine Dinucleotide.....	NADH
Pentose Phosphate Pathway	PPP
Energy Equivalent Liter	EEL
Ultraviolet	UV
Visible.....	Vis
Gas Chromatography	GC
Flame Ionization Detection.....	FID
Mass Spectrometry.....	MS
High Pressure Liquid Phase Chromatography	HPLC
Intermolecular Forces.....	IMF
Equilibrium Constant	K
Silica	SiO_2
Alumina.....	Al_2O_3
Normal Phase Liquid Chromatography.....	NPLC
Reverse Phase Liquid Chromatography.....	RPLC
Plate Height.....	H

Height Equivalent to A Theoretical Plate	HETP
Longitudinal Diffusion	B/U_x
Mass Transfer	CU_x
Particle Diameter	d_p
Ultrahigh Performance Liquid Chromatography	UPLC
Number of Plates	N
Refractive Index	RI
Evaporated Light Scattering	ELSD
Charged Aerosol Detection	CAD
Extinction Coefficient	ϵ
Constant Volume Heat	q_v
Internal Energy	ΔU
Molecular Oxygen	O_2
Center for Renewable and Alternative Fuel Technologies	CRAFT
Ethylene Bridged Hybrid	BEH
Relative Standard Deviation	RSD
95% Confidence Interval	CI
Ionic Liquids	IL
Direct Analysis in Real Time	DART
Mass to Charge Ratio	m/z
Scanning Electron Microscope	SEM

CHAPTER 1

INTRODUCTION AND BACKGROUND

1.1 Research Objectives

Fossil fuels have become an integral part of society by keeping us warm, transporting us from one place to another, providing electricity, and much more. Globally, we have become dependent on fossil fuels as a resource, even though they are limited because production takes much longer compared to the frequency of usage¹. No single country is responsible for global problems surrounding energy sources. However, since current energy systems cannot be maintained an alternative method must be developed, or permanent changes to the environment could be catastrophic².

A significant energy and environmental crisis has led to a call for other means of energy from sustainable sources. These new sources would provide a sustainable source of energy while being economically and environmentally viable. Many different sources of renewable energy are currently being developed and optimized including solar, hydroelectric, geothermal, wind, and biomass sources³. Each fuel source has a list of benefits and drawbacks but the focus of this body of work is concerned with potential production of biofuel from biomass sources.

Biomass is typically any plant source (or feedstock) high in a repeating biopolymer consisting of glucose monomers: cellulose. Different plants have different levels and availability of cellulose creating variable potential biofuel sources. Switchgrass (*Panicum virgatum*), a plant common to North America, is a leading biomass source in the United States⁴. Using physical and chemical treatments, the destruction of cellulose polymers into glucose occurs. These residual sugars can then be fed to microorganisms like yeast or algae eventually to produce bioethanol or biodiesel, respectively. Chemical breakdown of a substance by bacteria, yeasts, or other microorganism is the process of fermentation. The resulting broths derived from fermentation can be harvested and refined into a useable fuel source comparable to fossil fuels⁵.

This body of work presents a series of studies used to determine economic viability of switchgrass as an alternative fuel source. Specifically, the performed research can be summarized as: i) a quantitative study into fermentable sugars produced, ii) a calorimetric study into thermal energy values of untreated biomass, and iii) investigations of degradation of varying storage conditions for these two subjects. Objectives of this work were: i) to develop and optimize a method of analysis for sugar saccharification processes of biomass, ii) to investigate thermal energy capacities of residual biomass after saccharification processes, and iii) to study degradation of biomass kept in different storage conditions. This series of investigation was initiated to understand better the switchgrass fermentation process as a primary feedstock with the possibility for its use as a biomass alternative fuel source.

1.2 The Energy Crisis: Global Energy Use

Harnessing energy and its utilization is the single most important aspect of life processes and has taken many forms since the dawn of life on this planet. Energy is solely responsible for all organisms' growth and development. As time has progressed, exploitation of this energy, primarily from the sun, has become incredibly complex. With advents of the technological age, the need for mechanical work is ever increasing since machines need energy to be powered. This has caused a rapidly accumulating demand for sustained energy worldwide.

According to the United State Energy Information Administration (EIA), world energy consumption has been rising steadily since 1980, as shown in **Figure 1.1**⁶. Projection for global energy consumption will increase by 56% in the next 25 years⁷. The Organization for Economic Cooperation and Development (OECD) is a group of countries whom work with one another and non-OECD countries to help minimize energy consumption through economic growth and developmental policies⁸. Energy consumption projections are increasing at rapid rates in countries like China, India, and many the Middle East region whereas projections are at a lower rate in OECD countries like the United States, Russia and the United Kingdom⁷. Most research done to minimize energy consumption is being completed in OECD countries in hopes of non-OECD countries adopting alternative fuels to lessen their environmental impact.

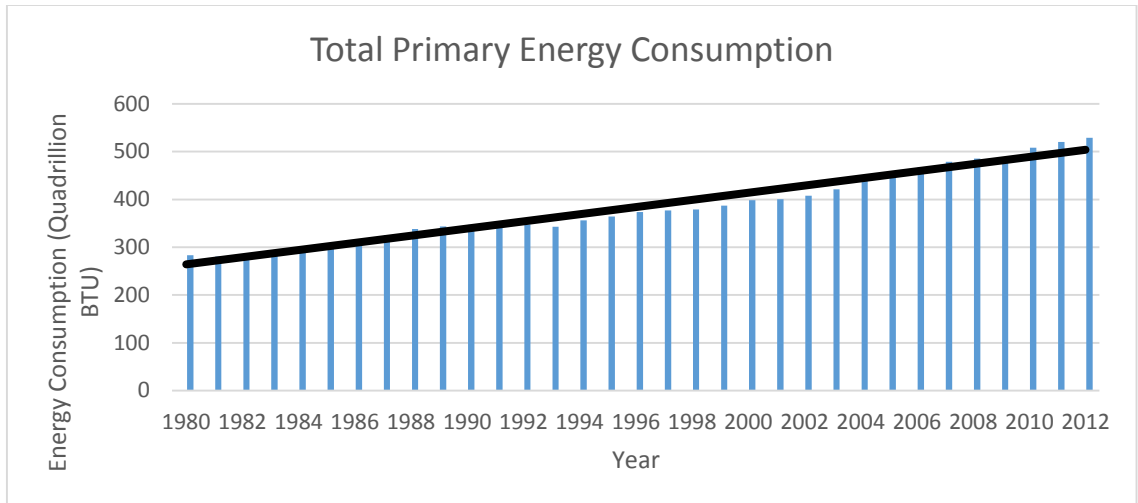


Figure 1.1. Total global energy consumption from years 1980 to 2012 in quadrillion British Thermal Units (BTU).

Note: The Line represents a general trend across years present.

Source: U.S. Energy Information Administration. International Energy Statistics. <http://www.eia.gov/cfapps/ipdbproject/iedindex3.cfm?tid=44&pid=44&aid=2&cid=ww,&syid=2008&eyid=2012&unit=QBTU> (accessed Feb 15, 2015).

Most prominent sectors of energy use in both OECD and non-OECD countries are forms of transportation. In 2012, petroleum and other liquids commonly used in transportation accounted for approximately 34% of total energy consumption globally⁷ with a majority of these energy consumption manifesting as fuel for vehicles. With more than one billion vehicles on this planet (and that number is expected to continually grow rapidly in coming years⁹), demand for transportation energy will constantly rise while non-renewable supplies fade. Therefore, development of renewable fuel sources to be used in transportation sectors of energy are of paramount importance.

1.2.1 Non-Renewable Fuel Sources

A non-renewable fuel source only exists in finite quantities on this planet. This is not to say these resources can never be made again, but rather the time it takes for their production is significantly longer than rate their of consumption. Sadly, these non-renewable energy sources are most commonly used with examples including nuclear fuels and fossil fuels. Proceeding sections elaborate on fossil fuels, and their consequences.

1.2.1.1 Diminishing Fossil Fuel Sources

Fossil fuels have been a major resource for energy dating back to the Industrial Revolution in the 18th century. Ever since their implementation as an energy source to power modern machines, demand has been constantly growing. Primarily formed through prehistoric plants and animals, these fuels are fashioned over a period equal to millions of years via remains of these organisms then decompose into organic material, namely hydrocarbons. These hydrocarbons were buried underneath continually changing topography until humans extracted them as a fuel source. Variability of organisms and location lead to differentiation of fossil fuels (coal, crude oil, natural gas)¹⁰. Unfortunately, millions of years are needed to make fossil fuels. This has created an expiration for them as a viable energy source.

By the year 2042, global oil reserves will be depleted, by 2044. natural gas will be exhausted and coal reserves will last until 2112¹. Although coal depletion will not be a major issue for another century, depletion of oil and natural gas is approaching rapidly.

If a renewable substitute is not found for oil in the next three decades, a global crisis for transportation energy will occur. After depletion of both oil and gas, coal may be made applicable to transportation through conversion of coal to liquid fuel. Consequently, the 2112 energy projection will be significantly truncated. Depletion of fossil fuels is not the only reason for renewable energy investigations, however, several environmental issues exist that must be addressed long before their projected expiration.

1.2.1.2 Consequences of Fossil Fuels

When fossil fuels are combusted, their products can be detrimental to both human health and the environment. The primary reaction that occurs is combustion of a hydrocarbon (C_xH_y) in the presence of oxygen yielding carbon dioxide (CO_2) and water (H_2O). Both compounds are necessary for life on this planet, Carbon dioxide is used in plant photosynthesis while water is needed by every living organism on the planet for various chemical reactions to sustain life. While plants utilize CO_2 , its overproduction can be, however, very environmentally detrimental.

Solar energy reaches the earth usually in the form of short wavelength, high-energy radiation (mainly visible, ultraviolet, and some infrared). This radiation is used as a primary energy source for many plants and other organisms to perform photosynthesis. A byproduct of this process is emission of a longer wavelength, lower energy infrared radiation. Normally this radiation would be directed to space, but high concentrations of greenhouse gases cause the earth to prevent it from leaving the atmosphere increasing

global temperature. Greenhouse gases are compounds found in earth's atmosphere that can absorb infrared radiation generated by the planet. Once radiation is absorbed, molecules vibrate and release radiation to other greenhouse gases. This cycle is perpetuated by a high concentration of greenhouse gas molecules in the atmosphere, causing the overall temperature of the planet to increase¹¹. Carbon dioxide itself is one of the most abundant greenhouse gases produced by fossil fuel combustion and one of the greatest factors of global climate change. Emission of CO₂ has been increasing rapidly since the 1950s and has led to significant global temperature increases¹².

Along with environmental consequences, many compounds are produced by fossil fuel consumption that cause toxic health effects on animal populations. Most pollutants take form as impurities in fossil fuel sources, and include but are not limited to: sulfur dioxide (SO₂), nitric oxides (NO_x), heavy metals (lead, mercury, etc.), dioxins, and several others¹³. Mechanisms and extent of toxicities differ between compounds but overall pollutants can cause irreversible and even fatal damage not limited to humans but also to many organisms of the entire animal kingdom. Pollutants disrupt natural development in pregnancies, generate free radicals to cause mutation in the body leading to carcinogenesis and overall disruption of natural bodily functions necessary to maintain homeostasis^{14,15}. Combinations of both environmental and health issues have led to current developments of renewable, environmentally favored energy resources.

1.2.2 Renewable Fuel Sources

Renewable fuel sources are similar to energy sources like fossil fuels, but the pollutants and CO₂ levels generated is significantly less. Typically derived from organic matter (biofuels) or naturally occurring phenomenon (wind, solar, hydroelectric power, etc.), these energy sources can be harnessed in a timely manner. For biofuels, the determining factor is time required to grow organic matter. Natural phenomenon conversely can be readily harnessed, but energy is dependent on uncontrollable variables like weather or geographical location. Renewable energy involves three major stages: i) energy saving on from consumer's perspective, ii) improvements in efficiency of energy production, and iii) replacement of fossil fuels by various energy means¹⁶. While the first stage requires action by people using energy, the latter two can be improved by energy providers and are the focus of proceeding sections.

1.2.2.1 The Need for Renewable Energy

Recent studies into expiration and impact of fossil fuel consumption for energetic means have revealed into the severity of many economic and environmental issues. Therefore, fuel technology research has shifted towards an alternative means of energy production. In an effort to entice renewable energy research and production, the United States government enacted the Energy Policy Act of 1992 to provide monetary incentive for energy from renewable sources¹⁷. Use of alternative energy could drastically decrease emission of greenhouse gases¹⁸. Although different energy options have

different greenhouse gas reductions, all options are better than current non-renewable fuel sources. While many different types of renewable fuel sources, each with their own advantages and disadvantages, a combination of all alternative energy options will lead to a long term, environmentally friendly, stable energy portfolio and economy.

1.2.2.2 Alternative Energy Options

As mentioned previously, main renewable energy sources can be broken down into four main categories: i) solar, ii) wind, iii) hydroelectric, and iv) biomass energy sources³. These energy sources provide a means of lowering greenhouse gas emission, but do not eliminate them. Many of these sources use natural phenomena to produce energy, but production, transportation, and application of energy derived from these sources still produce environmentally detrimental waste. Until a completely clean and efficient means of harnessing energy is developed, we are merely concerned with minimizing environmental impact.

i) Solar energy production attempts to mimic plants by utilizing energy directly from the sun. Rather than biochemical pathways to produce sugars, photovoltaic cells use light rays to excite dye energy rich compounds. These excited dyes then transfer electrons to a compound with a conduction band (empty π orbitals in semiconductors) that is similar in shape and energy. From there, electrons are sent along an electrode to produce electricity. This dye is then regenerated with an electrolyte, or compound with a high

electron density in a redox reaction¹⁹. Capacity to capture energy, life of photovoltaic cells, and sunlight exposure are major limiting factors for this energy source.

ii) Wind energy makes use of very tall wind turbines acting similar to a windmill. Kinetic energy from moving air is transferred to propeller-like blades, which cause a low speed shaft to turn. This shaft is attached to a gearbox that causes a high-speed shaft to turn. From here, the high speed shaft rotates and activates an induction generator, which then generates electricity²⁰. Mechanical work from turbines can then be converted into usable energy. However, this energy source is not without limitation. Large land areas with predictable and consistent wind patterns are needed for wind turbines to be constantly running to produce a sizable amount of energy. In addition, gearboxes connecting the low and high-speed shafts require regular maintenance. Finally, due to structure height, it may be susceptible to harsh weather conditions that could damage blades or other essential components.

iii) Hydroelectric energy can be divided into two primary components: freshwater and saltwater sources. Typically, freshwater sources use water at a higher altitude falling to lower altitude, causing a turbine at lower altitude to turn, and generating electricity. Freshwater bodies can be natural, human made reservoirs, or a human made contained system. Natural sources are existing rivers with a waterfall where turbine was built at the base. Human made reservoirs would create a dam either at an existing body of water or a new body of water would be built that would have a controlled flow to turbines below. Finally, human made contained system would be similar to

reservoirs, but a pump would be placed after turbines to regenerate the reservoir at higher altitude²⁰.

Other major hydroelectric energy source is from oceanic sources. Primary methods to harness oceanic energy are introduction of turbines on/near either the ocean surface or floor that utilizes waves to turn turbines to cause energy generation. In addition to these methods, use of buoys and their change in altitude causes by waves could also be used to perform mechanical work for electrical power genesis²⁰. Many limitations exist for both fresh and saltwater hydroelectric sources but generally these manifest in three main areas. These energy sources are dependent on water levels, which can make consistency of energy produced variable. The ecological impact of instrumentation that is needed for these renewable sources to be harnessed can disrupt natural animal and vegetation ecosystems. Finally, transportation of energy produced from these sources can be difficult at times.

iv) Biomass has been an energy source human kind has used since the invention of fire. Modern uses manifest primarily in two areas: thermal energy and liquid fuel. While energy released from biomass is similar to fossil fuels, main differences are levels of CO₂ and other air pollutants are lower (comparing biomass to coal on average²¹). Like coal, thermal energy produced by combustion of biomass is used to heat water into steam, which then turns steam turbines causing genesis of electricity. Alternatively, biomass can be pretreated to disrupt cellular structure and expose energy rich biopolymers. Through use of enzymes, namely cellulases and hemicellulases, components

of biomass can then be converted into simple carbohydrates. These carbohydrates can be fed to microorganisms, which are typically under anaerobic conditions, to produce liquid fuel sources (bioethanol and biodiesel) that can be readily used to power combustion engines and similar power technologies^{5,22,23}.

1.3 Biomass to Biofuel

Of all possible renewable sources discussed, the focus of this paper was the implementation of biomass to be readily converted into biofuels. Proceeding sections describe the use of biomass in an effort to create a fuels source comparable to fossil fuels. To achieve this, a discussion of practicality of biomass, its structural components, current methods of conversions, and different types of biofuels made from biomass are needed. Switchgrass is the biomass of concern for this body of work, along with bioethanol production and subsequent sections reflect this. The specific biomass chosen for the projects in Chapters 3 and 4 was switchgrass and information about that biomass is provided as well.

1.3.1 Biomass as a Fuel Energy

Although all non-renewable energy sources are of concern for depletion and environmental consequences, fossil fuels with respect to the transportation energy sector, is a matter that must be immediately addressed. With current research being completed and new government incentives for implantation of renewable fuel sources,

biomass sources appear to be an appropriate substitution. These efforts towards biofuel manufacturing has led to an increase in production of said fuels in the past three decades, as shown in **Figure 1.2**²⁴. Many venues in which optimization of biomass conversion to biofuels are currently being researched, but this body of work focuses on effects of long term storage on a promising switchgrass biomass source. By determining extent of degradation on both sugar production and thermal energy production, an assessment of effective storage methods can be achieved. Information presented in this text can be used to construct an economically competitive business model for switchgrass biofuel production. Biomass can be broken down into three major biological components of concern for biofuel production: lignin, hemicellulose and cellulose.

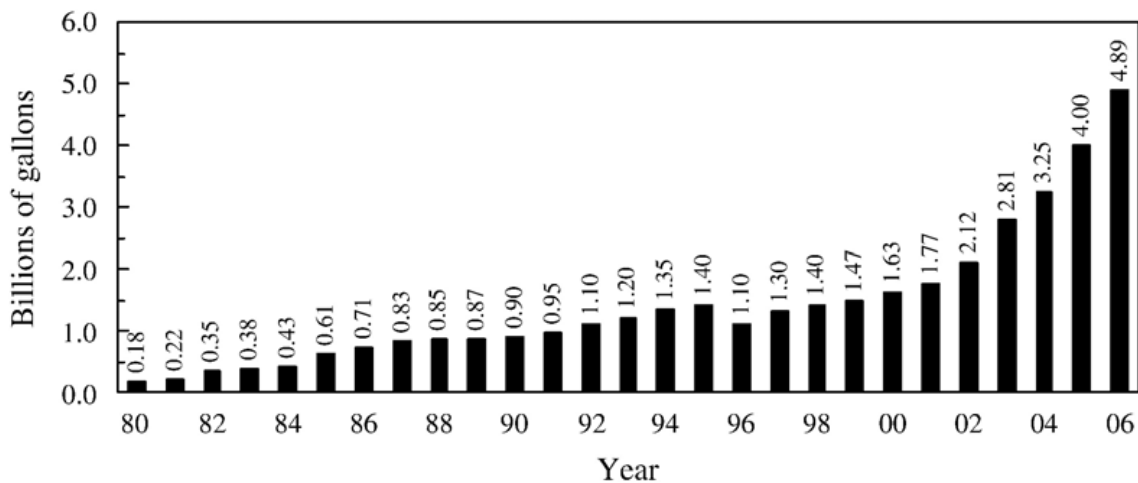


Figure 1.2. Annual ethanol production volumes (in billions of gallons) in the United States. Source: Bai, F.; Anderson, W.; Moo-Young, M., Ethanol fermentation technologies from sugar and starch feedstocks. *Biotechnology advances* **2008**, *26* (1), 89-105.

1.3.2 Biomass Components

Many different biomass sources are presently being used around the world. Each has varying amounts of components to make biomass a viable fuel source. A list of common lignocellulose materials and their component compositions are illustrated in **Figure 1.3**⁵. Not all of the listed components can be readily converted into fermentable sugars, but instead, may have applications in other renewable chemical processes.

lignocellulosic material	cellulose (%)	hemicellulose (%)	lignin (%)
hardwood stems	40–55	24–40	18–25
softwood stems	45–50	25–35	25–35
nut shells	25–30	25–30	30–40
corn cobs	45	35	15
grasses	25–40	35–50	10–30
paper	85–99	0	0–15
wheat straw	30	50	15
sorted refuse	60	20	20
leaves	15–20	80–85	0
cotton seed hairs	80–95	5–20	0
newspaper	40–55	25–40	18–30
waste papers from chemical pulps	60–70	10–20	5–10
primary wastewater solids	8–15		
solid cattle manure	1.6–4.7	1.4–3.3	2.7–5.7
coastal bermudagrass	25	35.7	6.4
switchgrass	45	31.4	12
swine waste	6.0	28	na

Figure 1.3. Component percentages of common agricultural residues and wastes.

Source: Kumar, P.; Barrett, D. M.; Delwiche, M. J.; Stroeve, P., Methods for pretreatment of lignocellulosic biomass for efficient hydrolysis and biofuel production. *Industrial & Engineering Chemistry Research* **2009**, *48* (8), 3713-3729.

1.3.2.1 Lignin

The outermost lining of plant cell walls in biomass is comprised of lignin. Lignin is a highly branched, amorphous biopolymer, which surrounds the plant as a protective coating, while allowing nutrients to diffuse into the plant. Lignin is typically composed of substituted aromatic monomers: most common monomers and dimers are shown in **Figure 1.4**²⁵. Different species of biomass sources may have varying predominant monomers. Primary causes of the amorphous nature of lignin are the free-radical enzyme assisted polymerizations that may occur at many different sites of phenolic monomers²⁶. The lignin in plants is responsible for protecting carbohydrate reservoirs, cellulose and hemicellulose. Lignin offers cell rigidity while also providing a hydrophobic vascular system for water and other nutrients into the plant²⁵. Unfortunately, the natural function of lignin in biomass is to protect carbohydrates from degradation but the goal of fermentation is to derogate those carbohydrates into sugar monomers to be fed to microorganisms to produce biofuels. Lignin may be the most hindering component of biofuel production, but it does have advantages of its own. Oxygenated polyaromatic lignin compounds are of great commercial and laboratory use²⁷. This has caused a great amount of research to be completed in an effort to separate lignin from cellulose and hemicellulose.

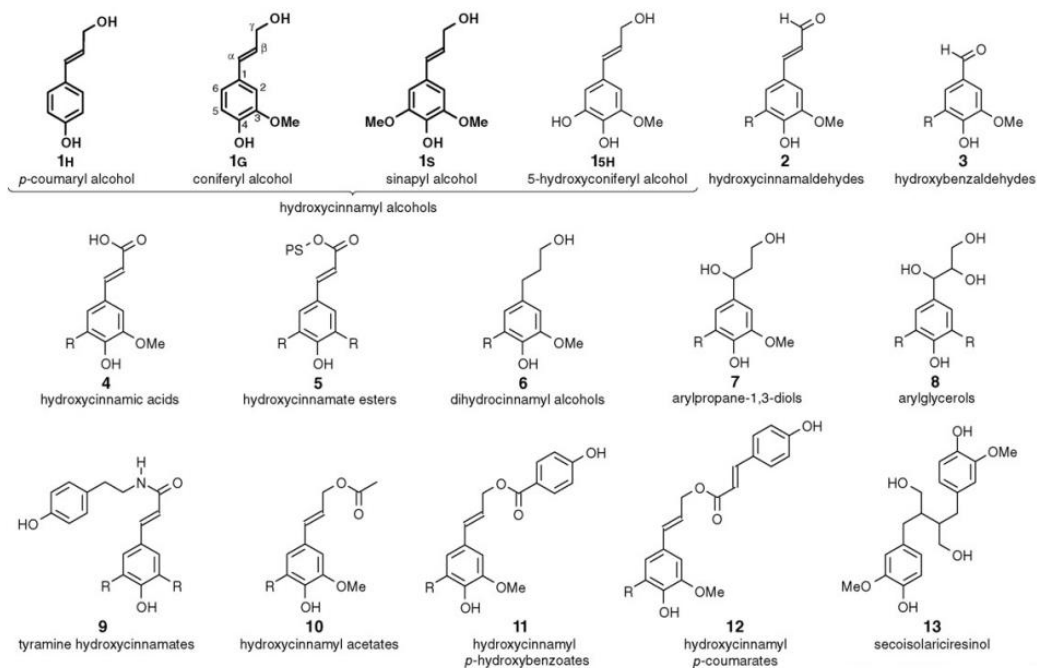


Figure 1.4. Structure of several lignin monomers and dimers.

Source: Vanholme, R.; Morreel, K.; Ralph, J.; Boerjan, W., Lignin engineering. *Current opinion in plant biology* **2008**, *11* (3), 278-285.

1.3.2.2 Cellulose and Hemicellulose

Both cellulose and hemicellulose are long chain carbohydrates composed of hexose and pentose sugars. Cellulose is comprised of β -1,4-linked glucose monomers and is interlaced between hemicellulose branches^{28,29}. Hemicellulose is comprised mainly of xylose, glucose, galactose, mannose, and arabinose sugars²⁹ and is directly attached to lignin polymers in cell walls. Once carbohydrates are separated from lignin, they become susceptible to enzymatic hydrolysis in an effort to depolymerize both starches into their respective sugar monomers. Main differences between these carbohydrates are the monomers in which they are composed and their proximity to lignin. Glucose and xylose can both be fermented into biofuels, but glucose can be directly converted into

bioethanol through glycolysis and alcoholic fermentation. First xylose will be converted into fructose before it can travel along the same metabolic pathways, whereas glucose has a more energetically favored metabolism pathway. Depending on the specific microorganism strains used for fermentation, enzymes may not readily be available to help in this process^{30,31}.

1.3.3 Switchgrass

Figure 1.3 shows many different plant sources used for the production of biofuels, each with varying components. A specific biomass source used in this body of work was switchgrass. This perennial, warm-season crop makes an ideal carbohydrate source for bioenergy production. Switchgrass grows naturally in prairies, shores, riverbank, marches, and other ecosystems but can be adapted to almost all regions of the continental United States. Low maintenance, high yield crop, and producing moderate to high biofuel concentrations and thermal energy production make it an outstanding renewable energy source for U.S. based biofuel refineries. The ability for it to grow almost anywhere in the country and under flexible conditions, make it great for localization of biofuel production to help minimize transportation costs during processing^{4,32,33}.

1.3.4 Biofuel

Any substance that produces more energy required for its genesis can be defined as a fuel. Energy produced from this fuel must be harnessed into performing

some form of mechanical work (*i.e.* transportational energy) or generate some form of storable energy (*i.e.* electricity). For a fuel to be considered a biofuel, substance origin must come from a biological source, typically plants. Finally, for biofuel to be considered a renewable fuel source, original biomass samples used to make biofuels must be able to grow and be cultivated in an adequate amount of time. Although fossil fuels at one point came from biological samples, the time it takes to reproduce the sources is in the order of thousands to millions of years. Biofuel in extreme cases would take no longer than a few decades to produce sizable amounts of biomass: for example, using wood as biomass. Typically, most biofuel sources are ones grown annually, biannually, or perennially.

1.3.4.1 Types of Biofuels

Biofuels are a colloquial term for all possible products yielding energy from biomass renewable sources³⁴. Two major biofuels used for transportation means are bioethanol and biodiesel. As the former implies, bioethanol is ethanol derived from complex carbohydrates in biomass sources. This alcohol cannot be directly extracted from biomass, nor can carbohydrates be directly converted to ethanol. Instead, the use of pretreatment technologies separate carbohydrates from biomass^{5, 35}. From there, the most common methods of carbohydrate de-polymerization and ethanol production are enzymatic hydrolysis and alcoholic fermentation, respectively. De-polymerization occurs via cellulase and hemicellulase enzymes³⁶. Multiple microorganism strains, each with

their own cellulases and hemicellulases, are capable of yielding bioethanol with different properties and efficiencies²².

Biodiesel is produced from biological oils; these can be either plant or animal in origin in a process called transesterification. During this reaction, there is an exchange of alkoxy groups (RO-) of long chain triglycerides with alkoxy groups of a short chain primary alcohol, namely methanol and ethanol³⁷. This produces methyl or ethyl esters fatty acids comprised of one or two carbon RO- groups from alcohol moieties, and long carbon R-OH groups from triglycerides. **Figure 1.5** shows transesterification of triglycerides from biological oils, with methanol, to produce biodiesels and glycerol, where catalysts may be either an acid, base, or enzyme³⁸. These ester fatty acids are high in energy and can be used by internal combustion engines to power vehicles.

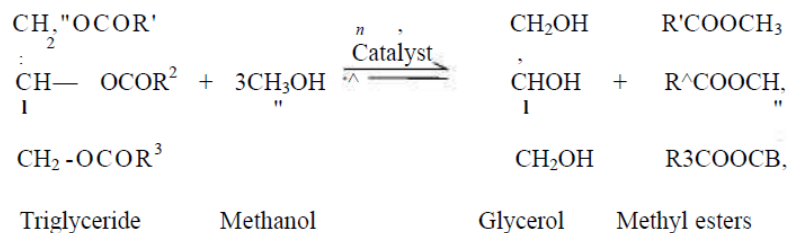


Figure 1.5. Transesterification reaction of triglyceride with methanol to produce glycerol and biodiesels (methyl esters).

Source: Meher, L.; Sagar, D. V.; Naik, S., Technical aspects of biodiesel production by transesterification—a review. *Renewable and sustainable energy reviews* **2006**, *10* (3), 248-268.

Both bioethanol and biodiesel have a positive net energy balance, meaning more energy is released from their combustion than energy required to produce them.

Given the structural nature of biodiesel having a longer carbon chain, biodiesel produces more energy over bioethanol. Unfortunately, on average, biodiesel produces more CO₂ and other pollutants than bioethanol. Both still yield a reduction in greenhouse gases when compared to traditional non-renewable fuels like gasoline and diesel⁵.

1.3.4.4 Current Conversion Processes for Lignocellulose Biofuel Production

Different ways of producing biofuels from lignocellulose are possible. General steps in this process occur in three phases: lignin disruption by pretreatment technologies, enzymatic hydrolysis, and fermentation processes. Pretreatment phases incorporate the greatest diversity in methods. Enzymatic hydrolysis makes use of two classes of enzymes, cellulase and hemicellulase, to convert separated components of lignocellulose into sugar monomers. Finally, fermentable sugars are fed to microorganisms to make a final conversion to bioethanol. After this process, bioethanol can be converted to biodiesel in a transesterification process described in Section 1.4.1. The focus of this body of work is production of bioethanol from lignocellulose switchgrass and proceeding sections will reflect this fact.

1.3.4.4.1 Pretreatment

As mentioned above, many pretreatment options for biomass sources exist. Main goals of these phases are to separate lignin polymer from cellulose and hemicellulose so de-polymerizing enzymes cellulase and hemicellulase can break down

sugar polymers into monomers readily and efficiently. Natural cellulose crystalline structure is very rigid due to hydrogen bonding. Chair conformations of glucose monomers force hydroxyl groups into equatorial positions, and aliphatic hydrogens into axial positions. This results in high intermolecular chain hydrogen bonding, causing difficulties in enzymatic hydrolysis³⁹. While hemicellulose is more amorphous in nature, both need extremely open polymeric faces for enzymatic hydrolysis to occur. Many different pretreatment options are needed and can be divided into two major categories: mechanical and chemical processes. Mechanical treatments aim to reduce particle size and degree of polymerization of cellulose and hemicellulose in biomass. This is conducted by the use of grinding, milling, heating, and an extruder to physically break down biomass into smaller components for better enzyme efficiency. Major disadvantages are high energy inputs required to perform these tasks³⁵.

Chemical pretreatments are numerous, each with their own advantages and disadvantages. One of the major classes of pretreatments involves solvation of lignin in alkali, acidic, or organic solvents. Oxidants, specifically for ozonolysis techniques, have also been used in an attempt to disrupt lignin-hemicellulose interactions. Ionic liquids have also been studied to determine if molten salts are capable of dissolving aromatic lignin monomers while maintaining cellulose and hemicellulose structures³⁵. Plethora of other pretreatment options are available, but are beyond the scope of this thesis.

1.3.4.4.2 Enzymatic Hydrolysis

Once lignin has been successfully separated from hemicellulose and cellulose, isolated enzymes are introduced into saccharification vessel to facilitate formation of fermentable sugars. The class of enzymes responsible for breakdown of cellulose is called cellulases. Numerous cellulases exist but most commercially available cellulases are made from fungal sources³⁶. Cellulose de-polymerization takes place via three major classes of cellulases working together: endocellulases, exocellulases, and β -glucosidases⁴⁰. Endocellulases are used to break cross-linked cellulose chains held together by hydrogen bonding of hydroxyl groups in glucose monomers. Once separate cellulose chains are exposed, exocellulases cleave long chained polymers into oligomers, typically between two and four monomers long. Finally, β -glucosidases cleave oligomers into individual monomers of glucose. All three reaction processes are illustrated in **Figure 1.6**⁴⁰.

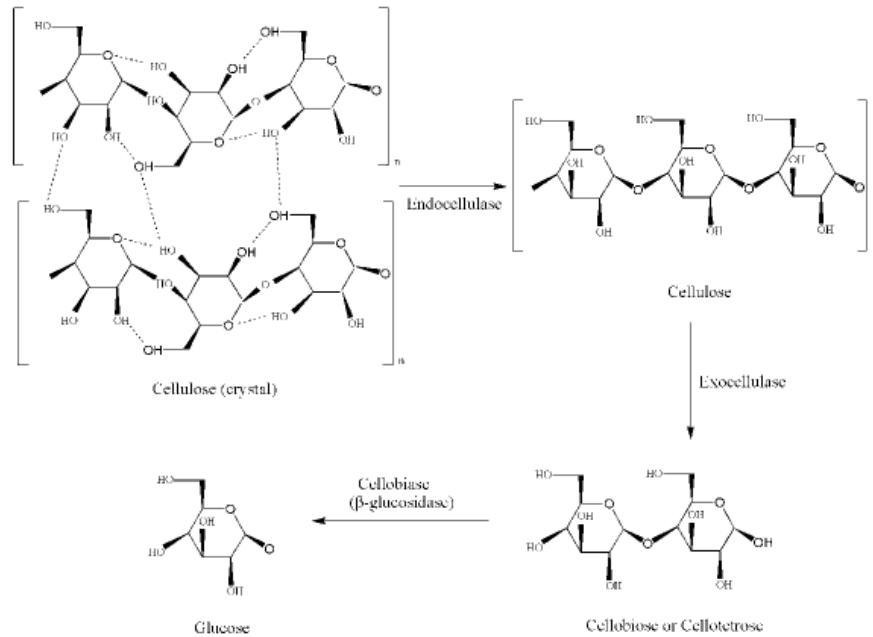


Figure 1.6. Conversion of crystalline cellulose to glucose through cellulase enzymes.
Source: Golan, A. E., Cellulase: Types and Action, Mechanism, and Uses. **2011.**

Hemicellulases work very similarly to cellulases as they break down sugar polymers comprised of hemicellulose. The main difference between the two is hemicellulases are not broken down into different functions for de-polymerization of a single monomer type. Hemicellulose consists of many different sugar monomers, typically xylose, mannose, galactose, rhamnose, and arabinose⁴¹. Because of this, an enzyme mixture (cocktail) is needed to ensure maximum de-polymerization. Typical enzymes include: xylanases, β -xylosidases, β -mannosidases, α -galactosidases, α -arabinases, and β -galactosidases. Xylanases are comprised of many different enzymes used to break amorphous chains of hemicellulose into oligomers. For oligomers of same sugar monomers, their respective α - or β -enzymes can then be used to cleave each

respective bond into individual monomers. When oligomers of different sugar monomers are created, special enzymes are used to cleave any combination of monomers⁴². The sheer number and complexity of combinations is out of the scope of this thesis, as this body of work is more concerned on resulting sugars produced.

1.3.4.5 General Fermentation Process for Ethanol Production

Once fermentable sugars are produced, they are fed to microorganisms under anaerobic conditions. Rationale for this is if oxygen is present, most microorganisms will undergo the Krebs cycle and oxidative phosphorylation pathways to produce high energy per sugar molecule. By restricting oxygen levels, anaerobic pathways are forced due to a lack of oxygen for aerobic pathways. During anaerobic conditions, low hydrogen levels can thermodynamically drive formation of acetate and carbon dioxide from ethanol and other compounds of interest. Fermentation typically occurs in closed containers in order to maintain high hydrogen levels for the reactions to occur⁴³. Genetic composition of organisms determines which anaerobic pathway is utilized. Diverse microorganisms are used to produce ethanol with their own affinities toward certain sugars. Most common microorganisms used are *Saccharomyces cerevisiae* species. A major advantage of this microorganism is its utilization of most hexose and pentose sugars for biofuel production. Hexose catabolism of *S. cerevisiae* is illustrated in **Figure 1.7**⁴⁴.

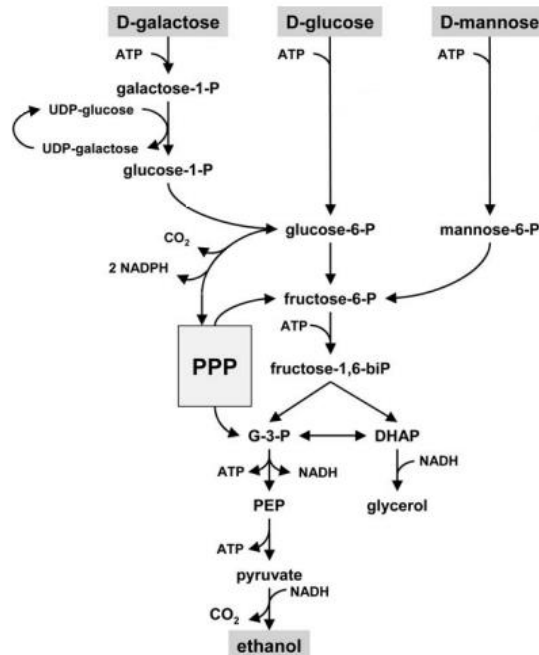


Figure 1.7. Hexose catabolism of *Saccharomyces cerevisiae*.

Adapted from: van Maris, A. J. *et al.* Alcoholic fermentation of carbon sources in biomass hydrolysates by *Saccharomyces cerevisiae*: current status. *Antonie Van Leeuwenhoek* **2006**, *90* (4), 391-418.

During breakdown of hexose sugars many intermediate compounds are formed. Major intermediates are: glucose-6-phosphate (G-6-P), fructose-6-phosphate (F-6-P), and pyruvate. Glucose-6-phosphate is product of both galactose and glucose catabolism. Fructose-6-phosphate is the centerpiece of this fermentation process as where all hexose and pentose sugars (from pentose phosphate pathway) meet. Finally, the end product is pyruvate from sugar breakdown, where it can either be converted into ethanol through anaerobic processes, or continue through aerobic pathways⁴⁴. Final conversion between pyruvate and ethanol is actually a two-step reaction. The first step is a decarboxylation of pyruvate to form acetaldehyde, via pyruvate decarboxylase, making use of thiamine

phosphate as a cofactor. Acetaldehyde is converted to ethanol using alcohol dehydrogenase, with aid of reduced Nicotinamide Adenine Dinucleotide (NADH)⁴⁵. Structures of compounds mentioned are shown in **Figure 1.8**. Xylose and other pentose sugars have similar metabolism properties, but rather than going through a hexolysis pathway, pentose sugars proceed through the Pentose Phosphate Pathway (PPP). This results in the conversion of pentose sugars to Fructose-6-Phosphate, and then a breakdown into pyruvate and bioethanol.

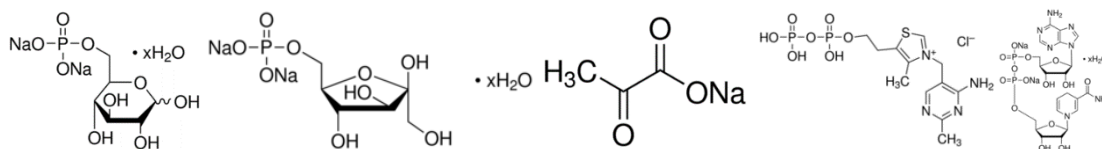


Figure 1.8. Structures (from left to right): glucose-g-phosphate, fructose-6-phosphate, pyruvate, thiamine phosphate, and NADH.

Notes: All compounds are shown with sodium salts or chloride counter ion for thiamine phosphate. Images taken from Sigma-Aldrich.com

1.3.4.2 Drawbacks of Biofuel

Although biofuels are an obvious replacement to fossil fuels, they are not without environmental, ecological, and economic consequences. Circa 2005, the net costs of corn bioethanol was \$0.46 per energy equivalent liter (EEL) of gasoline, and soybean biodiesel net costs were \$0.55 EEL of diesel. The term EEL refers to equivalent volume of a fuel needed to produce the same energy as one liter of gasoline. These EEL values compare to \$0.44/liter and \$0.46/liter for production costs of gasoline and diesel respectively. In order to achieve the \$0.46/EEL and \$0.55/EEL for bioethanol and biodiesel

respectively, the U.S. federal government implemented a \$0.20 and \$0.29 EEL for bioethanol and biodiesel, respectively¹⁸. While these make biofuels competitively viable, gasoline prices have recently seen a rapid decrease at the time of writing (July 2014 to Feb 2015)⁴⁶. Along with cost effectiveness, most internal combustion engines cannot be ran on biofuels alone. Instead, most biofuels produced are blended into gasoline and diesel to help reduce greenhouse gases, although some diesel engines can be ran solely from biodiesel⁴⁷. Cost competitiveness of biofuels is also dependent on federal subsidies, which can have economic consequences.

From an environmental perspective, overall greenhouse gas emissions are lower for biofuels than fossil fuels. Even so, at present, most biofuel production still involves the use of fossil fuel energy sources to provide energy for conversion of biomass to biofuel⁴⁷. Another major environmental concern of biofuels are pesticides and agrichemicals used to protect biomass. These chemicals are present in final biofuel products and can lead to discharge of nitrogen and phosphorous based greenhouse gases reducing net environmental balance of this renewable energy¹⁸. These problems were major concerns in first-generation biofuels, but in later generations, the impact of environmental factors has been dramatically reduced.

The last major type of problems with biofuel is ecological in nature. First generation biofuels were produced from food sources, namely corn for bioethanol and soybean for biodiesel¹⁸. This caused major controversy as fear of over consumption of food supplies would lead to increases in food costs and potential food shortages of any

biomass capable of producing biofuel. This issue was resolved in second generation biofuels primarily made from non-food sources such as lignocellulose and wood sources, as well as third generation biofuel made from microalgae⁴⁸. Although controversy has subsided, concern over plottable land for use of food versus biofuel production has not. As of 2009, only 1% of total plottable land was used for biomass production and produced only 1% total transportation energy⁴⁹. This is seemingly insignificant, but if second generation biofuels were to completely replace fossil fuels then plottable land required would dramatically increase. A combination these concerns make biofuels as a replacement to non-renewable fuel sources currently slow going, as they must be addressed and optimized before a complete overhaul of transportation energy sector is to take place.

CHAPTER 2

EXPERIMENTAL METHODS AND INSTRUMENTAL THEORY

2.1 Current Method of Analysis for Fermentation Products

Once biomass sources have been pretreated to remove lignin and enzymatically digested, fermentable sugars become the next major area of concern. Quality control and efficiency of sugar production are important factors leading to economic viability and cost competitiveness. This has led to several methods of analysis for sugar quantification over the years. The following sections discuss traditional and novel means for carbohydrate determination and quantification. Additionally, traditional method of analysis for thermal energy assessments is also described for oxygen bomb calorimetric studies.

2.1.1 Traditional Methods of Analysis for carbohydrates

Colorimetric Methods: These methods of analysis have been performed as early as 1947⁵⁰. Carbohydrates, themselves, do not readily absorb light in the ultraviolet (UV) or visible (Vis) light portion of the electromagnetic spectrum. Instead, different reagents can be used to replace one or more hydroxyl groups found on sugars with a compound or complex capable of absorbing UV-Vis light. Various reagents have been used throughout

the years, each with their own limits of quantitation and stability^{50,51,52,53}. In general, through acidic or alkaline conditions, chromophores are added to reducing sugars in solution. These chromophores may be aromatic in nature, or make use of transition metal complexes to provide a π -system where light in UV-Vis range can interact. This change results in absorbance of light at a given wavelength readily measured using a colorimeter or spectrophotometer. Early iterations of this analysis were done solely with colorimeters, which focus on a single wavelength. Advances in spectrophotometric instrumentation, such as spectrophotometers, have made measuring a range of wavelengths and recording their absorbance possible⁵⁴. Major problems arise from non-discrimination between different sugars, such as isomers, oligosaccharides and polysaccharides versus monosaccharides. In addition, the dependency of chromophores, and the potential not to add a chromophore to all carbohydrates in samples can cause a discrepancy in analyte concentration.

Gas Chromatography: Another common method of analysis for carbohydrates implores Gas Phase Chromatography (GC). This technique implements extremely long (typically 30 meters long) small diameter (0.25 m i.d.) metal coils packed with silica bound adsorbent material used to slow down and separate molecules passing through them⁵⁵. Dimensions of columns and stationary phase properties have changed drastically over the years but general methods have remained consistent. Along with colorimetric methods, this technique has been used for carbohydrate analysis for a long time, dating back to the 1960s^{56,57,58}. This method utilizes high temperature (250°C for example) sample

introduction chambers and carrier gases to aerosolizes liquid sample and provide needed kinetic energy to travel the column length. Materials inside columns are designed to have weak interactions with analytes in samples. Some of these analytes will interact with columns more causing a longer retention time while others will have practically no interactions causing a much shorter retention time. This technique is useful for carbohydrates because polysaccharides, oligosaccharides, and monosaccharides will separate better colorimetric studies. Hexose and pentose sugars will also be separated based on molecular weight. GC can also incorporate different detection sources; two most common being flame ionization detection (FID)^{56,57,58} and coupling to a Mass Spectrometer (MS)^{55,59} with respective detection sources. No technique is without drawbacks, and GC based methods are no exception. Largest downsides to any GC analysis are: long analytes run times (15-30 minutes), matrix interferences with samples can lead to a shifting of retention times, volatility of analytes is a major concern even with high temperature, degradation of sample due to high temperatures can occur, and often derivations are needed for adherence to a column so that separation can occur^{56,58}.

High performance Liquid Chromatography: Another common method of analysis for carbohydrates uses the technique of high pressure liquid phase chromatography (HPLC). This method is similar to GC based analysis but rather than aerosolizing samples, they remain in liquid phase. Another major difference between GC and LC are interactions analytes have with mobile phase. In GC, carrier gases act as the mobile phase, which carries analytes along the column, but does not have any direct

chemical interactions with analytes. In LC, analytes are dissolved in mobile phase, causing weak intermolecular forces (IMF) interactions with analytes. Theory behind this method of analysis will be expanded upon in later sections. Diverse column and mobile phase combinations are needed to do this type of analysis, each with varying success and applications^{60,61,62}. These variations and a plethora of detection devices make HPLC a versatile method of analysis but does share similar disadvantages with other traditional techniques.

2.2 Novel Method of Analysis for Fermentation Products

Proceeding sections describe analytical theory and basic operations of instruments used to perform analyses needed to quantitate biomass degradation and determine viability of storage methods for switchgrass fuel sources. By following molecular paths in sample solutions, a better understanding of the impact of this study will be illustrated. In order to achieve this, the interactions substances have with instrumentation and the chemical theory for data produced must be properly described. A more detailed explanation of the genesis of sample production is described in continuing chapters.

2.2.1 Liquid Chromatography

Chromatography was first coined by Mikhail Semenovitch Tswett in 1906 when describing a method for separating pigments in chlorophyll⁶³. Since then, there have been

many improvements and validation proofs of his original theory. The novel process used an adsorbent solid material, which a sample and a liquid that analytes were at least partially soluble in was introduced. This caused separation of individual components while passing through a packed solid column. This general theory for liquid chromatography is still used today, but in a much more advanced manner. Studies into interactions of solutes (i.e. analytes), in mobile phases (solvent that moves through columns) and stationary phases (adherent substance that does not move) have brought to light molecular levels interaction which cause this separation⁶⁴. Through these developed and tested theories, chromatography has become a major field of study and a branch of chemistry critical to almost any scientific experiment. The goal to any chromatographic technique is separation of components in a matrix (liquid or solid that analytes are contained in before column injection) as well as each individual analyte in a sample.

2.2.1.1 Separation Theory

In order for separation to occur in chromatography, analytes must have partial affinity to both mobile and stationary phases. Affinity, in this context, describes partition coefficient, or equilibrium constant (K) of a given analyte in two phases. Consider two extremes of this K value; assuming liquid phase is P_1 and stationary phase is P_2 shown in Equation 2.1⁶⁴.

$$K = \frac{[P_2]}{[P_1]} \quad \text{Equation 2.1}$$

If K is a very large number ($\geq 10^3$), almost all analytes are only in the mobile phase (100%) and are not in the stationary phase (0%). From this, there would be no separation between compounds in a sample and therefore, no visible response in the chromatogram (visual representation of separation based on detection method). Conversely, if K is a very small number ($\leq 10^{-3}$), once analytes reach stationary phase they will remain there no matter how much mobile phase is added. This too will cause no separation and can cause permanent column damage. For efficient separation time between analytes, they need to spend time in both phases somewhere between 0 and 100% over the time of the analysis.

The example above also implies there is only one type of compound in solution or all compounds have similar equilibrium constants for both stationary and mobile phases: which is inaccurate. Differences in K values for all compounds in solution are partially the cause of separation. Solutes having higher stationary phase K values will adhere to columns longer than ones those with lower values. Other major contributors to effective separation are interactions different compounds can have with one another while inside columns. Say, for instance, a pure sample of compound A elutes from a column in 5 minutes (or its retention time, t_r , is equal to 5). When compound B is introduced, there is a mixture of A and B through the column and B has intermolecular force attraction towards A, which now results in elution in 6 minutes. This interaction of

a compound in solution, with an analyte of interest, is a prime example of a matrix effect. Reducing matrix effects improves separation and experimental accuracy, which is why sample preparation has become a very important step in analytical separations.

Depending on analytes of interest, mechanisms for separation can vary. Analytes of concern for saccharification analysis were glucose and xylose whose structures are given in **Figure 2.1**. Amide column configuration and acetonitrile structure are shown in **Figure 2.2**. Hydrogen bonding is the main attractive force, which causes separation between the two sugars in this LC system. Carbonyl groups in the amide column act as a hydrogen bond acceptor, where amine groups act as a hydrogen bond donor. In sugars, hydroxyl groups both donate and accept hydrogen bonding. In acetonitrile mobile phase, nitrogen atoms of nitrile group act as hydrogen bond acceptors⁶⁵. In experiments presented (discussed in Chapter 3), the mobile phase also consisted of water, which acts as both a hydrogen bond acceptor and donor as well.

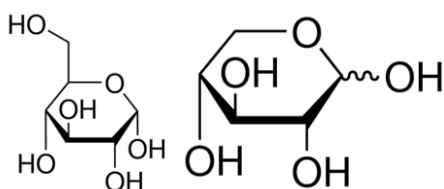


Figure 2.1. Structures of glucose (left) and xylose (right) are shown.
Note: Structures retrieved from Sigma-Aldrich.com.

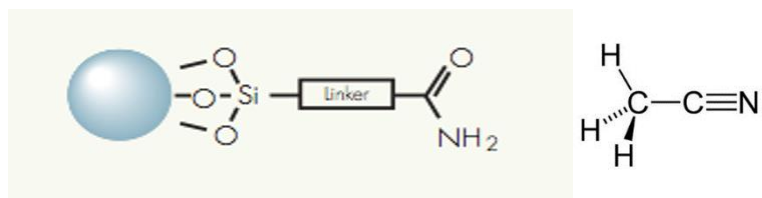


Figure 2.2. Structure of BEH amide column (left) and acetonitrile (right) are shown. Note: Images retrieved from Waters.com.

All compounds involved in this LC system have no ionic properties so hydrogen bonding is the highest intermolecular force observed and main cause of analyte affinity towards both mobile and stationary phase. Taking into consideration all possible hydrogen bonding in the system, equilibrium constants for glucose and xylose are quite involved. To simplify matters, the only difference between these two analytes is one CH₂OH group found on glucose. The extra hydroxyl group in glucose will cause separation compared to xylose because there will be more interactions with the stationary phase via hydrogen bonding. Technically, activity will be higher with the mobile phase as well, but concentrations of molecules are higher in the stationary phase, and the column acts as both a donor and acceptor negating this interaction. Relating back to examples in the preceding paragraphs, if mobile phase has no capacity for hydrogen bonding, equilibrium between time spent in stationary and mobile phases would be vastly more in the stationary phase.

2.2.1.2 Types of Liquid Chromatography

Separation of analytes from a matrix can occur in many different mechanisms. Prominent types of liquid chromatography are: adsorption, partition, ion-exchange, size-exclusion, and affinity chromatography. In adsorption chromatography, analytes are dissolved in a liquid solvent and as compounds reach the stationary phase, they adsorb, or adhere, to solid surfaces. Stationary phases in this type of chromatography are a tightly packed solid, usually silica (SiO_2) or alumina (Al_2O_3) based particles. Partition chromatography is very similar to adsorption, but rather than a tightly packed solid, this stationary phase is comprised of a liquid bonded to silica or similar surfaces⁶⁶. Usually partition chromatography is only used for GC based analysis, as open tubular diameter is too large for adequate equilibration between stationary and mobile phases. In this type of mobile phase, dissolved analytes are carried through the column, which spend differing amounts of time in the mobile gas and stationary liquid phases. This is also the most common type of chromatography for GC based analyses. For liquid chromatography, these two types can either be normal phase (NPLC) or reverse phase (RPLC). The major difference between the two is polarity of mobile and stationary phases. In NPLC, many stationary phases have a higher polarity than the mobile phase, and oppositely true for reverse phase⁶⁴.

Ion-exchange chromatography makes use of solid resins, like in adsorption chromatography, but anions or cations are covalently attached to a packed column. This is useful for pH dependent separations: usually proteins or other biochemical separations.

Different proteins have different isoelectric points, pI, which describes the pH level where a protein has an overall neutral charge. These differences in pI along with cations/anions density in ion-exchange columns lead to a separation based on overall charge density of proteins. Mobile phases for ion-exchange are a buffer prepared at a designated pH producing ions, which compete with charged amino acids in proteins. This competition eventually causes elution of proteins from the column. Depending on the experiment, analytes are typically ran with a lower buffer concentration. Then once non-analytes are removed, a higher buffer concentration is added to ensure all proteins are eluted from the column^{45,64}.

Size-exclusion chromatography, also known as gel filtration, separates analytes solely based on molecular size, regardless of net charge like in ion-exchange. Rather than a tightly packed solid stationary phase, size-exclusion makes use of a semi-solid gel. This gel bed, prepared for these experiments, is porous in nature. The pores are big enough to allow smaller molecules to fit into openings produced, while excluding larger molecules^{45,67}. It is important for the gel beds to remain hydrated because, if dried, there will be considerably less space between gel particles As well as creating air bubbles which are very detrimental to efficient separation. This is another type of chromatography common for protein analysis and purification. Mobile phases will also likely have a buffer to help dissolve proteins, but overall there is no interaction with stationary phases like in ion-exchange. Size-exclusion results in the largest molecules eluting first because they cannot fit into the pores of the stationary phase. Smaller molecules remain in pores until

mobile phases ions (proton or hydroxide ions depending on pH) compete with these molecules due to the reduced size of mobile phase ions. This is what causes the smaller analyte to elute later.

Affinity chromatography is the final major type of liquid based chromatography methods. Yet another common protein purification technique, affinity chromatography is similar to ion-exchange but instead of ions covalently attached to an immobilized column, specific chemical groups or antibodies are used⁶⁴. Rationale for this chromatography includes the fact most proteins have a very high affinity for certain molecules or proteins. Most commonly, these are substrates of a particular protein, other molecules have a binding site on proteins, or antibodies designed to attach to particular proteins. Similar to ion-exchange chromatography, a buffered mobile phase is used, and the concentration can be of importance when dealing with binding affinities, as they change with pH. When a mixture of various proteins are pushed through a stationary phase by a mobile phase, only analytes with specific affinity for covalently attached chemical group are retained in the column, while other will pass through with no interaction⁴⁵. This type of chromatography is unique because of a required two-step process where methods like ion-exchange can be facilitated with two steps. The first step is as described earlier in the paragraph, but the second step involves either flushing stationary phase with a high concentration of unbound chemical groups, or changing the pH to decrease binding strength of antibodies to a particular protein. Required specificity for this type of

chromatography makes it ideal when purification is important, but also tends to be most expensive, as each stationary phase is unique to each analyte.

With all different options available, a specific separation experiment can be implemented for analytes of interest. For this body of work, a normal phase adsorption chromatography technique was utilized. A polar stationary phase was chosen (amide column) with a nonpolar mobile phase solvent (acetonitrile). Specific interaction of analytes glucose and xylose with the amide column was described in preceding sections. In order to understand how this particular separation occurred, a general understanding of driving forces of separation is needed to be understood.

2.2.1.3 The Van Deemter Equation

The efficiency of a chromatographic system can be defined by the technique's ability to separate compounds from one another in a given matrix. In order to define how well this separation occurs, the van Deemter equation is used. The van Deemter equation is an empirical formula describing a relationship between linear flow rate and theoretical plate height⁶⁸. This equation encompasses four variables (eddy diffusion, longitudinal diffusion, mass transfer, and linear flow rate) affecting plate height of a column⁶⁹. Plate height (H), or height equivalent to a theoretical plate (HETP), is essentially the length of a column needed for one equilibration of analyte from mobile phase to stationary phase, and then back into mobile phase⁶⁴. Smaller plate heights equate to more equilibrium interactions of an analyte in a column, and a greater equilibrium rate equates to higher

resolution, and narrower solute bands in the column. Graphically, this manifests as thinner peaks in a chromatogram, as well as curves that are more Gaussian. The van Deemter equation is shown in Equation 2.2⁶⁴ with variable defined in following paragraphs.

$$H \approx A + \frac{B}{u_x} + Cu_x \quad \text{Equation 2.2}$$

Eddy diffusion is represented by term A in the van Deemter equation. The only variable independent of flow rate, meaning regardless of how fast or slow mobile phase is passing through the column, eddy diffusion will remain constant. This variable, also known as multiple flow paths, accounts for different routes in which a solute can travel through the stationary phase before reaching the end of a column. Stationary phases in chromatography (excluding open tubular partition columns) are typically packed columns all have varying size particles. The manner in which they are packed, how dense the composition, and particle size all contribute to generation of different path lengths and pathways⁶⁴. Some paths have more stationary phase interactions where others have less interaction. This interaction affects separation by causing elution of the same solute particles to elute at different retention times. These differences lead to peak broadening, which is indicative of a high plate height. No matter the packed column used, eddy diffusion will always be present, but decreasing particle size will lessen the impact of this variable. By decreasing particle size, more pathways are created, but a consequence is

pathways will be more uniform in length and therefore more consistent elution will occur. An illustration of eddy diffusion is given in **Figure 2.3**⁶⁴. This figure shows the effect of eddy diffusion on an ideal Gaussian peak, and dramatization of what would happen to the same peak given paths shown.

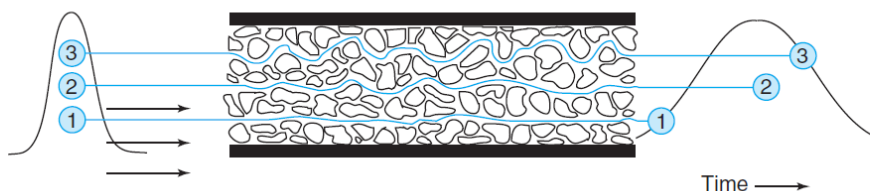


Figure 2.3. Theoretical illustration of band broadening via multiple flow paths (eddy diffusion) on a solute peak.

Source: Harris, D. C., *Quantitative Chemical Analysis*. 8th ed.; W. H. Freeman and Company: New York, 2010.

Next term in the van Deemter equation is longitudinal diffusion (B/u_x). Contribution to plate height, by this parameter, is defined by the tendency for a concentrated area of solute to diffuse into a larger, less concentrated area (equilibrium). Liquids, by nature, expand to fill the area in which they are contained, and mobile phase/analyte mixture is no different. When a sample is injected into the column, total concentration of analyte is in a localized volume. However, as bands of solute enter and begin passing through the column, natural repulsion of all molecules begins to create an equilibrium of distances between any two molecules^{64,69}. Resulting effects broaden band length for a given solute, which, in turn, increases plate height leading to a decrease in

resolution. Longitudinal diffusion is inversely proportional to linear flow rate, however. By increasing flow rate of the mobile phase for the experiment, forward forces of flow create a shift in the equilibrium of distances between any two molecules in a given solute band to be closer. This causes molecules of solute particles to concentrate, yielding a lower plate height, and therefore better resolution. Although raising flow rate increases resolution, by pushing separated solute out of the column faster, it also decreases separation of two different analytes. Recall the longer analytes spend in stationary phases the better separation will occur because of constant mobile/stationary phase equilibria. Greater flow rates will cause fewer interactions with stationary phases and therefore decrease separation of analytes.

Mass transfer (C_{u_x}) is the final component of the van Deemter equation. Conversely, to longitudinal diffusion, mass transfer is directly proportional to linear flow rate. If plate height gives us the distance in which one equilibrium occurs, in an LC column, mass transfer is defined as the rate in which equilibrium occurs^{69,64}. Energy is required for temporary interaction between solute and stationary phase to occur, which cause an analyte to adhere to the column. Similarly, energy is also needed to break intermolecular forces, which cause an analyte to dissociate from the column. Both interactions are spontaneous, but the frequency in which they occur affect the mass transfer variable. Mass transfer affects plate height because not all solutes adhere to the column at the same frequency; at any given moment, there is a portion of solute in both stationary and mobile phases. As time continues, solutes in mobile phase will travel further along the

column eventually adhering to different stationary phase binding sites. Original solutes are bound at an earlier site will eventually dissociate given enough time. With multiple sets of solutes binding in different places and taking different times (as a function of concentration), overall length of a column, in which total solute concentration occupies widens, causes an increase in plate height. **Figure 2.4** provides a visual representation of mass transfer⁶⁴.

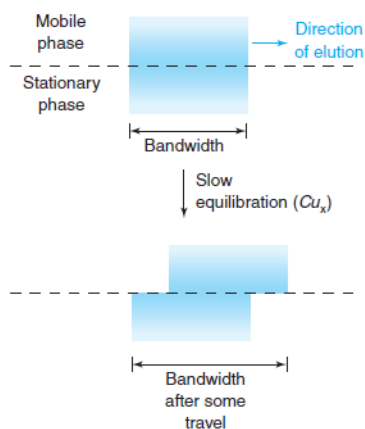


Figure 2.4. Visual representation of mass transfer in a chromatographic system.
Source: Harris, D. C., *Quantitative Chemical Analysis*. 8th ed.; W. H. Freeman and Company: New York, 2010.

Mass transfer is directly proportional to linear flow rate because when a portion of solutes bind, distance of mobile phase solutes travelled is increased. This causes an increase in total column length and consequently plate height. Both particle size and column temperature decrease this variable. Rationale for particle size is larger particles require more energy to separate solute from stationary phase. Therefore decreasing

particle diameter will provide a decrease in the time a solute is bound to a particular stationary phase site as well as making more binding sites per column volume with decreased particle diameter. Increased column temperature decreases mass transfer because it provides kinetic energy for both solute and mobile phase by decreasing viscosity of the mobile phase/sample mixture. Increased kinetic energy of the solute will yield in a higher probability of binding to stationary phase. If a solute has enough energy, however, it will effectively bounce off stationary particles because it will not only have enough energy to bind, but have enough residual kinetic energy to dissociate rapidly from the column. Greater mobile phase kinetic energy also contributes to a lower equilibration time because mobile phases can collide with both bound solutes and stationary sites to provide energy require for solute liberation from stationary particles. In short, increasing temperature provides a faster rate of making and breaking of intermolecular forces, which decreases the mass transfer component of the van Deemter equation and decreases plate height.

The many properties of a given chromatographic system give rise to many involved and complex variables when attempting to optimize plate height. Preceding paragraphs give a general overview of how these parameters of a given system affect plate height. Flow rate is one parameter to be controlled in almost every chromatography experiment and arguably affects plate height most directly. This is because flow rate is involved in two of the four variables components in the van Deemter equation. Greater flow rates are beneficial in longitudinal diffusion, but a hindrance in mass transfer. In light

of this, an optimized flow rates must be achieved for a given experiment. By plotting a graph of plate height as a function of flow rate, optimal efficiency can be accomplished. An example of plate height versus flow rate is given in **Figure 2.5**⁷⁰.

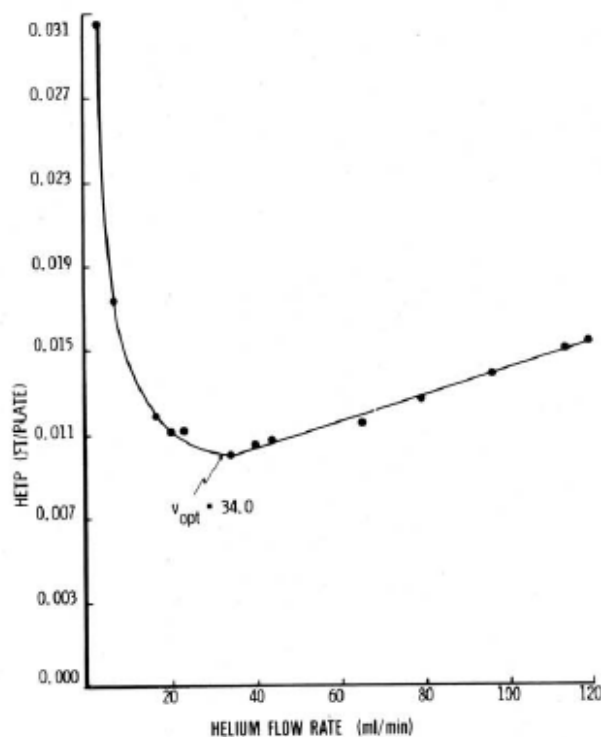


Figure 2.5. Graph of theoretical plate height versus flow rate of helium GC system. Source: Moody, H. W., The evaluation of the parameters in the van Deemter equation. *Journal of Chemical Education* **1982**, 59 (4), 290.

2.2.1.4 Ultrahigh Performance Liquid Chromatography

Traditional HPLC analysis involved the use of relatively large (5 μm) particle diameters (d_p). While these have been more than adequate in the past for many different applications, it was determined by decreasing particle diameter faster flow rates and

better resolution can be achieved. This led to the first generation of Ultrahigh Performance Liquid Chromatography (UPLC) system to be developed by ACQUITY in 2004⁶⁸. The main idea behind this system was to take advantage of smaller particles sizes increase efficiency. As d_p becomes smaller than 2.5 μm there is no significant increase in efficiency (plate height)^{68,71}. So this raises the question of why columns with sub-2 μm d_p have become so important? Although efficiency does not increase, it also does not decrease with higher linear flow rates. A comparison of van Deemter equations for different particle diameters are given in **Figure 2.6**⁷². As evident from the figure, decreasing particle size reduces plate height, therefore, increases number of plates (N), and improving resolution. Using 1.7 μm d_p particles in a column would not only lead to improved resolution, but would also allow you to increase linear velocity without greatly compromising plate height. This creates arguably the best advantage of UPLC over HPLC by an increased flow rate; lower run times are available for the equivalent resolution.

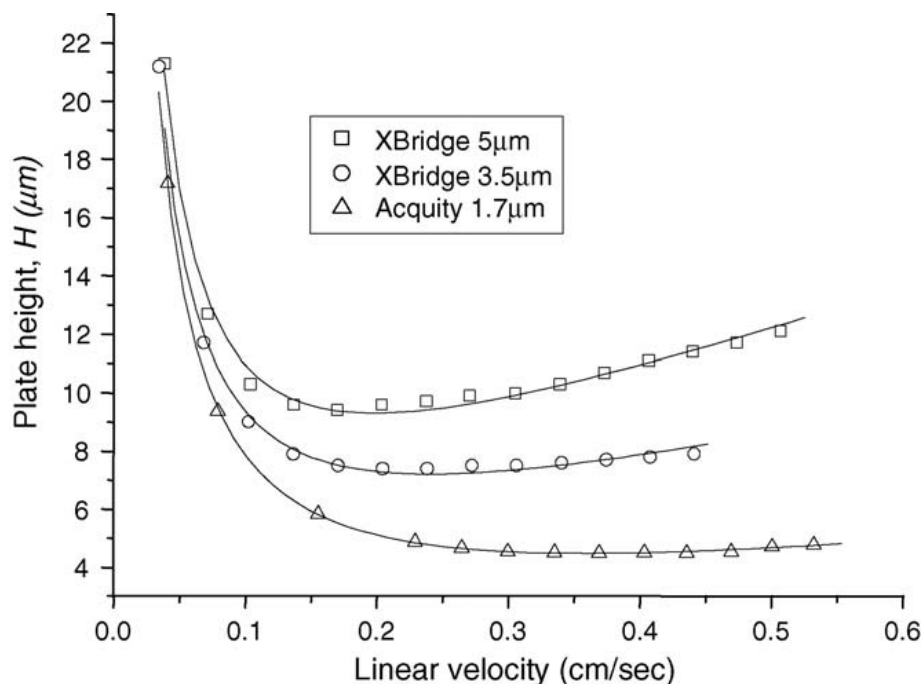


Figure 2.6. van Deemter plots for acetophenone on Acquity and XBridge column C₁₈ at three particle diameters: 5 μm, 3.5 μm, and 1.7 μm.

Source: de Villiers, A.; Lestremau, F.; Szucs, R.; Gélébart, S.; David, F.; Sandra, P., Evaluation of ultra performance liquid chromatography: Part I. Possibilities and limitations. *Journal of Chromatography A* **2006**, 1127 (1), 60-69.

Smaller particle diameter changes every variable of the van Deemter equation.

Eddy diffusion is interesting because by making more particles in a packed column, there would be more pathways an analyte can travel. At the same time, however, these new pathways are more uniform in length and resistance, making solute elution in a less broadened band. Longitudinal diffusion is changed because of the UPLC system, but more indirectly of particle diameter than eddy diffusion. In a UPLC system, having smaller particles equates to higher flow rate, therefore longitudinal diffusion is decreased because the two are inversely proportional. Solute, in a band in the column, is less likely to diffuse against the flow if the flow is greater. This would be the equivalent of swimming

against the current in a very slow moving versus a very rapid river. Finally, mass transfer is the only term that is detrimental to plate height contribution. This term is directly proportional to flow rate, therefore, increasing plate height. Rationale for this is solute is bound temporarily to particles in the column, and unbound particles are traveling further due to increased flow rate. Going back to the river example, if a person was to be stuck on a rock or log in the middle of said river, all his or her friends would have traveled much further in a rapid river before he or she could dislodge themselves. Although one of the terms is increased, overall effects of smaller particles on plate height are beneficial, resulting in lower plate height and higher number of plates.

Although decreasing d_p further would decrease run times and increase the potential for higher flow rates, complications can arise. Two major problems arise from further decreasing d_p . The production of small particles is excessively difficult, making consistency of the column more varying. In addition, as particle size decreases and linear flow rate increases, backpressure of the system also increases, which can cause mechanical failure if the pumps in the LC system cannot handle those increased pressures. In 2004, small particle stationary phases were possible by introduction of LC systems capable of handling pressures of 1000+ bar by having two serial flow pumps which divide backpressure so the system is not overloaded⁶⁸. A consequence of these novel systems was increased friction between mobile and stationary phases. This friction can lead to varying temperature profiles along the column itself. For a system to really be uniform and create Gaussian curves, with good resolution, a uniform temperature needs to be

achieved⁷³. In my experimentation, a higher uniform temperature (80°C) was used. Increasing column temperature decreases the viscosity of the mobile and therefore differences in the temperature profile are reduced.

2.2.1.5 Detection Sources

Once the sugars are separated, they travel towards the detector. Several detectors are commercially available, each with their own unique mechanism of detection. Main methods of LC analytical detection include: ultraviolet (UV), refractive index (RI), evaporated light scattering (ELSD), mass spectrometry (MS), and charged aerosol detection (CAD). Analyte level of detection varies between these detection sources. Generally, detectors with higher specificity have lower levels of detection, whereas more universal detectors are applicable to almost every type of sample, but may not be able to reach smaller levels of detection.

Ultraviolet Detection: This detection source works on the same premise as spectrophotometric methods such as colorimetric and UV-Vis spectroscopy. After mobile phase leaves the column, with analytes separated, flow direction takes a 90° turn and flows for a set length, usually 1 cm long. At this point, the eluate is bombarded with light in UV-Vis ranges. Some light will be absorbed by mobile phase and analyte, and the rest will be transmitted to the detector⁶⁴. Typically, if the samples were ran by themselves, Beer-Lambert's law would be needed to determine concentration, which could be problematic for the determination of the molar extinction coefficient (ϵ). This can be

easily remedied, with the use of standards, to either make a standard ratio, or more likely create a standard curve with multiple concentrations. Major problems that can arise are very similar with traditional spectroscopic methods, namely analytes must be readily able to absorb UV-Vis light. Another major issue, in this detection method, is the absorbance capacity of the mobile phase has to be considered. Although blank samples can be run to establish a baseline, if a baseline absorption is high, it can cause problems in quantitation.

Refractive Index: Light travels in a vacuum at a speed of approximately 3×10^8 meters per second. In absence of a vacuum, light travels slightly slower. The difference between the two rates is defined as a substance's refractive index (RI). RI detectors have two compartments, one for pure solvent and the other for the eluate. By bombarding both compartments with light, a difference between pure mobile phase and analyte dissolved mobile phase can be obtained. The analyte will refract the light more than only mobile phase, which then light from both cells travel to a photodiode array. The magnitude of refraction is proportional to the concentration of analyte⁷⁴. While this detection technique is essentially universal because all substances refract light to some degree, this detector is also the worst in terms of detection level. Depending on the level of detection needed, RI detectors are the most valuable for their application and price, but if low levels of analyte detection are needed, another detector is required.

Evaporative Light-Scattering: This detection method also makes use of like similar to UV and RI detectors. Rather than observing light absorbance or refraction, respectively, ELSD observes light scattering of solid solute particles. The main difference

is this detection method measures light, which does not pass through, but rather is reflected or bounced off analytes. In order to get solid particles, eluate is nebulized using nitrogen gas and travels through small diameter holes to form uniform aerosolized droplets. From here, mobile phase is evaporated off using a temperature-controlled tube. What is left over is a solid solute which is then bombarded with light and scattering patterns observed⁶⁴. Major advantages to this detection method is it produces a signal independent of the identity of the sample; smaller solute particles make smaller peaks, and vice versa. This can also be a major disadvantage because if any kind of coelution occurs, distinction between two analyte peaks is impossible. Another major drawback of this method is solutes have to be less volatile than mobile phase or solid particles will not form. Due to the increased temperature, analytes would remain in liquid or gas phase and not properly scatter light.

2.2.1.6 Charged Corona Aerosol Detection

The last major analytical detection method is the Charged Corona Aerosol Detector (CAD). This detector was the analytical detector used for this experiment because of its extremely low detection limit (10-fold more sensitive than ELSD and 5-fold more sensitive than UV), and elimination of analyte derivation needed for UV detection⁷⁵. This detection method is a derivation of ELSD as both use solid particles from nebulized eluate to produce an electrical signal interpreted by computer software. A general schematic of the CAD is shown in **Figure 2.7**⁷⁶.

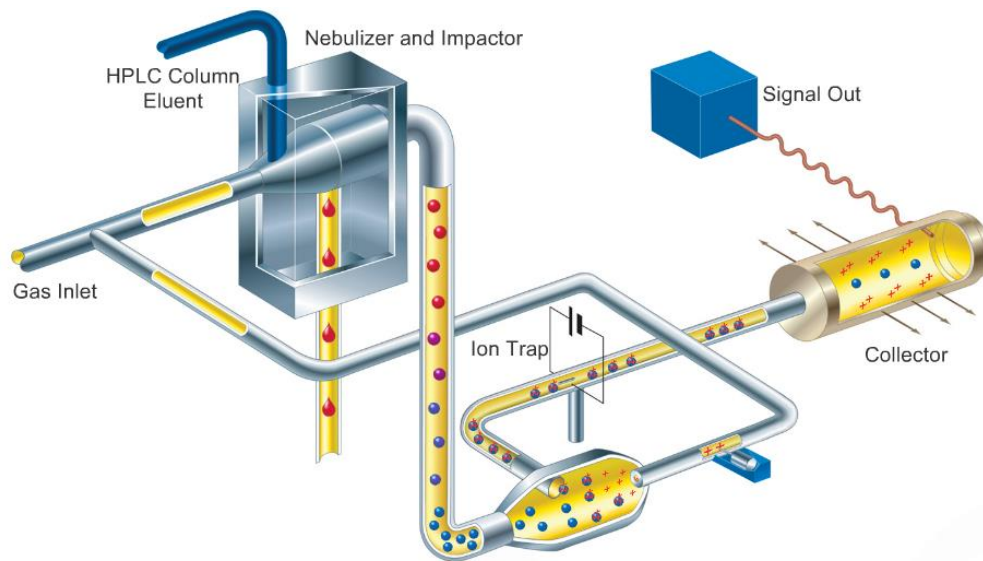


Figure 2.7. Schematic of Charged Corona Aerosol Detector is presented.

Source: Dionex. Charged Aerosol Detectors. <http://www.dionex.com/en-us/products/liquid-chromatography/lc-modules/detectors/charged-aerosol/lp-85214.html> (accessed Feb 15 2015).

Like in ELSD, the LC eluate is introduced into a nebulizing chamber with nitrogen gas as a nebulizing agent. Once aerosolized, mobile phase and analyte droplets are passed through a heated drying tube, which separates mobile phase from solutes, leaving solid particles. These particles are introduced into an ionization chamber where charged gas particles collide with analytes to transfer charges. Nitrogen particles are charged by using a positively charged corona wire, usually platinum⁷⁵. These positively charged nitrogen particles collide with both solid analyte and aerosolized mobile phase, which may have not been drained. This charge then is transferred to both types of particles and is fed into a narrow tube. At this point, the positively charged particles are met with a positively

charged ion trap or ion gate. Voltage of this ion trap is set so smaller particles (i.e. mobile phase particles) whose charge is more localized, due to particle size, cannot pass, but larger particles can delocalize charge, due to larger surface area, are able to pass through the ion trap. This is the last of several steps to remove as much mobile phase particles as possible. From here, analyte particles travel to the collector, where eventually they collide with the metal walls and an electric signal can be observed⁷⁶. The metal walls are electron rich and outer-most electrons can be readily removed by positively charged analyte particles. The loss of an electron creates an electron hole in the metal, to which other nearby electrons will move to help delocalize the now partial positive charge on the metal. This movement of electrons generates an electric current, which is then measurable by the electrometer.

The beauty of this detector is solutes can be made into solid particles (i.e. less volatile than mobile phase) but the identity of the particle does not matter. Analyte concentration in the proceeding experiments (Chapter 3) needed a detector capable of nanogram carbohydrate detection and CAD was able to deliver those levels⁷⁷. Nothing is without drawbacks, however, and CAD is no different. Because CAD is a relatively universal detector it more susceptible to matrix effect in comparison to UV detectors⁷⁸. This can be averted with proper sample preparation. In addition, the mobile phase, specifically when buffers are used, can be problematic. If a mobile phase has any nonvolatile component, the baseline detector will be increased, and therefore, can yield skewed results⁷⁵.

One major drawback of this detector is the variable detector response with different mobile phases. If molecules in the mobile phase can be easily crystalized then a higher detector baseline will be observed. This is usually caused by the conjugate ion of acids/bases used to pH mobile phases. Another drawback is this detection source can be non-linear in nature at low levels (nanogram levels of analyte)⁷⁹. This can be alleviated with the use of calibration curves via a quadratic regression instead of typical linear regressions⁸⁰. Despite these problems, corona aerosol detection is a great, nearly universal detector for extremely sensitive or low level experiments.

2.2.2 Oxygen Bomb Calorimetry

In addition to carbohydrate concentrations, an assessment of the raw thermal energy produced by untreated biomass sources was needed to assess switchgrass viability as a fuel source. Rationale for this study was another potential use of biomass as a renewable energy source. Rather than the time consuming, costly process of biofuel generation, biomass can be compressed and fed directly into boiler system or residential stoves to provide thermal energy. Traditional methods of thermal energy determination are calorimetric in nature. These traditional methods were sufficient for our needs and as such, no novel procedure was developed for this portion (see Chapter 4 for experimental procedure).

In general, theory behind this method of analysis includes a closed system where only heat can be transferred (not mass), with energy produced by combustion of a solid

or liquid primarily manifested as heat energy. Designing an experiment with a controlled system (reaction vessel, contents of the vessel) and its surroundings (water bath, outermost container) allows for quantification of this transferred heat. If this combustion is held at a constant volume, the heat (q_v) is equal to the total change in internal energy (ΔU_{total})⁸¹. An excess of molecular oxygen (O_2) is introduced to the vessel to ensure the limiting reactant is the hydrocarbon source.

Composition of biomass makes determination of the heat capacity difficult, and therefore, direct measurement of thermal energy produced problematic. To correct this, a substance of known molecular weight and heat capacity (water) surrounds the reaction vessel so all heat produced by combustion of a biomass is transferred to surrounding water bath and the calorimeter itself. This water bath is also held at constant volume, equilibrated using a stirring mechanism, and monitored via high accuracy temperature probe⁸². By accounting for the heat transferred to water, as well as the calorimeter itself, the total heat of combustion can be found for a sample. A visual representation of this apparatus is shown in **Figure 2.8**⁸¹. Using this system, Equation 2.3⁸¹ can be implemented to determine $\Delta U_{\text{combustion}}$. In this equation m_s is the mass of the sample, M_s is the molecular weight of the sample, m_{H_2O} is the mass of water used in the bath, M_{H_2O} is the molecular weight of water, $C_{p,m}(H_2O)$ is the molar constant pressure heat capacity of water, ΔT is the change in temperature of the water, and $C_{\text{calorimeter}}$ is the heat capacity of the calorimeter⁸². The $C_{\text{calorimeter}}$ term must be determined experimentally using a standard of known $\Delta U_{\text{combustion}}$ (Benzoic Acid).

$$\frac{m_s}{M_s} \times \Delta U_{\text{combustion}} + \frac{m_{H_2O}}{M_{H_2O}} \times C_{p,m}(H_2O) \times \Delta T + C_{\text{calorimeter}} \times \Delta T = 0 \quad \text{Equation 2.3}$$

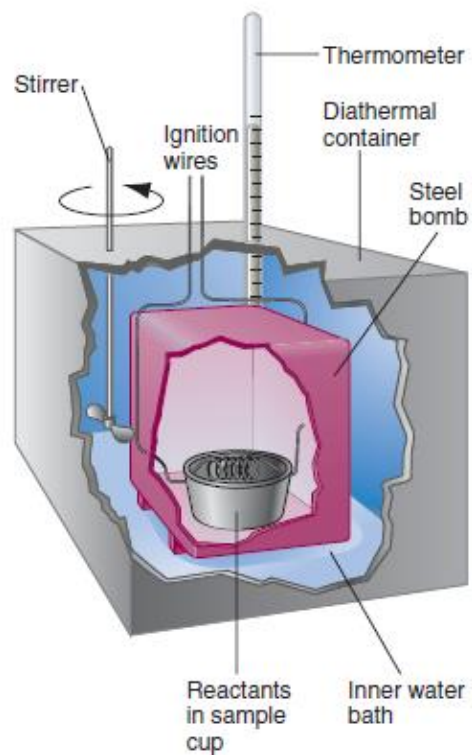


Figure 2.8. Sample schematic of bomb calorimeter.

Source: Engel, T.; Reid, P., *THERMODYNAMICS, STATISTICAL THERMODYNAMICS, AND KINETICS*. 3rd ed.; Pearson: Boston, 2012.

CHAPTER 3

SACCHARIFICATION STUDY USING UPLC-CAD

3.1 Introduction

The complex nature of biomass as a sample can lead to a high amount of molecular components, which are of no concern to the researcher. These components are commonly called a matrix and their effects on the analytes in question are therefore called matrix effects. In chromatography, matrix effects present themselves as molecules that can affect the elution order and retention time of the analytes in question. Exact mechanisms for matrix effects vary greatly on the analyte and matrix themselves but regardless of their origin, these effects must be reduced from samples to generate separation with maximum efficiency⁸³.

This chapter focuses on the production of fermentable sugars, glucose and xylose, from switchgrass and their quantitation using UPLC-CAD. Using effective pretreatment and filtration techniques, samples with virtually no matrix effect were analyzed using UPLC-CAD with the aid of standards. A previous study⁸⁴ already established initial parameters for analysis, but further method optimization was needed to minimize run time while maintaining adequate resolution.

3.2.1 Sample Preparation

Biomass samples were prepared at EKU's Center for Renewable and Alternative Fuel Technologies (CRAFT) department by Dr. Bruce Pratt and Gary Selby. Switchgrass was harvested in February of 2012. Mowing, windrowing and baling were done on the same day. Baling was done with a 1.2 x 1.2 m round baler and bales were secured with nylon net wrapping. Bales weighed an average of 290 kg. Round bales were moved and stacked in a 3-2-1 pyramidal configuration. Bales either were stored undercover in a hoop structure or outside in a well drained graveled lot as shown in **Figure 3.1**. Bales stacked outside were either left uncovered or protected with a waterproof nylon tarp.



Figure 3.1. Storage conditions for switchgrass samples: hooped (left) uncovered (middle), and tarped (right).

Switchgrass samples were collected monthly with a 0.6 m hay probe for 13 consecutive months. Probed samples were divided into thirds representing the outer 1/3 portion, middle 1/3 portion, and center of the bale. A composite sample from the entire bale was also collected. Switchgrass samples were processed in a Wiley mill with a 2 mm

screen. Samples were pre-treated in with a 1% NaOH (wt./volume) at 90°C for 1 hr. Samples were triple washed, pH adjusted to 5.0 with citric acid, and temperature brought up to 50°C. Novozyme Cellic® CTec and HTec⁸⁵ were added (.088 μL/mg fiber) and saccharification continued for 72 hrs. To terminate enzymatic saccharification samples were heated to 90°C for 1 hour and supernatant was harvested. These filtered samples were then placed into UPLC vials with screw-top septum lids and stored in a -22°C freezer until analysis by UPLC-CAD. A total of 156 samples were created based on month of the sample (1 to 13), storage method (hooped, tarped, or uncovered) and bale position of sample (first, second, third, or whole bale). Each sample was run in sextuplicate, triplicate from initial sample generation and duplicate from instrumental analysis.

3.2.2 Reagents

Glucose, C₆H₁₂O₆, (99% purity) and Xylose, C₅H₁₀O₅, (99% purity) were purchased from Sigma-Aldrich (St. Louis, MO, USA), structures shown in **Figure 2.1**. HPLC grade Methanol, CH₄O, and Acetonitrile, C₂H₃N, were purchased from Thermo Fischer Scientific (Fair Lawn, NJ, USA). Ultra-pure 18 MΩ distilled H₂O was produced in house using NANOpure Ultra Water Purification System (Barnstead/Thermolyne Inc., Dubuque, IA, USA). All chemicals and reagents were used without further purification or degassing. All mass measurements were made on an analytical grade scale.

3.2.3 Standard Preparation

Standard amounts (0.1000 g) of xylose and glucose were weighed out and dissolved in a 100 mL volumetric flask with distilled water. Each stock solution was vortexed and kept in a -22°C freezer until the day of use. From stock solution, 500 µL of each standard were pipetted into 1.5 mL microcentrifuge vials and vortexed for a concentration of 0.5 µg/µL for each sugar. Standard mixtures were then transferred into UPLC autosampler vials and prepared for sequencing. Three sets of standards and three sets of blanks, containing only distilled water, were prepared for every 34 samples. Blanks were run between standard injections and sample injections to prevent carry-over. Standards were placed in the beginning, middle, and at the end of each 40-slot tray. Up to three trays were used during one sequence. Injection volumes for standards were: 0.05, 0.25, 1.00, 1.50, and 2.50 µL. Rather than preparing multiple standard solutions at different concentrations, different injections volumes were chosen to perform the same varying levels of the two sugars in standards to generate calibration curves. Calibration curves were generated from the average of all standards used in sequence and a quadratic regression equation was generated to use to sample calculations.

3.2.4 Instrumentation

The instrument used in this portion of the study was the Dionex Ultimate 3000 RS UHPLC system (Thermo Scientific, San Jose, CA, USA). UPLC system consisted of a pump, autosampler, temperature controlled column, and CAD modules as outline in

Figure 3.2. Methanol was used as the pre-wash phase solvent, and 80% acetonitrile 20% distilled water was used as the mobile phase during the saccharification analysis studies. ACQUITY UPLC Ethylene Bridged Hybrid (BEH) Amide column (130Å, 1.7 µm, 2.1 mm X 100 mm) was used for separation in saccharification studies (Waters Corporation, Milford, MA, USA). Corona Aerosol Detector was used as detection source for Dionex 3000 RS system.

Fundamentals of the operations and theory behind this instrument are described in Chapter 2. Mobile phase flow rate of 0.250 mL/min was used. Amide Column were set at 80°C during analysis and kept at room temperature when in standby. Analysis was performed on column with pressures exceeding 1450 psi. Software interface for UPLC system was Chromeleon 7, which allowed independent control over individual modules of Dionex 3000 RS. Samples were introduced via 40-slot trays in autosampler, fitted with septum screw tops. An injection volume of 0.05 µL was used for all samples. Samples were injected into column via needle injector located in the autosampler. Original method was provided by Waters Corporation but optimizations described above were used for specific application⁸⁴.

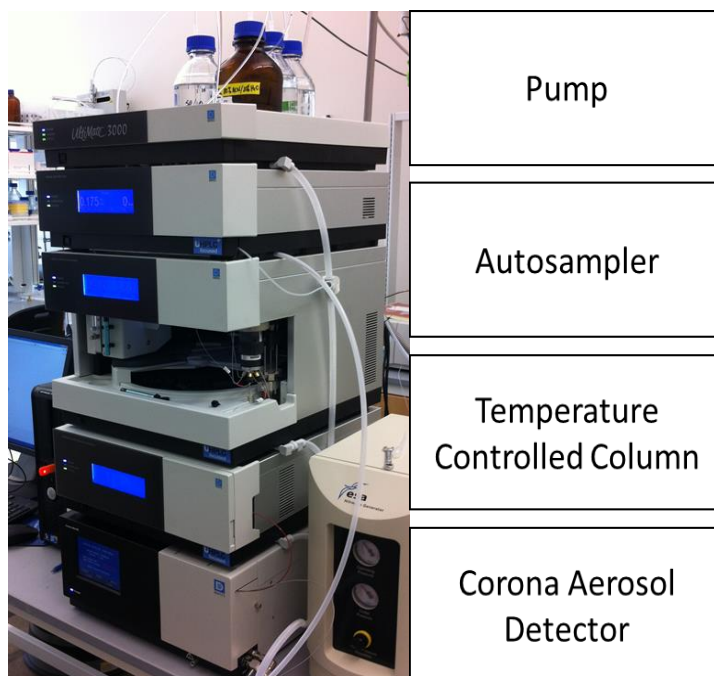


Figure 3.2. Dionex Ultimate 3000 RS UHPLC system (left) and block diagram (right).

3.3 Standard Results

A total of 36 standard curves were generated for glucose (18) and xylose (18) throughout the course of this study. This was derived from three standard sets placed in 40 slot trays with samples as described in Section 3.2.3. All generated curves had coefficient of determination values, R^2 , above 0.99 with a mean of 0.9989 for both xylose and glucose. Relative standard deviation (RSD) for gross sample statistics were 0.0828% and 0.1051% respectively for xylose and glucose. Overall standards were accurate and precise. This lead to the assumption of instrument reliability and reproducibility for all 936 samples that were ran. R^2 values are outlined in **Table 3.1**. Standard R^2 values for standard calibration curves.

Table 3.1. Standard R² values for standard calibration curves.

<i>Date</i>	<i>Xylose R²</i>	<i>Glucose R²</i>
08.14.2013	0.9992	0.9982
08.14.2013	0.9985	0.9998
08.14.2013	0.9995	0.9997
08.16.2013	0.9983	0.9970
08.16.2013	0.9999	0.9998
08.16.2013	1.0000	1.0000
08.21.2013	0.9996	0.9997
08.21.2013	0.9998	0.9990
08.21.2013	0.9990	0.9997
08.30.2013	0.9993	0.9998
08.30.2013	0.9992	0.9994
08.30.2013	0.9985	0.9992
09.05.2013	0.9993	0.9996
09.05.2013	0.9990	0.9979
09.05.2013	0.9981	0.9988
09.16.2013	0.9986	0.9990
10.09.2013	0.9965	0.9971
10.09.2013	0.9986	0.9969
Average	0.9989	0.9989
Std Dev	0.0008	0.0011
RSD (%)	0.0828	0.1051

Sample calibration curves with quadratic regression for xylose and glucose are shown in **Figure 3.3** and **Figure 3.4**. Standard error bars were present on all calibration curves, but standard deviations were low enough that points on the graph obscured said bars. Quadratic regression was decided due to the response from CAD detector. Remaining calibration curves are shown in **Appendix A**.

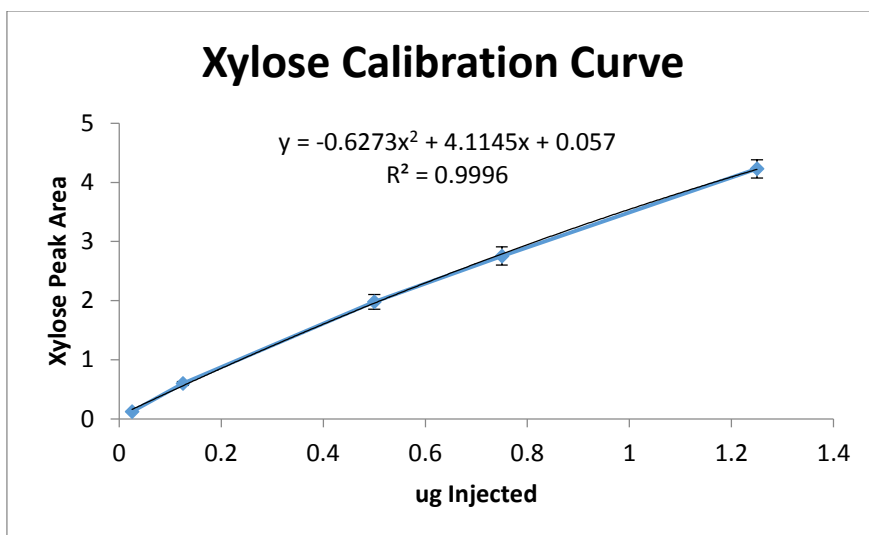


Figure 3.3. Representative xylose calibration curve for saccharification analysis where concentration (μg) is plotted against peak area.

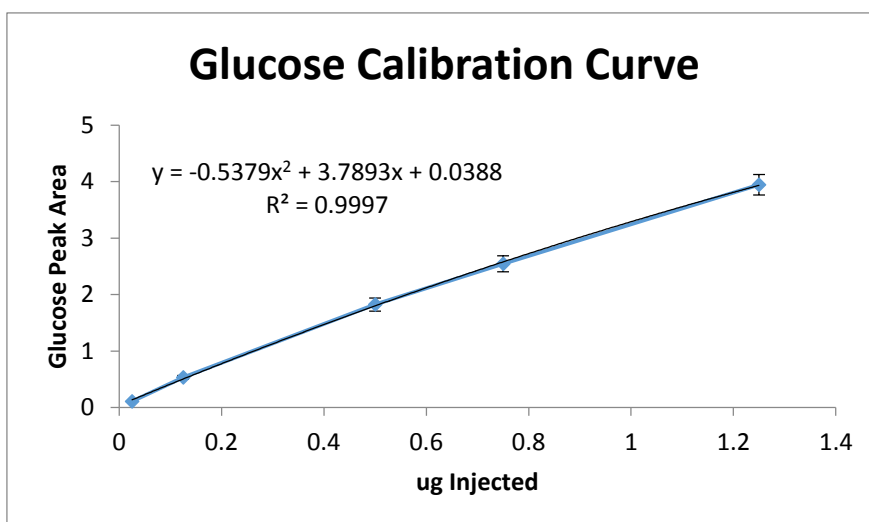


Figure 3.4. Representative glucose calibration curve for saccharification analysis with concentration (μg) plotted against peak area.

A sample chromatogram of xylose and glucose standard peaks is shown in **Figure 3.5**. Resolution of peaks in the figure was 1.59, which indicated adequate separation of sugars in column to perform quantitation. Calculations are based off of half height width

values, shown in Equations 3.1 and 3.2⁶⁴. In this equation, Δt_r refers to the change in retention time of the two adjacent peaks. The term $w_{1/2av}$ refers to the average width of the two peaks at $\frac{1}{2}$ the total peak area.

$$Resolution = \frac{0.589\Delta t_r}{w_{1/2av}} \quad \text{Equation 3.1}$$

$$Resolution = \frac{0.589 \times (1.998 - 1.642)}{(0.120 + 0.144)/2} = \frac{0.210}{0.132} = 1.59 \quad \text{Equation 3.2}$$

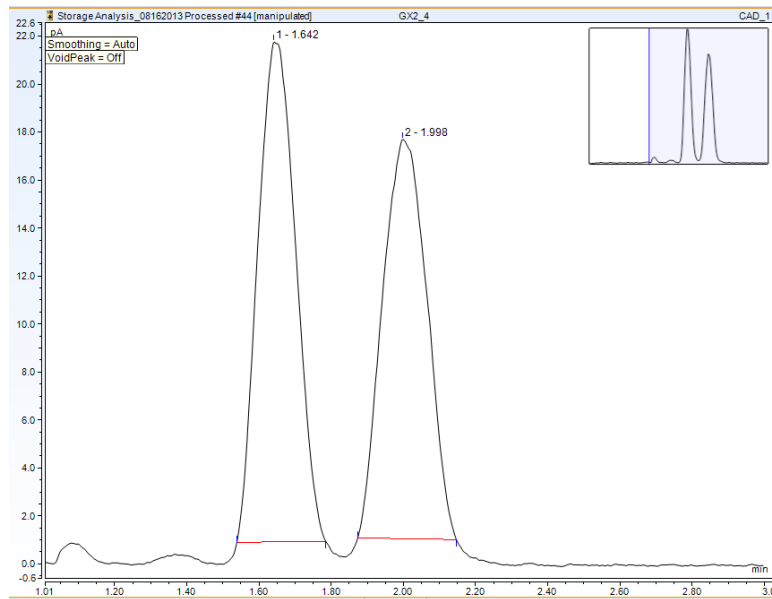


Figure 3.5. Example chromatogram of standards sugars is shown with the elution order of xylose (left) and then glucose (right).

Sample calculations for concentration determination, based on standard quadratic regression, are shown in Equations 3.3 and 3.4. Quadratic regression was chosen due to response from CAD detector.

$$\frac{-B + \sqrt{B^2 - (4 * A * (C - \text{Sugar Peak Area}))}}{2A} \quad \text{Equation 3.3}$$

$$\frac{-4.1145 + \sqrt{4.1145^2 - 4 * -0.6273 * (0.057 - 1.2146)}}{2 * -0.6273}$$

Equation 3.4

3.4 Sample Results

A total of 947 chromatograms were produced from samples (data not shown). All sample chromatograms were similar to standards in both retention time and resolution. An example chromatogram for samples is shown in **Figure 3.6**. The resolution for this sample chromatogram was found to be 1.86 based on Equation 3.1. Both standard and samples resolutions varied according to concentration, higher concentrations tended to be less resolute than smaller concentrations but all resolutions were adequate for distinct peak identification. Sample calculations for concentration determination based on standard quadratic regression are shown in Equations 3.3. Terms A, B, and C change according to the standard curve corresponding to particular data sets. Integration of peak areas were done manually for all chromatograms using Chromeleon 7 software. Some samples were either below or above detection levels of standard concentrations. To address this, samples were rerun with either higher or lower injection volumes and the different injection volume was accounted for in calculating sugar concentration.

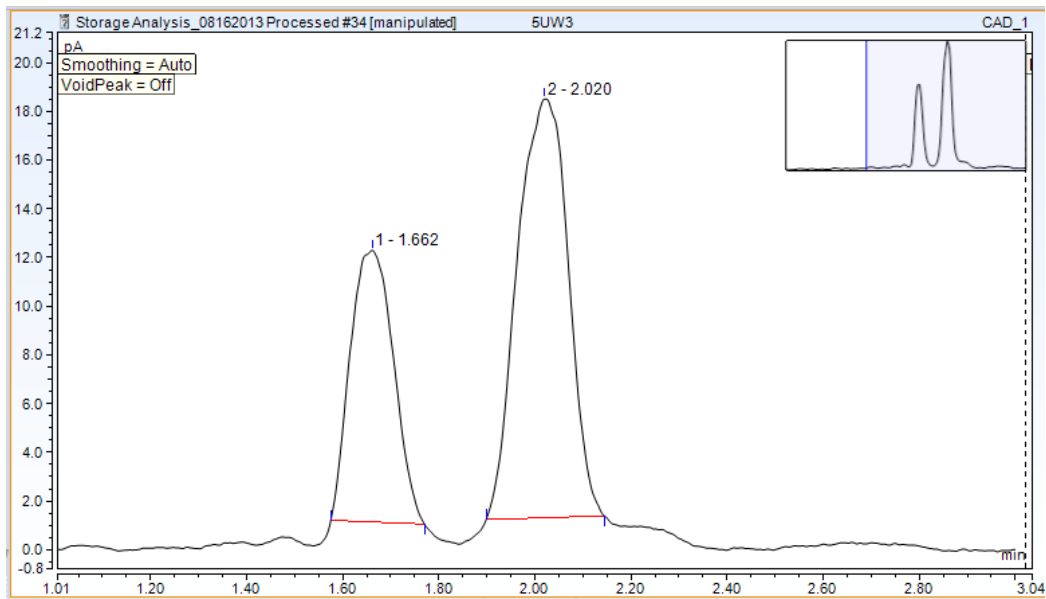


Figure 3.6. Example chromatogram of sample 5UW3 is shown with the elution order of xylose (left) and then glucose (right).

Once compiled and organized, averages, standard deviations, relative standard deviations, and 95% confidence intervals were calculated based on month number, storage structure, and position in bale separately. These data are shown in

Table 3.2,

Table 3.3, and **Table 3.4.** A total of 925 xylose and glucose concentrations were reported (data not shown) with 23 missing values. These values corresponded to concentrations disregarded due to Grubbs' test for outliers. Remaining samples were used to calculate 95% confident intervals (CI) based on Student's T-test according to a previous study⁸⁶. These CIs were produced for each month, each structure, and each sampling positions.

Table 3.2. Saccharification concentration based on month.

Month	Xylose N	Xylose N Missing	Xylose g/L Average	Xylose g/L Std Dev	Xylose g/L RSD	Xylose 95% CI	Glucose N	Glucose N Missing	Glucose g/L Average	Glucose g/L Std Dev	Glucose g/L RSD	Glucose 95% CI
Feb'12	72	1	6.063	1.524	25.136	0.358	72	1	11.978	2.684	22.408	0.631
Mar	70	3	5.130	0.932	18.168	0.222	71	2	10.153	1.962	19.324	0.464
Apr	72	1	5.348	1.170	21.877	0.274	72	1	11.353	2.390	21.052	0.562
May	75	1	4.827	0.938	19.432	0.215	76	0	10.514	1.965	18.689	0.449
Jun	76	1	5.646	1.426	25.257	0.326	76	1	12.063	2.582	21.404	0.590
Jul	72	0	5.360	1.303	24.310	0.307	72	0	10.334	2.526	24.444	0.593
Aug	72	0	5.181	0.907	17.506	0.213	72	0	10.163	1.425	14.021	0.334
Sep	71	1	4.552	1.140	25.044	0.270	71	1	9.254	2.148	23.212	0.508
Oct	69	3	4.851	1.178	24.284	0.283	70	2	9.883	2.116	21.411	0.505
Nov	67	5	5.884	1.157	19.663	0.282	67	5	11.777	2.023	17.178	0.493
Dec	70	2	5.677	1.069	18.830	0.255	70	2	11.592	2.276	19.634	0.542
Jan '13	70	2	4.651	1.035	22.253	0.246	70	2	10.261	2.198	21.421	0.524
Feb '13	69	3	4.847	0.989	20.404	0.238	69	3	10.221	2.046	20.018	0.491

Table 3.3. Saccharification concentration based on structure.

Structure	Xylose N	Xylose N Missing	Xylose g/L Average	Xylose g/L Std Dev	Xylose g/L RSD	Xylose 95% CI	Glucose N	Glucose N Missing	Glucose g/L Average	Glucose g/L Std Dev	Glucose g/L RSD	Glucose 95% CI
Uncovered	309	6	5.173	1.201	23.213	0.135	309	6	10.700	2.422	22.636	0.271
Tarped	308	10	5.216	1.264	24.224	0.238	309	9	10.665	2.334	21.885	0.262
Hoop	308	7	5.310	1.239	23.336	0.139	310	5	10.849	2.318	21.366	0.259

Table 3.4. Saccharification concentration based on sample position with total concentrations for all samples.

Sample Position	Xylose N	Xylose N Missing	Xylose g/L Average	Xylose g/L Std Dev	Xylose g/L RSD	Xylose 95% CI	Glucose N	Glucose N Missing	Glucose g/L Average	Glucose g/L Std Dev	Glucose g/L RSD	Glucose 95% CI
1st Third	232	5	5.334	1.319	24.717	0.171	232	5	10.801	2.422	22.424	0.304
2nd Third	236	6	5.370	1.240	23.098	0.159	237	5	11.001	2.334	21.216	0.304
3rd Third	228	7	5.106	1.112	21.787	0.145	230	5	10.493	2.318	22.091	0.300
Whole	229	5	5.115	1.240	24.250	0.161	229	5	10.650	2.318	21.765	8.588
Total	925	23	5.233	1.235	23.596	0.080	928	20	10.738	2.357	21.950	0.152

From these statistics, graphical representations were produced to better visualize whether degradation had occurred in samples. Error bars represent standard deviation based on Equation 3.7. Monthly graphs, **Figure 3.7**, represent averages of all storage methods and bale positions for each month during the course of the study.

Storage graphs, shown in **Figure 3.8**, represent averages of different structure methods for all months and bale positions. Bale position graphs, shown in **Figure 3.9**, represent averages for different bale positions for all months and storage conditions.

$$\sqrt{\frac{\sum (x - \bar{x})^2}{(n-1)}}$$

Equation 3.7

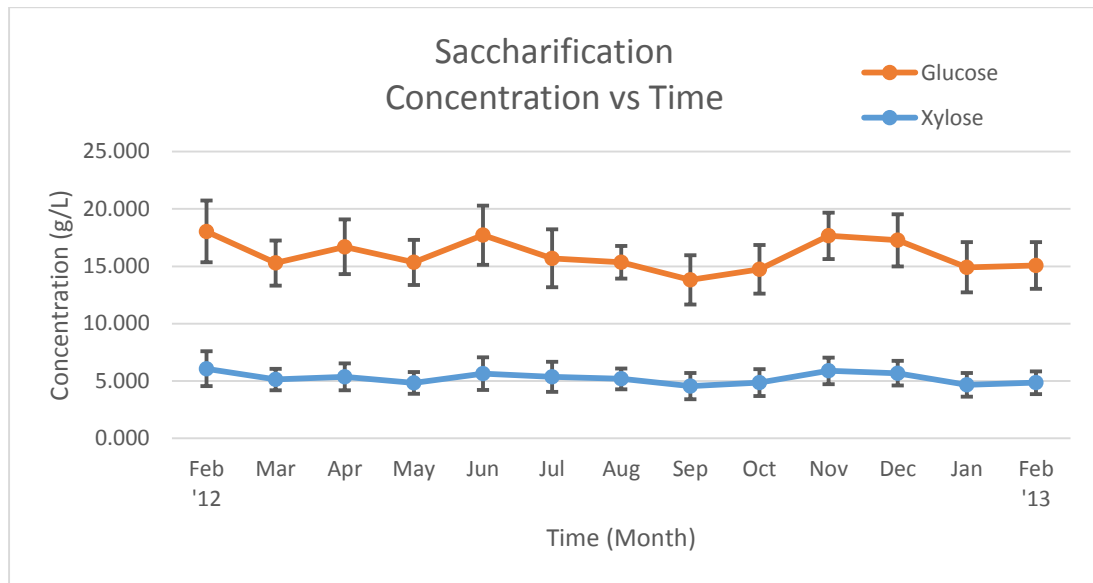


Figure 3.7. Monosaccharide concentration (g/L) versus time for saccharification study.

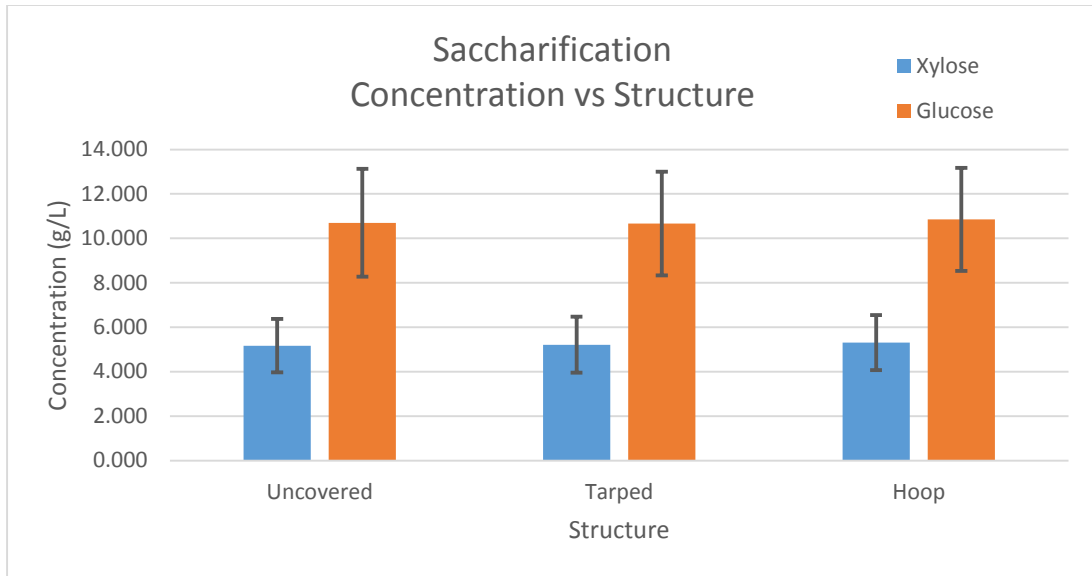


Figure 3.8. Monosaccharide concentration versus structure for saccharification study.

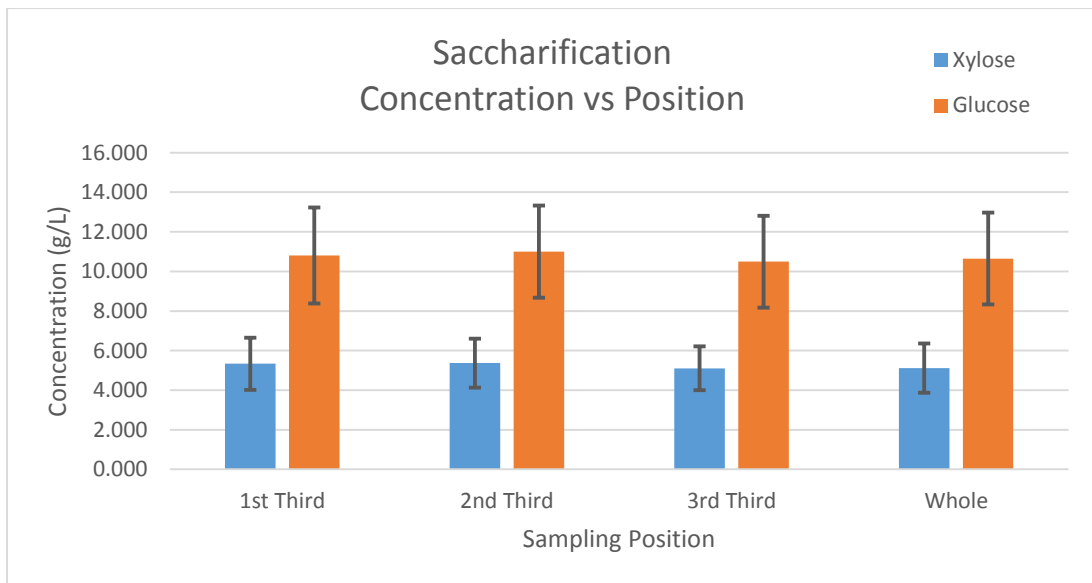


Figure 3.9. Monosaccharide concentration versus sampling position for saccharification study.

3.5 Data Discussion

Separation and detection of the fermentable sugars, xylose and glucose, from one another within the saccharified switchgrass samples were easily performed. Overall, standard calibration curves showed the precision and accuracy UPLC offers when compared to other methods of sugar analysis. Using generated calibration curves similar to **Figure 3.3** and **Figure 3.4** a series of saccharification samples were analyzed. Based on the results shown in Section 3.2.6 a few conclusions can be drawn from this experiment.

Glucose and xylose were successfully separated from any residual matrix and quantitation was made possible. Algae and yeast subsequently produce bioethanol or biodiesels from glucose most readily. Xylose can be converted to glucose using xylose (glucose) isomerase or traveling through the pentose phosphate pathway, making the sugar useful but not ideal³¹. Minimal biomass degradation occurred regardless of the storage condition, which, in turn, meant minimal loss in sugar concentration occurred as a function of time, storage, or sample position. This is evident by the time, structure, and sampling graphs that were compiled. Standard deviations and confidence intervals of all figures for this sample study are slightly higher than anticipated, but this is believed to be due to the scale and nature of samples analyzed. Typically, agricultural samples such as switchgrass tend to have great variance and weather conditions, location, sun exposure, and other factors could lead to the standard deviations observed. Despite this, no significant changes in sugar concentration; for a one year period under any storage method, even with slightly elevated standard deviations; were observed. Factors, which

led to this increase in standard deviation, were precipitation and humidity during analysis, as well as climate differences between months. This was during not only storage, but also when switchgrass was growing before harvest. Based on the low standard deviation of the standard curves, overall high R^2 values for all calibration curves, and the resolution of the peaks in both the standards and samples; it can be inferred that high standard deviation arise from the samples themselves and not the instrument.

The main goal of this study was to determine if the improved storage facilities were needed to maintain switchgrass over the course of one year, which is the typical amount of time a commercial company would store switchgrass before growing new crops. Based upon the figures produced from this study, samples taken as a composite for the entire year, there is virtually no difference in xylose and glucose concentrations produced whether the bales are housed in hooped structures, or outside either with tarps and completely uncovered. The purpose of testing different sampling position of the bales was to determine if the outer portion, which was more exposed to moistures and other weather conditions, were more susceptible to degradation than the inner portions, which were naturally better protected. Based on **Figure 3.9**, this is shown not to be a major determining factor.

3.6 Saccharification Study Conclusion

The data presented are very important for making biomass conversion into biofuel as an alternative fuel source economically viable because it means essentially no

additional storage costs for the biomass. If biomass is to compete with fossil fuel for energy production, it needs to be as cost effective as possible. Although the methods of saccharification or sugar source can be interchanged, there is not an appreciable amount of degradation between a built hoop structure and leaving samples in an uncovered gravel lot. As with any kind of experiment, limitations and unforeseen factors occur, the biggest of which would be storage climate. All bales were stored on ECU's farm in Richmond, KY for the duration of the study where climates are moderate, winters on average are not severe and summers tend not to be overly dry. Other geographical locations where weather is much more severe may affect the storage conditions. This study also only focused on switchgrass, which is local to this part of the globe, but other biomass sources may have not produced the same results.

CHAPTER 4

BIOMASS THERMAL ENERGY ASSESSMENT

4.1 Introduction

More forms of energy can be produced from biomass other than those from carbohydrate sources. This energy is primarily manifested as thermal energy by either direct combustion for warmth in residential environments, or in a boiler system to move steam turbines to produce electricity. With respect to alternative energy, the latter is of more concern to us than the former. This chapter describes the method of analysis for the determination of thermal energy in switchgrass samples as a possible alternative to fossil fuel sources. Bomb calorimetry was used to determine thermal energy production. Theory pertaining to this technique is described in Section 2.2.2. This study was conducted in tandem with the saccharification study described in the previous chapter, and as such was also used as a confirmatory analysis to determine if degradation of thermal energy occurred in biomass samples held in different storage conditions over one year. In addition to this, a quantification of usable energy produced from the combustion of switchgrass samples available was also necessary to determine its viability with other biomass sources. These assessments further prove the practicality of switchgrass as an alternative fuel source to be used in the ever-demanding energy market.

4.2.1 Sample Preparation

Samples were prepared in the same manner as Section 3.2.1. Only composite samples were prepared for this study for the sake of time, thus reducing total trials run to 108. Monthly and structural samples were investigated to confirm primary objectives of the original study. Once the samples were processed through the Wiley mill with 2 mm screens they were not subjected to pretreatment or saccharification processes. These procedures were excluded to ensure raw biomass would be used in the thermal energy assessment. Samples were contained in glass jars at room temperature until calorimetric procedures were performed.

4.2.2 Standard Preparation

The standard used for this experiment was benzoic acid, $C_7H_6O_2$, obtained from Sigma-Aldrich (St. Louis, MO, USA). Its structure was shown in **Figure 4.1**. This particular standard was not used for the generation of a calibration curve. Rather benzoic acid was used as a means to determine the $C_{\text{calorimeter}}$. This was accomplished using Equation 2.3 and solving for $C_{\text{calorimeter}}$, using -771271.511 (cal/g) as the value for $\Delta U_{\text{combustion}}$. Three benzoic acid trials were ran during the course of the experiments, and an average of $C_{\text{calorimeter}}$ was used in sample calculations.

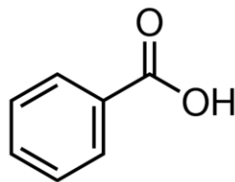


Figure 4.1. Structure of benzoic acid.

Note: Image retrieved from Sigma-Aldrich.com

4.2.3 Instrumentation

Instrument chosen for this analysis was the Parr 1341 Plain Jacket Bomb Calorimeter (Parr Instrument Company, Moline, IL). A picture of the instrument is provided in **Figure 4.2**. This included a main jacket container (center back), an inner water bath (2nd left), a bomb vessel and a metal screw cap, jacket top with mechanical stirrer (left most), inner water bath (2nd left), main jacket (center back), bomb screw lid (center front), bomb container (center right), digital thermometer (2nd right most), and ignition switch (right most). Sample holder and ignition wire not shown. The thermometer was the Parr Model 6775 Digital Thermometer, and Parr provided ignition wire as well.



Figure 4.2. Parr 1341 Plain Jacket Bomb Calorimeter.

4.2.4 Experimental Procedure

Samples were weighed (either 0.500 g or 1.000 g) and placed into calorimetry sample holder. Smaller sample weights were chosen if the total samples provided contained less than 2 grams of material. Approximately 10 cm of ignition wire was used for each trial. Ignition wire was placed approximately 1 mm from the actual sample. Deionized water (1 mL) was pipetted into the bottom of the bomb to absorb nitrogen oxides may be formed during combustion. Once the bomb head was assembled, it was placed in the bomb, which making sure the rubber seal was intact to avoid unwanted explosions. The container was sealed using the screw top metal lid and the gas valve was firmly closed. Oxygen was added to the sealed chamber via an oxygen tank until an internal pressure of 20-25 atm was reached. Backpressure of the oxygen transfer apparatus was relieved using a valve on the oxygen tank. From here, the prepared bomb

was set in the empty water bath container, the positive and negative electrodes were attached to their respective inlets on the charged calorimeter. The empty water bath with the charged bomb was placed in the outermost jacket of the instrument. Volumetric flasks were used to fill the water bath container with deionized water (2 L) after the charged bomb was added to ensure accurate volume. The cover to the jacket was placed on the top, to ensure both the thermometer and mechanical stirrer were not obstructed. The temperature was allowed to equilibrate for five minutes via stirrer and the initial temperature was recorded. The bomb was ignited next and the temperature changes were observed until the highest temperature change occurred. All electrical connections were turned off, the mechanical stirrer was stopped, and the instrument was disassembled. The spent bomb was placed in a hood and the vent valve was slowly opened and allowed to expel gas until the pressure subsided. Water was poured down the drain. The bomb was disassembled and cleaned thoroughly between each trial. Calculations were done based off change in temperature. Benzoic standard was run periodically to ensure instrumental stability.

4.3 Standard Results

Three benzoic acid standards were run during the course of these studies. Typically, standards were run at one to two week intervals to ensure instrumental reliability. Values for $C_{\text{calorimeter}}$ of the three benzoic acid standards are shown in **Table 4.1**. The average $C_{\text{calorimeter}}$ of the benzoic acid standards, 532.32 Cal/g (± 194.18 at 95% CI),

was used in all calculations for samples. Sample calculations for determination of $C_{calorimeter}$ are shown in Equations 4.1 through 4.3. No values were eliminated via Grubb's test.

$$\frac{m_s}{M_s} \Delta U_{combustion} + \frac{m_{H_2O}}{M_{H_2O}} \times C_{p,m}(H_2O) \times \Delta T + C_{calorimeter} \times \Delta T = 0 \quad \text{Equation 4.1}$$

$$C_{calorimeter} = \frac{-\left[\frac{m_s}{M_s} \Delta U_{combustion} + \frac{m_{H_2O}}{M_{H_2O}} C_{p,m}(H_2O) \Delta T\right]}{\Delta T} \quad \text{Equation 4.2}$$

$$C_{calorimeter} = \frac{-\left[\frac{1.088 \text{ g}}{122.12 \text{ g mol}^{-1}} \times -771271.511 \text{ Cal mol}^{-1} + \frac{2000 \text{ g}}{18.02 \text{ g mol}^{-1}} \times 17.995 \text{ Cal mol}^{-1} \text{ K}^{-1} \times 2.625 \text{ K}\right]}{2.625 \text{ K}} = 620.48 \frac{\text{Cal}}{\text{g}} \quad \text{Equation 4.3}$$

Table 4.1. Benzoic acid standard raw and corrected values.

Sample	$C_{calorimeter}$ (Cal/g)	Average (Cal/g)	532.32
<i>Benzoic Acid Standard 1</i>	620.48	Std Dev (Cal/g)	78.15
<i>Benzoic Acid Standard 2</i>	471.52	RSD (%)	14.68
<i>Benzoic Acid Standard 4</i>	504.97	95% CI (Cal/g)	194.18

4.4 Sample Results

A total of 108 samples were run and temperature changes recorded (data not shown). Sample calculations for thermal energy produced during calorimetric procedure are shown in Equations 4.4 through 4.6. Combustion values were then converted to BTU/lb. using Equation 4.7. Any samples inconsistent within triplicate trials were rerun. This phenomenon was usually caused by saturating the chamber too quickly with oxygen, which led to the sample leaving the holder, not combusting. Once compiled and organized, averages, standard deviations, relative standard deviations, and 95%

confidence intervals (CI) were calculated based on month number and storage structure. As mentioned above, the sample position parameters were not the focus of either project and after determining sample position was irrelevant, only composite samples were ran. Grubb's test as well as Student's T-test were ran to determine outliers and CI respectively. No values were deemed outliers. Each sample was ran in triplicate, thus creating 9 total samples for monthly values and 36 for structure values (3 structures times 12 months).

Table 4.2 and **Table 4.3** summarize the data for this experiment.

$$m_s \Delta U_{combustion} + \frac{m_{H_2O}}{M_{H_2O}} C_{p,m}(H_2O) \Delta T + C_{calorimeter} \Delta T = 0 \quad \text{Equation 4.4}$$

$$\Delta U_{combustion} = \frac{-\left[\frac{m_{H_2O}}{M_{H_2O}} C_{p,m}(H_2O) \Delta T + C_{calorimeter} \Delta T\right]}{m_s} \quad \text{Equation 4.5}$$

$$\Delta U_{combustion} = \frac{-\left[\frac{2000 \text{ g}}{18.02 \text{ g mol}^{-1}} \times 17.995 \text{ Cal mol}^{-1} \text{ K}^{-1} \times 1.648 \text{ K} + 532.32 \text{ Cal K}^{-1} \times 1.648 \text{ K}\right]}{1.0497 \text{ g}} = -3971.32 \frac{\text{Cal}}{\text{g}} \quad \text{Equation 4.6}$$

$$\frac{-3971.32 \text{ Cal}}{1 \text{ g}} \times \frac{1 \text{ BTU}}{252.164 \text{ Cal}} \times \frac{453.592}{1 \text{ lb.}} = -71432.71 \frac{\text{BTU}}{\text{lb.}} \quad \text{Equation 4.7}$$

Table 4.2. Thermal energy values (in British Thermal Units per pound) for switchgrass samples monthly statistics.

<i>Month</i>	<i>N</i>	<i>BTU/lb. Average</i>	<i>BTU/lb. Std Dev</i>	<i>BTU/lb. RSD</i>	<i>95% CI</i>
<i>Feb'12</i>	9	7738.0	313.0	4.0	240.0
<i>Mar</i>	9	7642.0	522.0	6.8	402.0
<i>Apr</i>	9	7501.0	418.0	5.6	322.0
<i>May</i>	9	7527.0	390.0	5.2	300.0
<i>Jun</i>	9	7561.4	227.1	3.0	174.6
<i>Jul</i>	9	7313.0	361.0	4.9	278.0
<i>Aug</i>	9	7722.0	312.0	4.0	240.0
<i>Sep</i>	9	7403.9	129.3	1.7	093.4
<i>Oct</i>	9	7670.0	364.0	4.7	280.0
<i>Nov</i>	9	7361.9	185.7	2.5	142.7
<i>Dec</i>	9	7429.6	248.4	3.3	190.9
<i>Jan '13</i>	9	7459.0	519.0	7.0	399.0

Table 4.3. Thermal energy values (in British Thermal Units per pound) for switchgrass samples structure statistics with total for all samples.

<i>Structure</i>	<i>N</i>	<i>BTU/lb. Average</i>	<i>BTU/lb. Std Dev</i>	<i>BTU/lb. RSD</i>	<i>95% CI</i>
<i>Uncovered</i>	36	7592.1	337.6	4.4	114.2
<i>Tarped</i>	36	7498.3	419.9	4.4	142.1
<i>Hoop</i>	36	7491.9	317.6	4.2	170.4
Total	108	7527.4	360.7	4.8	68.8

Based on these values sets, graphical representations were produced to better visualize whether degradation had occurred in samples and to confirm the conclusions drawn from the saccharification study. Error bars on both figures represent standard deviations calculated based on Equation 3.7. **Figure 4.3** represents thermal energy produced as a function of time for untreated switchgrass samples. **Figure 4.4** represents thermal energy produced as a function of structure for untreated switchgrass samples.

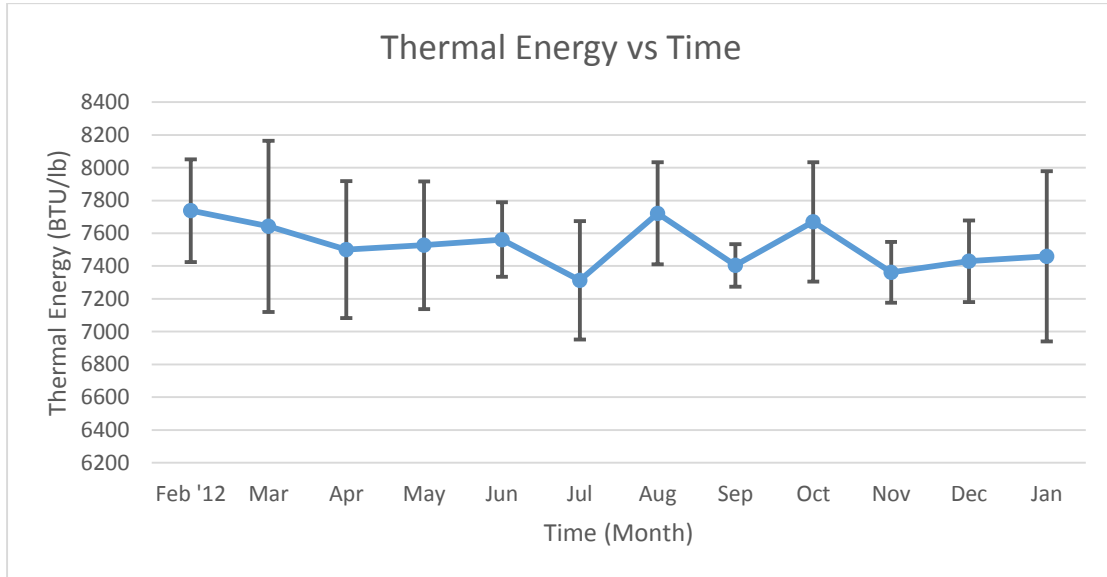


Figure 4.3. Thermal energy (in BTU/lb) produced by untreated switchgrass over 12 months.

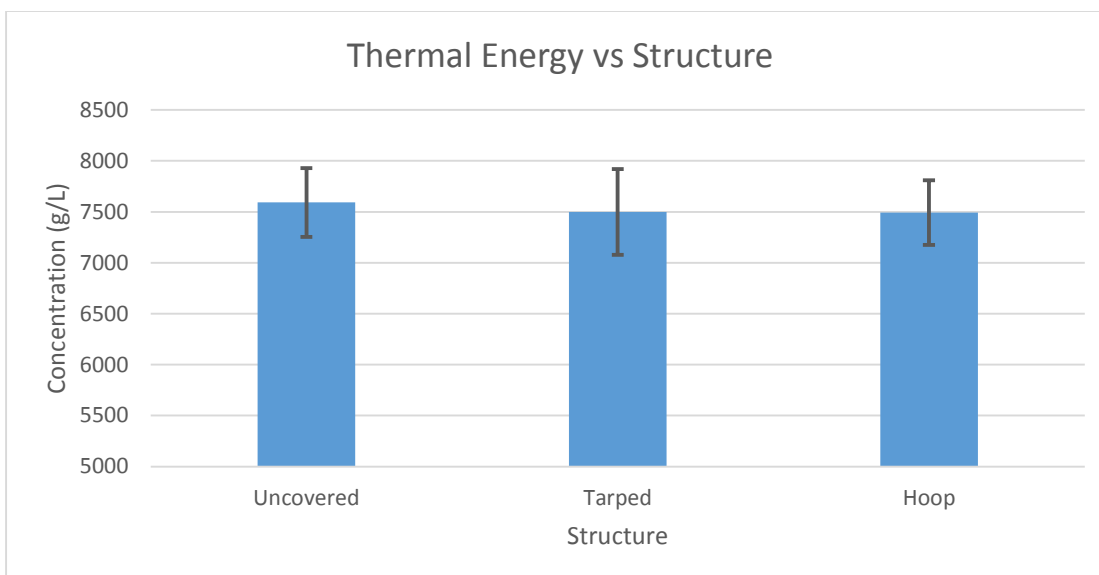


Figure 4.4. Thermal energy (in BTU/lb.) produced by untreated switchgrass of three different storage structures.

4.5 Data Discussion

Values produced from this project were very similar to saccharification studies into the degradation of switchgrass storage conditions and storage time for the use for biofuels. Based on standard deviations and 95% confidence intervals a clear lack of degradation occurred in the samples with respect to thermal energy produced. This project was primarily used as a confirmatory study of the original saccharification project. Overall, the method of analysis using calorimetric procedures was effective for our purposes. Originally, a previous student researcher had run some samples, but because of instrumental misfire, all 108 samples were rerun to ensure the data were consistent. There was virtually no sample preparation other than the Wiley milling processing from my perspective. It appeared that some samples were more grounded than others were. This may have affected thermal energy values slightly, but not significantly. The thermal

values produced during this project were consistent with literature values for switchgrass and other perennial grasses.

Based on observed BTU/lb. values, switchgrass used for this analysis was slightly lower than literature values. Based on multiple sources, the range of switchgrass heating values were between 7766 and 8555 BTU/lb.^{87,88,89} and the total average heating value for samples was 7527.4 BTU/lb. The lower of the values was not a significant amount, less than 10% of the average of the literature values. There may have been a number of different factors, which could have caused this lower value, most of which were unlikely to be on the analysis perspective. Switchgrass is a feedstock crop and as such is affected greatly by annual rainfall, fertilizers used, weather conditions in general, and several other unavoidable geographical factors. Compared to other grass heating values⁹⁰, switchgrass was relatively consistent and so no major concern about the decreased heating values should be inferred from this data.

4.6 Thermal Energy Assessment Conclusion

Overall, multiple conclusions can be drawn from the data collected during these experiments. Firstly, no significant degradation occurred in biomass under minimal (uncovered in a well-drained gravel lot) conditions for a time of one year. Secondly, thermal energy produced by raw, untreated, unpacked biomass is only slightly lower than previous literature values and still applicable for commercial use. Finally, a realistic business model for the use of switchgrass based biofuel and thermal energy generation

is more than possible with a storage time of one year with little cost to storage and maintenance.

Although thermal energy yield may not be optimal, use as an alternative energy source to fossil fuels is still possible. Both studies showed the application of switchgrass as a second generation biomass for the use of energy production. Either depending on type of energy needed fermentation processes or direct combustion are viable options. For commercial use of untreated biomass however, an alternative sample production may be needed. If switchgrass could be grown, harvested, milled, and compressed into easily manageable pellets to be used in either a boiler system or residential heating stoves, then storage and direct usage may be easier.

CHAPTER 5

LIGNIN DISSOCIATION USING IONIC LIQUIDS

5.1 Introduction

As mentioned in Chapter 1, the pretreatment phase of biomass conversion to biofuel is arguably the most important stage. The effectiveness of the separation of lignin from hemicellulose and cellulose is what ultimately determines how high sugar yield can be. Although studies into the glucose yields based on total cellulose content was not addressed during these projects, strive toward 100% conversion is always the main goal of the experimental process. The pretreatment method used for samples in Chapter 3 are describe in Section 3.2.1. Dilute base catalyzed dissociation of biomass is one of the original pretreatment options. A relatively new pretreatment option is the use of ionic liquids (IL) to dissolve aromatic monomers of lignin in biomass. These room temperature, molten salts are usually comprised of either an aromatic cation or anion and an inorganic counter ion. The aromatic nature of the IL are what make lignin dissolution possible. The following study is a preliminary project, which investigates the use of these IL, and potential characterization using both microscopic and mass spectrometric methods.

5.2 Instrumentation

Two major instruments were used during the development of this project. The first was a Leica DM EP Polarized Microscope (Leica Microsystems Inc., Buffalo NY, USA). A magnification of 40x was used to see visually lignin extract dissolve in small amounts of IL. Second instrument used was the Thermo Scientific LTQ XL Mass Spectrometer (Thermo Scientific, Fair Lawn, NJ, USA) with a Direct Analysis in Real Time (DART) SVP ion source (Ion Sense, Saugus, MA). These apparatuses are shown in **Figure 5.1** and **Figure 5.2** respectively. In addition, both a cartoon illustration⁹¹ as well as an actual close-up of the DART ion source are shown in **Figure 5.3**. Once lignin extracts had fully dissolved, characterization was attempted using the ambient pressure DART ion source at different temperatures and ion selection modes. The rationale for using these particular instruments is both qualitative and quantitative in nature. The microscopic portion of this project was to determine the best IL candidate based on dissolution on both short-term (30 minutes) and long-term (24 hours) timescales. Once dissolution was achieved, if it was achieved, attempted characterizations based on mass to charge (m/z) ratios of the mass spectra produced were used to attempt to distinguish the dissolution patterns of the lignin-IL interactions.



Figure 5.1. Leica DM EP Polarized Light Microscoped used to visually observe lignin-IL interactions.



Figure 5.2. Thermo Scientific LTQ XL with DART ion source used to characterize lignin-IL interactions.

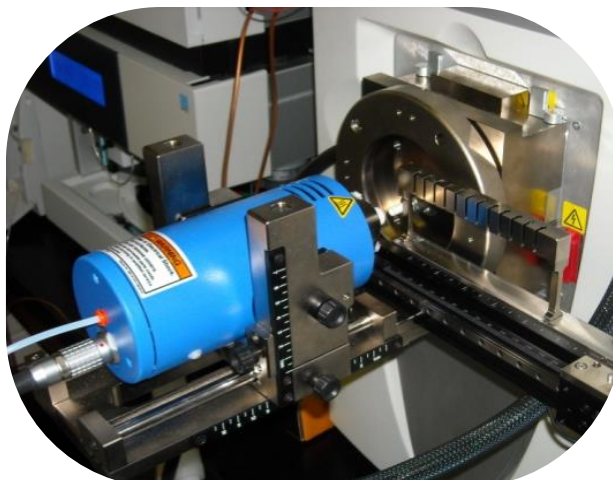
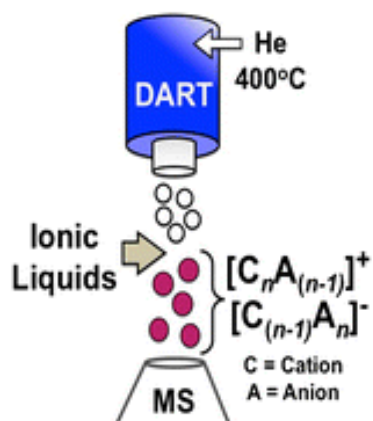


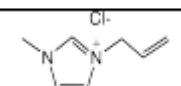
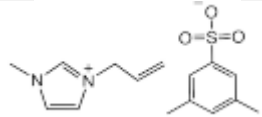
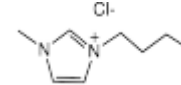
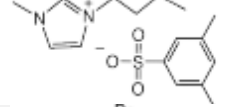
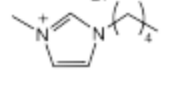
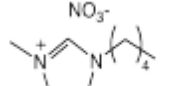
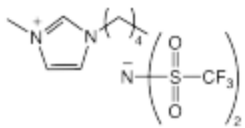
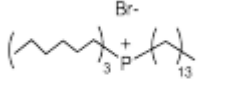
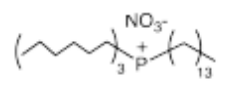
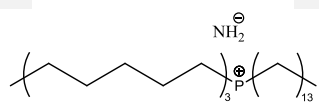
Figure 5.3. Cartoon illustration⁹¹ (left) and photo close-up of DART ion source used (right).

5.3 Experimental Procedure

Ten different ionic liquids were available for analysis.

Table 5.1 shows the chemical formulas, names and structures of all IL used. Samples were also investigated to determine how different extraction conditions or switchgrass samples affect dissolution. Low lignin concentrations in whole biomass samples made initial method development and monomer characterizations difficult. As such, the primary sample for this project was a lignin extract from switchgrass samples, extracted using formic acid at 50 °C.

Table 5.1. Chemical formulas, names, and structures of ionic liquids used in lignin dissolution project.

Chemical Formula	Chemical Name	Structure
[AMIM][Cl]	1-Allyl-3-methylimidazolium chloride	
[AMIM][XS]	1-Allyl-3-methylimidazolium xylene sulfonate	
[BMIM][Cl]	1-Butyl-3-methylimidazolium chloride	
[BMIM][XS]	1-Butyl-3-methylimidazolium xylene sulfonate	
[PMIM][Br]	1-Pentyl-3-methylimidazolium Bromide	
[PMIM][NO ₃]	1-Pentyl-3-methylimidazolium Nitrate	
[PMIM][NTf ₂]	1-Pentyl-3-methylimidazolium bis(trifluoromethylsulfonyl)imide	
[THTDP][Br]	Trihexyltetradecylphosphonium Bromide	
[THTDP][NO ₃]	Trihexyltetradecylphosphonium Nitrate	
[THTDP][NH ₂]	Trihexyltetradecylphosphonium Amide	

Note: Images taken from Mazzotta, M.; Pace, R.; Wallgren, B.; Morton, S.; Miller, K.; Smith, D., Direct Analysis in Real Time Mass Spectrometry (DART-MS) of Ionic Liquids. *J. Am. Soc. Mass Spectrom* **2013**, 24 (10), 1616-1619.

5.3.1 Microscopic Analysis of Lignin Extract Dissolution

A glass slide was tarred on an analytical balance. Lignin extract was added, and the mass was recorded. Then, glass slides and lignin were tarred again, ionic liquid was added, and then the mass was recorded again. The main reason for this is the viscosity of IL; delivering a consistent volume was almost impossible, but by taking mass measurements, volume could be calculated based on density. Immediately after IL contact with lignin, samples were put under the Leica polarized microscope. To record data, pictures with a mobile phone (8 Mega pixel auto focus camera) were taken at five minute intervals for 30 minutes. Visual data were obtained for all combinations of samples and IL. For qualitative comparison, the $t = 0$ minutes and $t = 30$ minutes were used to assess the effectiveness of lignin-IL interactions. Once completed, samples were stored in 1.5 mL plastic conical vials for a time of 24 hours before introduction into DART-MS. Some samples showed no dissolution at $t = 30$ minutes, but after $t = 24$ hours some or all lignin appeared to be dissolved. For these samples, pictures were also taken of the vial. Typically, the color of pure IL was a light yellow to light tan color, but after successful dissolution of lignin, color changed to dark brown or black.

5.3.2 DART-MS Analysis of Dissolved Lignin in Ionic Liquids

Dissolved samples in IL were introduced into DART inlet via glass Dip-IT tips. DART gas temperature was determined to be most efficient at 400 °C. Samples were ran in both positive and negative ion mode, but positive mode appeared to given the best results.

Many peaks were produced during this time. A previous study had already investigated the MS peaks arising from IL samples in the DART-MS⁹¹. LTQ Tune was the software used to control the mass spectrometer, Xcalibur was used to view and manipulated the spectra produced, and finally the SVP software was used to control the DART ion source. Peaks produced during this project were compared to those of just ionic liquids themselves to differentiate between solvated m/z peaks and un-solvated m/z peaks. From here, investigations in reoccurring losses between solvated peaks were found.

5.4 Preliminary Results

Results for this project were divided into two major categories: microscopic pictures of lignin-IL interactions and mass spectra. Each IL's capacity to dissolve lignin extract was divided into characterized into 4 categories: noticeable dissolution at t = 30 minutes, noticeable dissolution at t = 24 hours, partial dissolution at t = 24 hours, or no dissolution at all. The lignin extract used for this categorization was formic acid extraction at 50 °C. Categories for IL dissolution capacity are shown in

Table 5.2, and example photographs of [BMIM][Cl] with lignin extract showing the dissolution progression are shown in **Figure 5.4**. Only [AMIM][Cl] and [BMIM][Cl] were found to have noticeable dissolution at t = 30 min, and as such are the only combinations yielding photographable dissolution. Ionic Liquids under the category of t = 24 hr showed some microscopic observable dissolution, but under higher magnification (100x). Those

with no dissolution were considered poor solvent choices for lignin, and as such, no further studies were investigated. Ionic liquids with any kind of dissolution would be introduced into the DART-MS instrument for analysis.

Table 5.2. Categorization of each IL's capacity to dissolve lignin extract.

<i>Ionic Liquid</i>	<i>Dissolution Category</i>
[AMIM][Cl]	Dissolution at t = 30 min
[AMIM][XS]	Dissolution at t = 24 hr
[BMIM][Cl]	Dissolution at t = 30 min
[BMIM][XS]	Dissolution at t = 24 hr
[PMIM][Br]	Dissolution at t = 24 hr
[PMIM][NO ₃]	Dissolution at t = 24 hr
[PMIM][NTf ₂]	No Dissolution
[THTDP][Br]	Partial Dissolution at t = 24 hr
[THTDP][NO ₃]	Partial Dissolution at t = 24 hr
[THTDP][NTf ₂]	No Dissolution

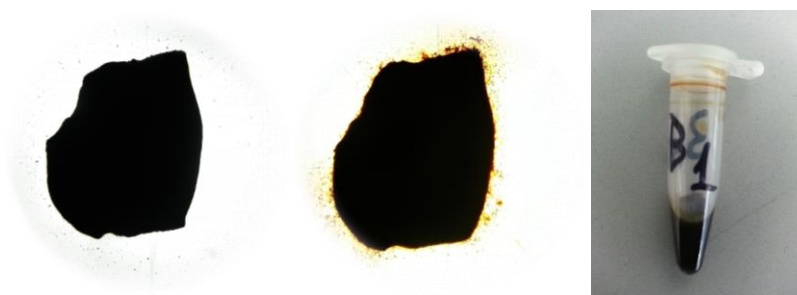


Figure 5.4. Dissolution of lignin extract in [BMIM][Cl] at t = 0 min (left), t = 30 min (middle), and t = 24 hr.

Once spectra were obtained, un-solvated peaks were identified and marked according to a previous study⁹¹ as well as unknown peaks assumed to be solvated peaks. To ensure these peaks were not mistakenly identified background peaks the MS continued to scan for ions for approximately 30 seconds to one minute after sample

introduction, and background ions were subtracted from sampling sections. The samples themselves were introduced over the course of approximately one minute and an average of the individual scans were taken for consistency. From these identified solvated peaks, reoccurring 148, 174, and 198 m/z losses were observed. An example spectrum of [BMIM][Cl] lignin interaction is shown in

Figure 5.5 with the maroon stars representing known IL peaks and the black hexagons representing the unknown solvated peaks. Other mass spectra for [AMIM][Cl], [AMIM][XS], [BMIM][XS], [PMIM][Br], [PMIM][NO₃], [THTDP][Br], and [THTDP][NO₃] interactions with lignin extract are shown in **Appendix B**.

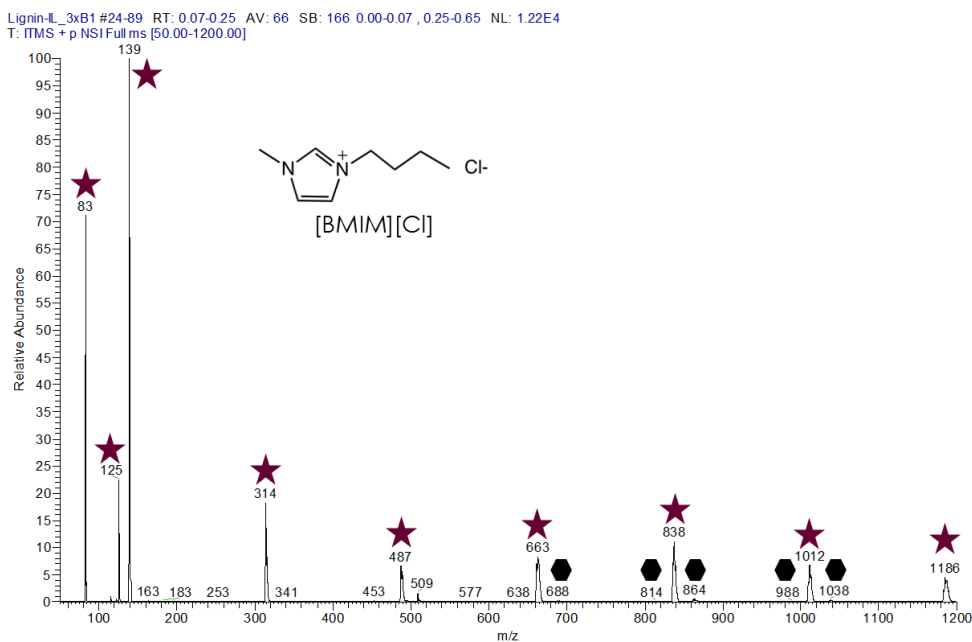


Figure 5.5. DART positive (+) ion mode spectrum with lignin extract (FA 50 °C) after dissolution with [BMIM][Cl].

5.5 Project Discussion

Overall, this project was genuinely interesting and had promise for understanding lignin dissolution in ionic liquids. There were a few reasons why progress in this project has halted. The cost of the ionic liquids are relatively high and, if continued, this work would have not been covered by a research grant, thus making funding a major issue. The relative volumes used for each analysis was less than one milliliter, but if continual testing was needed in order to perform tandem (MS-MS) studies volume used would start to accumulate. In addition, there was not a genuine concern for the continuations of this project, as our agricultural collaborator, Dr. Bruce Pratt, had written a grant to determine the degradation extent in switchgrass samples. Most of this project was run in the downtime of the automated LC protocol described in Chapter 3. The final factor, which lead to a standstill in this research, was difficulty deriving lignin monomers or dissolution patterns of solvated peaks. Specifically, ILs tend to form solvent clusters in solution and appear, as such, in spectra. This makes the distinct characterization of monomers of lignin difficult. Therefore, a very high mass accuracy MS system would be needed in order to derive lignin monomer identities. In addition to this, the amorphous nature of lignin also makes consistent characterization more difficult than in a more patterned polymer.

Despite setbacks, this project could still very easily be brought back to life. Lignin-IL samples have not been discarded at the time of writing (April 8th 2015) and can readily be used for MS sampling. Unfortunately, the hard drive of computer housing microscopic photographs of the dissolution process had corrupted and as such, all pictures but the

ones shown in **Figure 5.4** were lost. Pictures were also on the mobile phone originally was used to take the photographs, but the motherboard on the phone was also corrupted.

5.6 Future Directions for Lignin Study using Microscopy and DART-MS Methods

Due to the lack of photographs, the first order of business would be to retake all of the interactions between lignin and ionic liquids. At first, pictures were taken at 5 minutes intervals with the thought dissolution would occur rapidly. It became evident even the best IL, [AMIM][Cl] and [BMIM][Cl], do not kinetically solvate pure lignin in this period. As such, if new photographs were to be taken, it would be better to take them at longer intervals, potentially 30 minute intervals, to see a more dramatic effect. Once that would be complete, a higher magnification would yield more qualitative information. Our agricultural collaborator had access to a Scanning Electron Microscope (SEM) and the increased resolving power of the SEM would give even information about how lignin dissolves. This would likely be the practical extent of the microscopy aspect of this project.

From the MS aspect, many more areas of research can be investigated to help illuminate the solvation pattern and monomer identities of lignin once in solution. The first would be applying the same method used in Section 5.3.2 to all spectra collected using highest possible mass calculations to determine the exact mass of these reoccurring losses. Once successful, a set of tandem experiments at varying fragmentation energies, and potentially different fragmentation mechanisms, could be implemented in the hope to produce fragments of pure lignin monomers. This can be taken one step further and

another fragmentation can be used (MS^3) to confirm monomer structure. The main problem with MS^3 of these sample sets would be concentration of a particular monomer. For these types of experiment an ion-trap based MS (like the LTQ XL) would be ideal because multiple fragmentation stages can occur without the need for additional mass analyzers (compared to a triple quadrupole system).

CHAPTER 6

CONCLUSIONS AND FUTURE DIRECTIONS

6.1 Introduction

In the past few decades, there has been an increase in the need and desire for alternative fuel research. As natural fossil fuel sources began to show signs of depletion, it is clear energy derived from these sources would not be infinite or even in high enough quantities to power our civilization for the next two centuries. In addition to this, society began to observe increased health and environmental risks for using this type of fuel. A combination of both factors has led to many different avenues of alternative fuel research. Biofuel has become arguably the most important because of its ability to be introduced into current transportation sectors.

By creating a less toxic, renewable energy source to be readily implemented into transportation vehicles, the transition will be overall cheaper and easier on a global scale. This ideal has directed the genesis of first generation biofuels. These were bioethanol and biodiesel sources coming from food crops already being produced. The concern for using food sources as fuel and the continual need for improvement led to second generation biofuels. These are similar to first generation, but are derived from non-food sources (like switchgrass). Through continuing improvements and innovations, a third generation of

biofuels from biomass has arisen. These newest biomass sources are created from microalgae. They offer an even more applicable business model for biofuel production.

As with any research, the applicability of the work is what eventually determines its significance. As such, an investigation into the degradation of switchgrass was needed to determine housing conditions and to help access economic costs. Through the projects presented in this body of work, we have shown only minimal to no housing conditions are needed for this particular sample to produce adequate carbohydrates to be used for fermentation to create biofuels as well as a thermal energy assessment for direct energy applications.

6.2 Saccharification Study Conclusions

Overall, these projects show the reliability and uses of both Ultrahigh Performance Liquid Chromatography and Oxygen Bomb Calorimetry for the assessment of biofuel intermediates and thermal energy production. The saccharification project was the first completed and it was clear no degradation had occurred during the yearlong experiment regardless of housing conditions or sampling positions. The conclusions of both studies were validated by both the instrument consistency and the accuracy of the standards. Although some sample had to be rerun and even still, some of those sample values had to be discarded due to Grubb's test, sheer sample size, standard deviations, and confidence intervals are evidence enough degradation did not occur. The agricultural nature of the samples is what led to the increased relative standard deviations. Even so,

the average RSD across all samples was 23.6 and 22.0 % for xylose and glucose respectively. The slightly higher RSD and overall lower concentrations of xylose compared to glucose are within reason. This can be attributed to xylose being the main component of hemicellulose, which is an amorphous mixture of different monosaccharaides. Whereas glucose is derived from cellulose, a structured polymer of repeating glucose monomers. The averages and confidence intervals between different storage structures and sampling positions were almost identical and therefore statistically indifferent.

6.3 Calorimetric Study Conclusions

Although this information would have been sufficient to say confidently no degradation occurs and storing switchgrass in an uncovered lot is a viable option, a thermal energy assessment was employed to act as a confirmatory test for the previous project. As expected, the values produced were similar. The experimental procedure for the calorimetric study was much more time consuming than the automated LC study and as such the sample size was reduced to 108 from 936 by eliminating the sampling position from sample and reducing replicates to three from six. RSD for the entirety of the calorimetry samples was 4.8%, which is well within reliable tolerance. Overall the values were slightly lower than expected but only minimally (less than 10%).

Lower than expected values were not the only problem this project had, however. Originally, samples were supposed to be post-saccharification samples, so to further help assess the economic impact of using switchgrass for biofuel production. Ideally, after

switchgrass has been milled, pretreated, and saccharified the leftover, or residual, biomass could then be dried and compacted into heating pellets. These heating pellets could then be used in a boiler system, which in term would provide local energy for a continuation of the biofuel production. This would dramatically help reduce energy costs as well as waste disposal. Unfortunately, samples received from our agricultural collaborator were not residual, but instead untreated switchgrass.

In addition to this, during the experiments, more often than not, there were some kind of residual ash content of the biomass inside the calorimeter. This may explain decreased BTU/lb. values derived from that study, but for a true thermal value, complete combustion would need to occur. One of the major future directions of calorimetric studies would be investigations into why not all of the sample combusted. Furthermore, switchgrass, or any biomass, is complex mixtures of many different compounds, proteins, and other substances. Many of those are not made solely of hydrocarbons, and therefore gas produced by burning biomass is not completely carbon dioxide and water. For any kind of implementation into a residential environment, it would be necessary to determine the gas phase identity of compounds and their toxicities. This could easily be done using a Gas Chromatography system with appropriate sampling methods.

6.4 Lignin Dissociation Conclusions

Chapter 5's focus was over a project, which did not make enough traction or have enough interest to be continued at the time the biomass storage project was being

completed. This has led to a standstill in the research and with the corruption of the microscopy; photographs would make the revival of said project an uphill battle. Overall, of the three projects presented the lignin dissociation was by far the most interesting and most enjoyable. For accurate analysis, however, additional instrumentation would be needed. Mainly in the use of a Scanning Electron Microscope or other higher resolving power apparatus to attempt to see on a molecular level what is occurring. Ionic liquids offer the unique property of replenishment for pretreatment options. These compounds by nature have virtually no vapor pressure, and only under extreme conditions will go into gas phase. This would allow a business model where IL would be used in pretreatment, then proceed through some form of separation (likely an ion-exchange or other type of chromatography) to reuse them for future pretreatments. This would again greatly help reduce economic and environmental impacts of biomass conversion. Another caveat of this particular pretreatment is lignin-IL interactions are likely not destructive and the application for lignin as a biopolymer for commercial use is definitely appealing. In short, this project had (and still has) a great deal of potential, but additional funding and labor would be needed for successful research in this area.

6.5 Closing Remarks

This body of work presents not only the information provided and conclusions drawn from data acquired, but also the potential for a variety of future research. There is great security in this research because new and optimal energy production will also be a

great concern to any civilization. I am very glad I was able to do this research; I have learned a great deal during this process. This program, this research, and my experiences during my time here have given me great insight into the scientist I want to become. I have learned what parts of research I really enjoy and what parts I loathe; but the former is just as important as the latter.

LIST OF REFERENCES

1. Shafiee, S.; Topal, E., When will fossil fuel reserves be diminished? *Energy policy* **2009**, *37* (1), 181-189.
2. Bradshaw, M. J., Global energy dilemmas: a geographical perspective. *The Geographical Journal* **2010**, *176* (4), 275-290.
3. Outka, U., Siting renewable energy: Land use and regulatory context. *Ecology Law Quarterly* **2010**, *37*, 1041.
4. Wright, L. L.; Perkacj, R. D.; Turnhollow, A. F.; Eaton, L. M., Switchgrass Production in the USA. *IEA Bioenergy* **2011**, *43*, 1-18.
5. Kumar, P.; Barrett, D. M.; Delwiche, M. J.; Stroeve, P., Methods for pretreatment of lignocellulosic biomass for efficient hydrolysis and biofuel production. *Industrial & Engineering Chemistry Research* **2009**, *48* (8), 3713-3729.
6. U.S. Energy Information Administration. International Energy Statistics. <http://www.eia.gov/cfapps/ipdbproject/iedindex3.cfm?tid=44&pid=44&aid=2&cid=ww,&syid=2008&eyid=2012&unit=QBTU> (accessed Feb 15, 2015).
7. U.S. Energy Information Administration. Annual Energy Outlook 2014. [http://www.eia.gov/forecasts/aeo/pdf/0383\(2014\).pdf](http://www.eia.gov/forecasts/aeo/pdf/0383(2014).pdf) (accessed Feb 15, 2015).
8. Organisation for Economic Co-operation and Development (OECD). About the OECD. <http://www.oecd.org/about/> (accessed Feb 15, 2015).
9. Sperling, D.; Gordon, D., Two billion cars: driving toward sustainability. **2009**.
10. U.S. Department of Energy. How Fossil Fuels were Formed. http://www.fe.doe.gov/education/energylessons/coal/gen_howformed.html (accessed Feb 17, 2015).
11. U.S. Environmental Protection Agency. Causes of Climate Change. <http://www.epa.gov/climatechange/science/causes.html> (accessed Feb 15, 2015).
12. Hansen, J.; Kharecha, P.; Sato, M.; Masson-Delmotte, V.; Ackerman, F.; Beerling, D. J.; Hearty, P. J.; Hoegh-Guldberg, O.; Hsu, S.-L.; Parmesan, C., Assessing “dangerous climate change”: required reduction of carbon emissions to protect young people, future generations and nature. *PloS one* **2013**, *8* (12), e81648.
13. Williams, A.; Jones, J.; Ma, L.; Pourkashanian, M., Pollutants from the combustion of solid biomass fuels. *Progress in Energy and Combustion Science* **2012**, *38* (2), 113-137.
14. Kampa, M.; Castanas, E., Human health effects of air pollution. *Environmental pollution* **2008**, *151* (2), 362-367.
15. Lavric, E. D.; Konnov, A. A.; De Ruyck, J., Dioxin levels in wood combustion—a review. *Biomass and Bioenergy* **2004**, *26* (2), 115-145.
16. Lund, H., Renewable energy strategies for sustainable development. *Energy* **2007**, *32* (6), 912-919.
17. U.S. Environmental Protection Agency. Renewable Energy Production Incentives. <http://www.epa.gov/osw/hazard/wastemin/minimize/energyrec/rpsinc.htm> (accessed Feb 15, 2015).

18. Hill, J.; Nelson, E.; Tilman, D.; Polasky, S.; Tiffany, D., Environmental, economic, and energetic costs and benefits of biodiesel and ethanol biofuels. *Proceedings of the National Academy of Sciences* **2006**, *103* (30), 11206-11210.
19. Tennakone, K.; Kumara, G.; Kumarasinghe, A.; Wijayantha, K.; Sirimanne, P., A dye-sensitized nano-porous solid-state photovoltaic cell. *Semiconductor Science and Technology* **1995**, *10* (12), 1689.
20. Letcher, T. M., Future energy: improved, sustainable and clean options for our planet. **2008**.
21. U.S. Environmental Protection Agency. Biomass Combined Heat and Power Catalog of Technologies. http://www.epa.gov/chp/documents/biomass_chp_catalog.pdf (accessed Feb 15, 2015).
22. Lin, Y.; Tanaka, S., Ethanol fermentation from biomass resources: current state and prospects. *Applied microbiology and biotechnology* **2006**, *69* (6), 627-642.
23. Ragauskas, A. J.; Williams, C. K.; Davison, B. H.; Britovsek, G.; Cairney, J.; Eckert, C. A.; Frederick, W. J.; Hallett, J. P.; Leak, D. J.; Liotta, C. L., The path forward for biofuels and biomaterials. *science* **2006**, *311* (5760), 484-489.
24. Bai, F.; Anderson, W.; Moo-Young, M., Ethanol fermentation technologies from sugar and starch feedstocks. *Biotechnology advances* **2008**, *26* (1), 89-105.
25. Vanholme, R.; Morreel, K.; Ralph, J.; Boerjan, W., Lignin engineering. *Current opinion in plant biology* **2008**, *11* (3), 278-285.
26. Adler, E., Lignin chemistry—past, present and future. *Wood science and technology* **1977**, *11* (3), 169-218.
27. Huber, G. W.; Iborra, S.; Corma, A., Synthesis of transportation fuels from biomass: chemistry, catalysts, and engineering. *Chemical reviews* **2006**, *106* (9), 4044-4098.
28. Alonso, D. M.; Bond, J. Q.; Dumesic, J. A., Catalytic conversion of biomass to biofuels. *Green Chemistry* **2010**, *12* (9), 1493-1513.
29. Jørgensen, H.; Kristensen, J. B.; Felby, C., Enzymatic conversion of lignocellulose into fermentable sugars: challenges and opportunities. *Biofuels, Bioproducts and Biorefining* **2007**, *1* (2), 119-134.
30. Krahulec, S.; Petschacher, B.; Wallner, M.; Longus, K.; Klimacek, M.; Nidetzky, B., Fermentation of mixed glucose-xylose substrates by engineered strains of *Saccharomyces cerevisiae*: role of the coenzyme specificity of xylose reductase, and effect of glucose on xylose utilization. *Microbial cell factories* **2010**, *9* (1), 16.
31. Kuyper, M.; Hartog, M. M.; Toirkens, M. J.; Almering, M. J.; Winkler, A. A.; Dijken, J. P.; Pronk, J. T., Metabolic engineering of a xylose-isomerase-expressing *Saccharomyces cerevisiae* strain for rapid anaerobic xylose fermentation. *FEMS yeast research* **2005**, *5* (4-5), 399-409.
32. Ogden, C.; Ileleji, K.; Johnson, K.; Wang, Q., In-field direct combustion fuel property changes of switchgrass harvested from summer to fall. *Fuel Processing Technology* **2010**, *91* (3), 266-271.

33. U.S. Department of Agriculture. Switchgrass plant Fact Sheet. https://plants.usda.gov/factsheet/pdf/fs_pavi2.pdf (accessed Feb 15, 2015).
34. Agarwal, A. K., Biofuels (alcohols and biodiesel) applications as fuels for internal combustion engines. *Progress in Energy and Combustion Science* **2007**, *33*, 233-271.
35. Alvira, P.; Tomás-Pejó, E.; Ballesteros, M.; Negro, M., Pretreatment technologies for an efficient bioethanol production process based on enzymatic hydrolysis: a review. *Bioresource technology* **2010**, *101* (13), 4851-4861.
36. Bayer, E. A.; Chanzy, H.; Lamed, R.; Shoham, Y., Cellulose, cellulases and cellulosomes. *Current opinion in structural biology* **1998**, *8* (5), 548-557.
37. Amin, S., Review on biofuel oil and gas production processes from microalgae. *Energy Conversion and Management* **2009**, *50* (7), 1834-1840.
38. Meher, L.; Sagar, D. V.; Naik, S., Technical aspects of biodiesel production by transesterification—a review. *Renewable and sustainable energy reviews* **2006**, *10* (3), 248-268.
39. Himmel, M. E.; Ding, S.-Y.; Johnson, D. K.; Adney, W. S.; Nimlos, M. R.; Brady, J. W.; Foust, T. D., Biomass recalcitrance: engineering plants and enzymes for biofuels production. *science* **2007**, *315* (5813), 804-807.
40. Golan, A. E., Cellulase: Types and Action, Mechanism, and Uses. **2011**.
41. Saha, B. C., Hemicellulose bioconversion. *Journal of Industrial Microbiology and Biotechnology* **2003**, *30* (5), 279-291.
42. Shallom, D.; Shoham, Y., Microbial hemicellulases. *Current opinion in microbiology* **2003**, *6* (3), 219-228.
43. Béguin, P.; Aubert, J.-P., The biological degradation of cellulose. *FEMS microbiology reviews* **1994**, *13* (1), 25-58.
44. van Maris, A. J.; Abbott, D. A.; Bellissimi, E.; van den Brink, J.; Kuyper, M.; Luttik, M. A.; Wisselink, H. W.; Scheffers, W. A.; van Dijken, J. P.; Pronk, J. T., Alcoholic fermentation of carbon sources in biomass hydrolysates by *Saccharomyces cerevisiae*: current status. *Antonie Van Leeuwenhoek* **2006**, *90* (4), 391-418.
45. Berg, J. M.; Tymoczko, J. L.; Stryer, L., *Biochemistry*. W. H. Freeman: New York, 2010.
46. U.S. Energy Information Administration. U.S. All Grades All Formulations Retail Gasoline Prices. http://www.eia.gov/dnav/pet/hist/LeafHandler.ashx?n=pet&s=emm_epm0_pte_nus_dp&f=m (accessed Feb 15, 2015).
47. Agarwal, A. K., Biofuels (alcohols and biodiesel) applications as fuels for internal combustion engines. *Progress in energy and combustion science* **2007**, *33* (3), 233-271.
48. Nigam, P. S.; Singh, A., Production of liquid biofuels from renewable resources. *Progress in Energy and Combustion Science* **2011**, *37* (1), 52-68.
49. Brennan, L.; Owende, P., Biofuels from microalgae—a review of technologies for production, processing, and extractions of biofuels and co-products. *Renewable and sustainable energy reviews* **2010**, *14* (2), 557-577.

50. King, E.; Garner, R., The colorimetric determination of glucose. *Journal of Clinical Pathology* **1947**, *1* (1), 30.
51. Lever, M., A new reaction for colorimetric determination of carbohydrates. *Analytical biochemistry* **1972**, *47* (1), 273-279.
52. Dubois, M.; Gilles, K. A.; Hamilton, J. K.; Rebers, P.; Smith, F., Colorimetric method for determination of sugars and related substances. *Analytical chemistry* **1956**, *28* (3), 350-356.
53. Miller, G. L., Use of dinitrosalicylic acid reagent for determination of reducing sugar. *Analytical chemistry* **1959**, *31* (3), 426-428.
54. Uyeda, K.; Racker, E., Regulatory Mechanisms in Carbohydrate Metabolism VIII. THE REGULATORY FUNCTION OF PHOSPHATE IN GLYCOLYSIS. *Journal of Biological Chemistry* **1965**, *240* (12), 4689-4693.
55. Koek, M. M.; Muilwijk, B.; van der Werf, M. J.; Hankemeier, T., Microbial metabolomics with gas chromatography/mass spectrometry. *Analytical chemistry* **2006**, *78* (4), 1272-1281.
56. Sweeley, C. C.; Bentley, R.; Makita, M.; Wells, W., Gas-liquid chromatography of trimethylsilyl derivatives of sugars and related substances. *Journal of the American Chemical Society* **1963**, *85* (16), 2497-2507.
57. Crowell, E. P.; Burnett, B. B., Determination of the carbohydrate composition of wood pulps by gas chromatography of the alditol acetates. *Analytical Chemistry* **1967**, *39* (1), 121-124.
58. CAYLE, T.; VIEBROCK, F.; Schiaffino, J., Gas chromatography of carbohydrates. *Cereal Chem* **1968**, *45*, 154-161.
59. Fox, A.; Lau, P.; Brown, A.; Morgan, S.; Zhu, Z.; Lema, M.; Walla, M., Capillary gas chromatographic analysis of carbohydrates of *Legionella pneumophila* and other members of the family Legionellaceae. *Journal of clinical microbiology* **1984**, *19* (3), 326-332.
60. Fu, D.; Oneill, R. A., Monosaccharide composition analysis of oligosaccharides and glycoproteins by high-performance liquid chromatography. *Analytical biochemistry* **1995**, *227* (2), 377-384.
61. Yasuno, S.; Murata, T.; Kokubo, K.; Yamaguchi, T.; Kamei, M., Two-mode analysis by high-performance liquid chromatography of *p*-aminobenzoic ethyl ester-derivatized monosaccharides. *Bioscience, biotechnology, and biochemistry* **1997**, *61* (11), 1944-1946.
62. Yang, X.; Zhao, Y.; Wang, Q.; WANG, H.; MEI, Q., Analysis of the monosaccharide components in *Angelica* polysaccharides by high performance liquid chromatography. *Analytical Sciences* **2005**, *21* (10), 1177-1180.
63. Gehrke, C. W.; Wixom, R. L.; Bayer, E., *CHROMATOGRAPHY-A CENTURY OF DISCOVERY 1900-2000. THE BRIDGE TO THE SCIENCES/TECHNOLOGY JOURNAL OF CHROMATOGRAPHY LIBRARY VOLUME 64 (JCL)*. Elsevier: 2001.
64. Harris, D. C., *Quantitative Chemical Analysis*. 8th ed.; W. H. Freeman and Company: New York, 2010.

65. Le Questel, J. Y.; Berthelot, M.; Laurence, C., Hydrogen-bond acceptor properties of nitriles: a combined crystallographic and ab initio theoretical investigation. *Journal of Physical Organic Chemistry* **2000**, *13* (6), 347-358.
66. Dorsey, J. G.; Cooper, W. T.; Siles, B. A.; Foley, J. P.; Barth, H. G., Liquid chromatography: theory and methodology. *Analytical Chemistry* **1998**, *70* (12), 591-644.
67. Snyder, L. R.; Kirkland, J. J.; Dolan, J. W., *Introduction to modern liquid chromatography*. John Wiley & Sons: 2011.
68. Swartz, M. E., UPLC™: an introduction and review. *Journal of Liquid Chromatography & Related Technologies* **2005**, *28* (7-8), 1253-1263.
69. Van Deemter, J. J.; Zuiderweg, F.; Klinkenberg, A. v., Longitudinal diffusion and resistance to mass transfer as causes of nonideality in chromatography. *Chemical Engineering Science* **1956**, *5* (6), 271-289.
70. Moody, H. W., The evaluation of the parameters in the van Deemter equation. *Journal of Chemical Education* **1982**, *59* (4), 290.
71. Swartz, M. E., Ultra performance liquid chromatography (UPLC): An introduction. *Separation Science Re-Defined, LCGC Supplement* **2005**, *8*, 8-14.
72. de Villiers, A.; Lestremau, F.; Szucs, R.; Gélébart, S.; David, F.; Sandra, P., Evaluation of ultra performance liquid chromatography: Part I. Possibilities and limitations. *Journal of Chromatography A* **2006**, *1127* (1), 60-69.
73. Gritti, F.; Guiochon, G., Complete temperature profiles in ultra-high-pressure liquid chromatography columns. *Analytical chemistry* **2008**, *80* (13), 5009-5020.
74. Waters Corporation. Waters 2414 Refractive Index Detector Operator's Guide. <http://www.waters.com/webassets/cms/support/docs/71500241402rb.pdf> (accessed Feb 17, 2015).
75. Inagaki, S.; Min, J. Z.; Toyo'oka, T., Direct detection method of oligosaccharides by high-performance liquid chromatography with charged aerosol detection. *Biomedical Chromatography* **2007**, *21* (4), 338-342.
76. Dionex. Charged Aerosol Detectors. <http://www.dionex.com/en-us/products/liquid-chromatography/lc-modules/detectors/charged-aerosol/lp-85214.html> (accessed Feb 15 2015).
77. Bailey, B.; Ullucci, P.; Bauder, R.; Plante, M.; Crafts, C.; Acworth, I., Carbohydrate Analysis using HPLC with PAD, FLD, Charged Aerosol Detection, and MS Detectors. *Thermo Fisher Scientific, MA, USA* **2014**.
78. Crafts, C.; Bailey, B.; Plante, M.; Acworth, I., Validating Analytical Methods with Charged Aerosol Detection.
79. Hutchinson, J. P.; Remenyi, T.; Nesterenko, P.; Farrell, W.; Groeber, E.; Szucs, R.; Dicoski, G.; Haddad, P. R., Investigation of polar organic solvents compatible with Corona Charged Aerosol Detection and their use for the determination of sugars by hydrophilic interaction liquid chromatography. *Analytica chimica acta* **2012**, *750*, 199-206.

80. Dixon, R. W.; Peterson, D. S., Development and testing of a detection method for liquid chromatography based on aerosol charging. *Analytical chemistry* **2002**, *74* (13), 2930-2937.
81. Engel, T.; Reid, P., *THERMODYNAMICS, STATISTICAL THERMODYNAMICS, AND KINETICS*. 3rd ed.; Pearson: Boston, 2012.
82. Atkins, P.; De Paula, J., *Physical chemistry for the life sciences*. W. H. Freeman and Company: 2011.
83. Taylor, P. J., Matrix effects: the Achilles heel of quantitative high-performance liquid chromatography–electrospray–tandem mass spectrometry. *Clinical biochemistry* **2005**, *38* (4), 328-334.
84. Waters Corporation. Acquity UPLC BEH Amide Columns Application Notebook. <http://www.waters.com/webassets/cms/library/docs/WA64081.pdf> (accessed Feb 17, 2015).
85. Novozymes. THE KEY TO NOVOZYMES' CELLULOSIC ETHANOL INNOVATIONS. <http://bioenergy.novozymes.com/en/cellulosic-ethanol/cellic/Documents/Cellic%20brochure.pdf> (accessed Feb 15, 2015).
86. Smith, D.; Smith, L.; Shafer, W.; Klotz, J.; Strickland, J., Development and validation of an LC-MS method for quantitation of ergot alkaloids in lateral saphenous vein tissue. *Journal of agricultural and food chemistry* **2009**, *57* (16), 7213-7220.
87. Clarke, S.; Preto, F., *Biomass burn characteristics*. Ministry of Agriculture, Food and Rural Affairs: 2011.
88. Jenkins, B.; Baxter, L.; Miles, T., Combustion properties of biomass. *Fuel processing technology* **1998**, *54* (1), 17-46.
89. Demirbas, A., Potential applications of renewable energy sources, biomass combustion problems in boiler power systems and combustion related environmental issues. *Progress in energy and combustion science* **2005**, *31* (2), 171-192.
90. Domalski, E. S.; Jobe, T. J.; Milne, T. A., Thermodynamic data for biomass conversion and waste incineration. **1986**.
91. Mazzotta, M.; Pace, R.; Wallgren, B.; Morton, S.; Miller, K.; Smith, D., Direct Analysis in Real Time Mass Spectrometry (DART-MS) of Ionic Liquids. *J. Am. Soc. Mass Spectrom* **2013**, *24* (10), 1616-1619.

APPENDIX A:

Calibration curves generated from xylose and glucose standards prepared for
saccharification study.

Notes: These curves were used to determine sample sugar concentrations. Each curve represents three standards with different injection volumes averaged and used for 40-slot container in the UPLC autosampler.

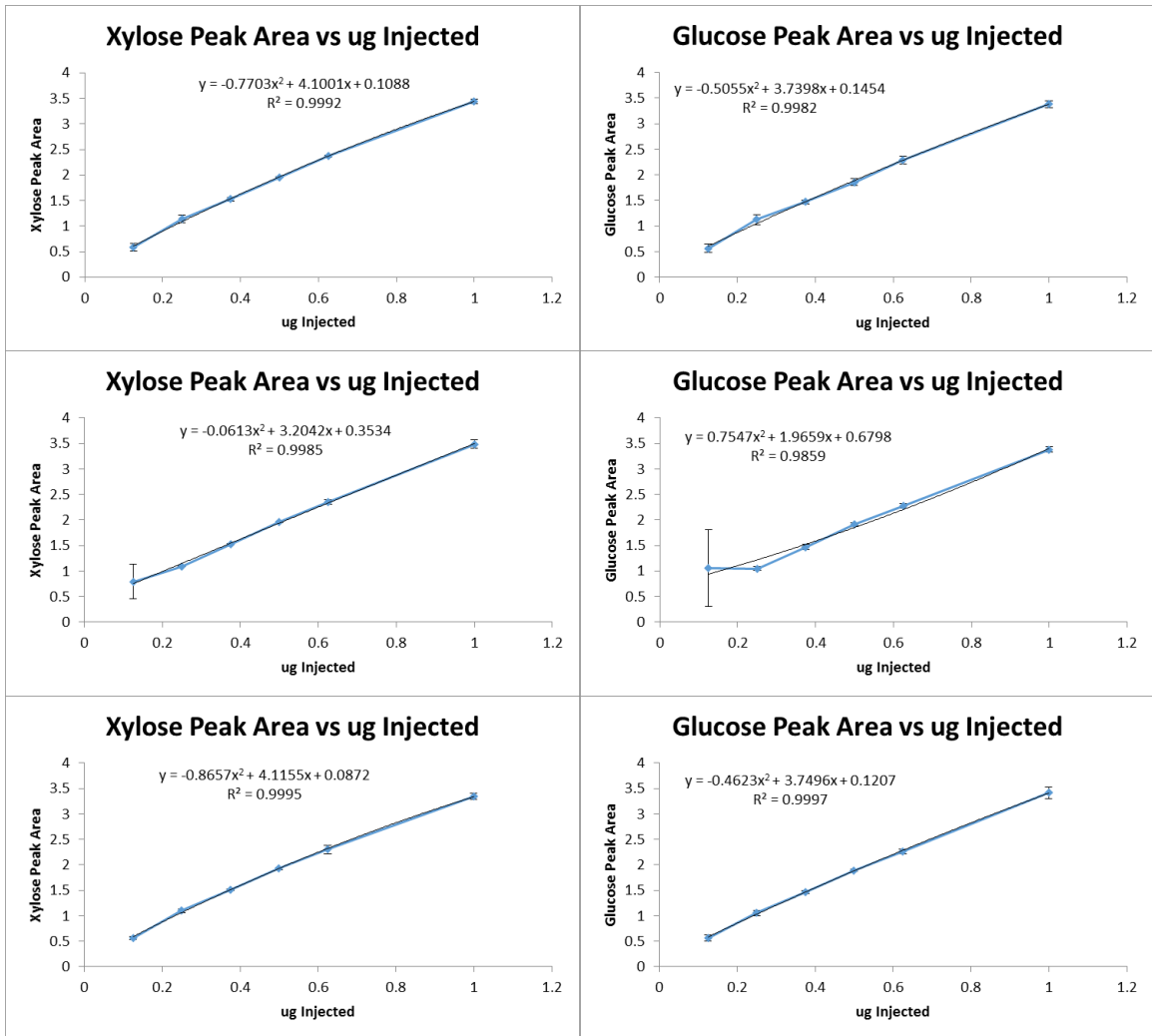


Figure A.1. Xylose and glucose calibration curves for 08142013 data sets.

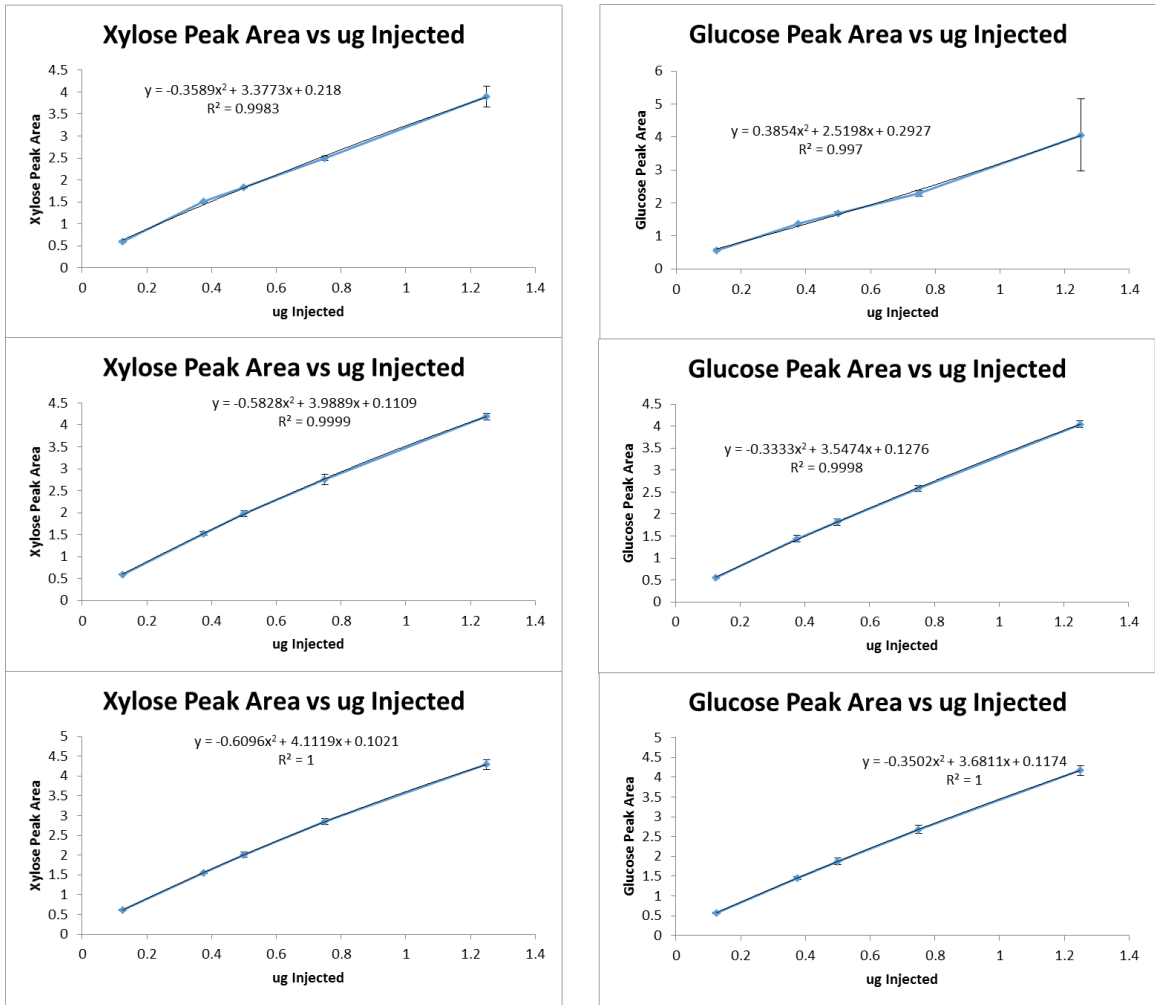


Figure A.2. Xylose and glucose calibration curves for 08162013 data sets.

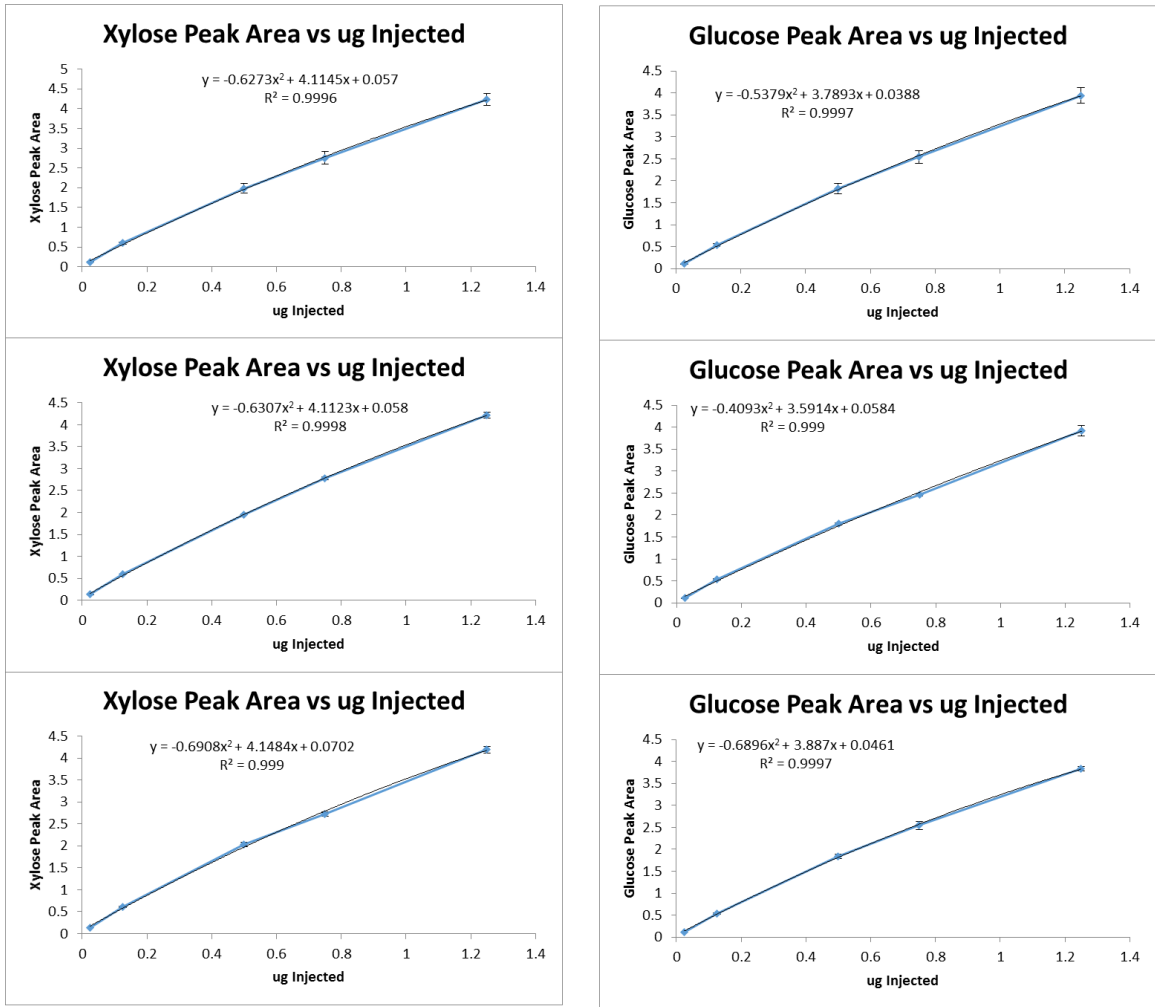


Figure A.3. Xylose and glucose calibration curves for 08212013 data sets.

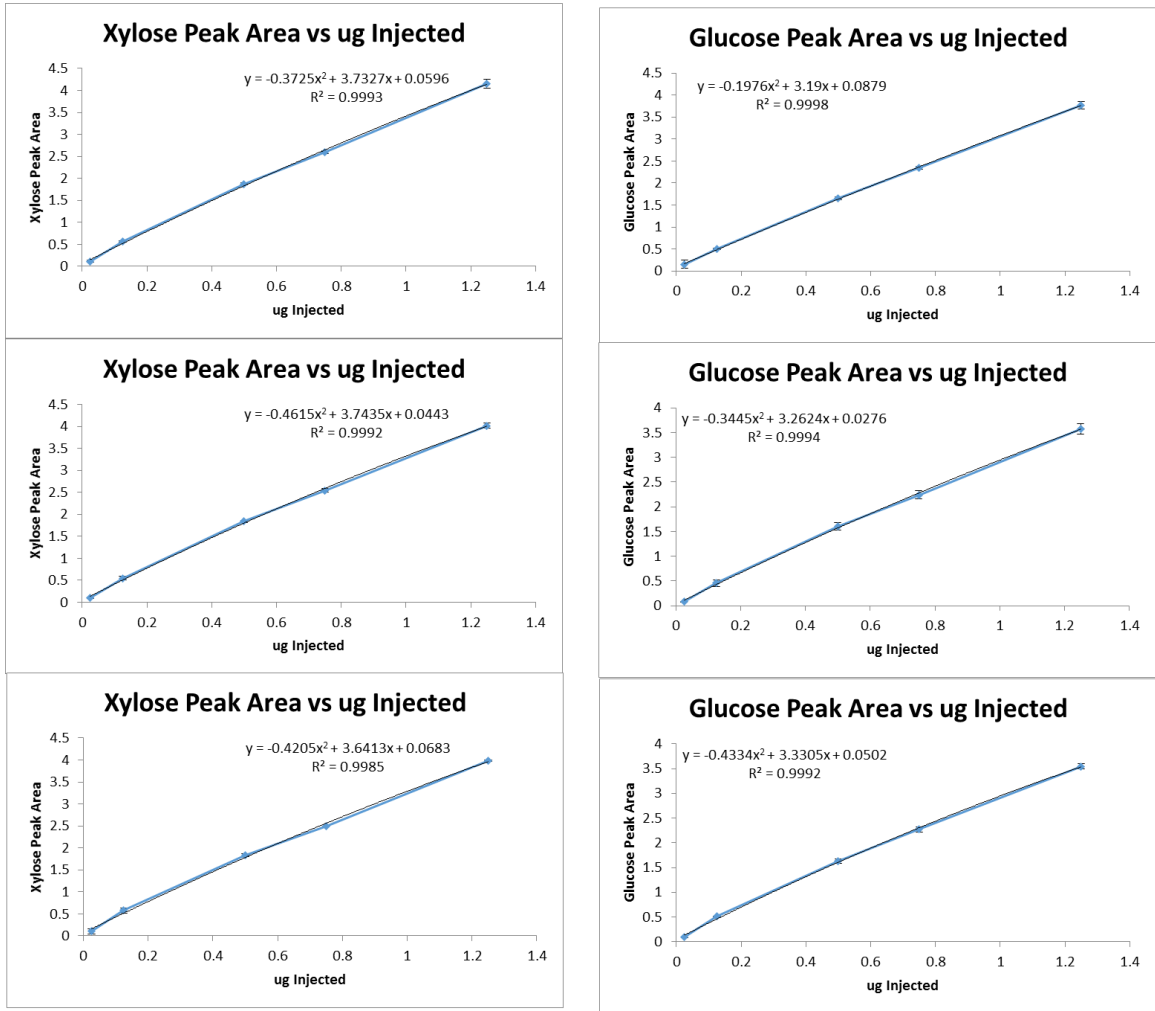


Figure A.4. Xylose and glucose calibration curves for 08302013 data sets.

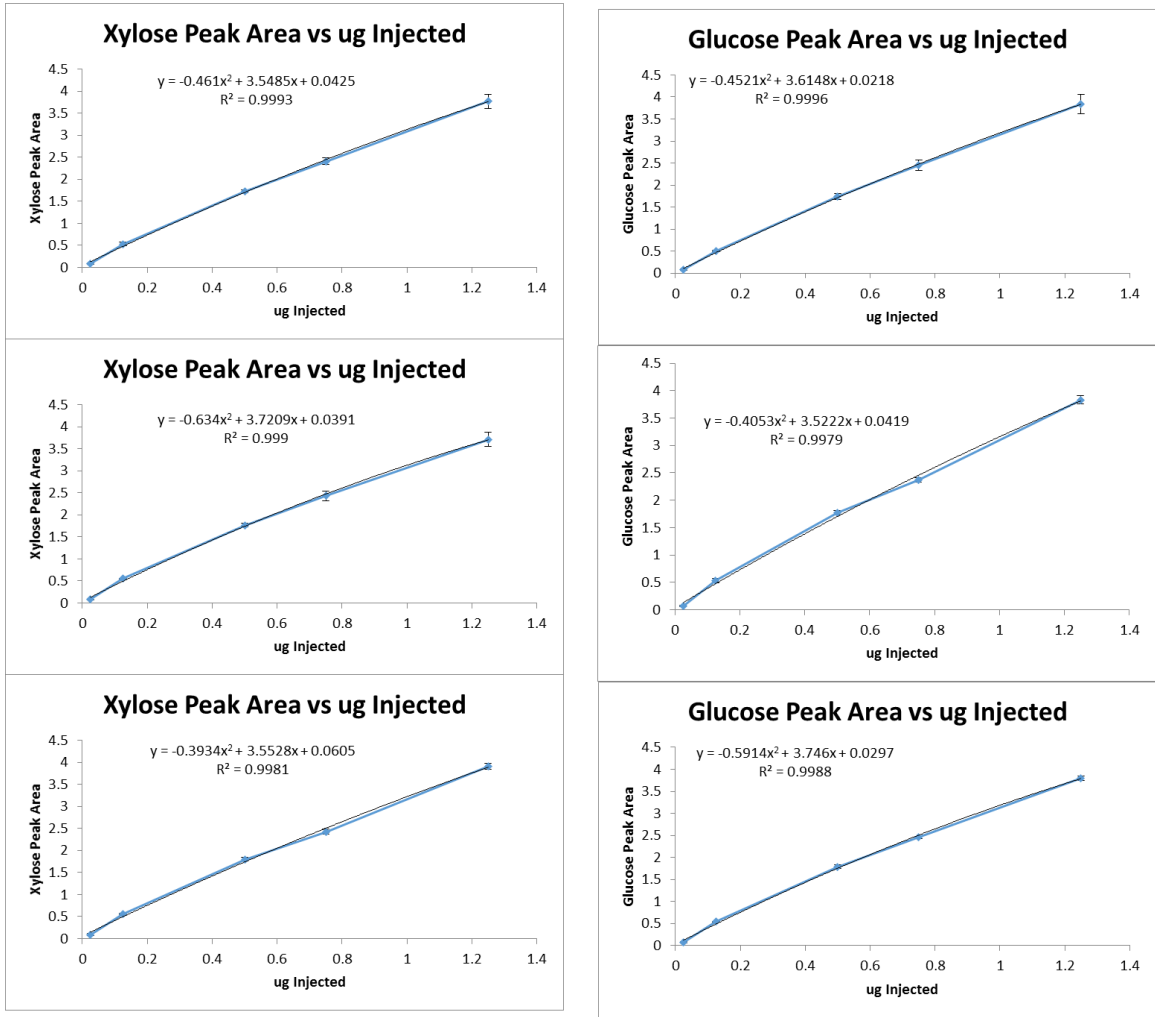


Figure A.5. Xylose and glucose calibration curves for 09052013 data sets.

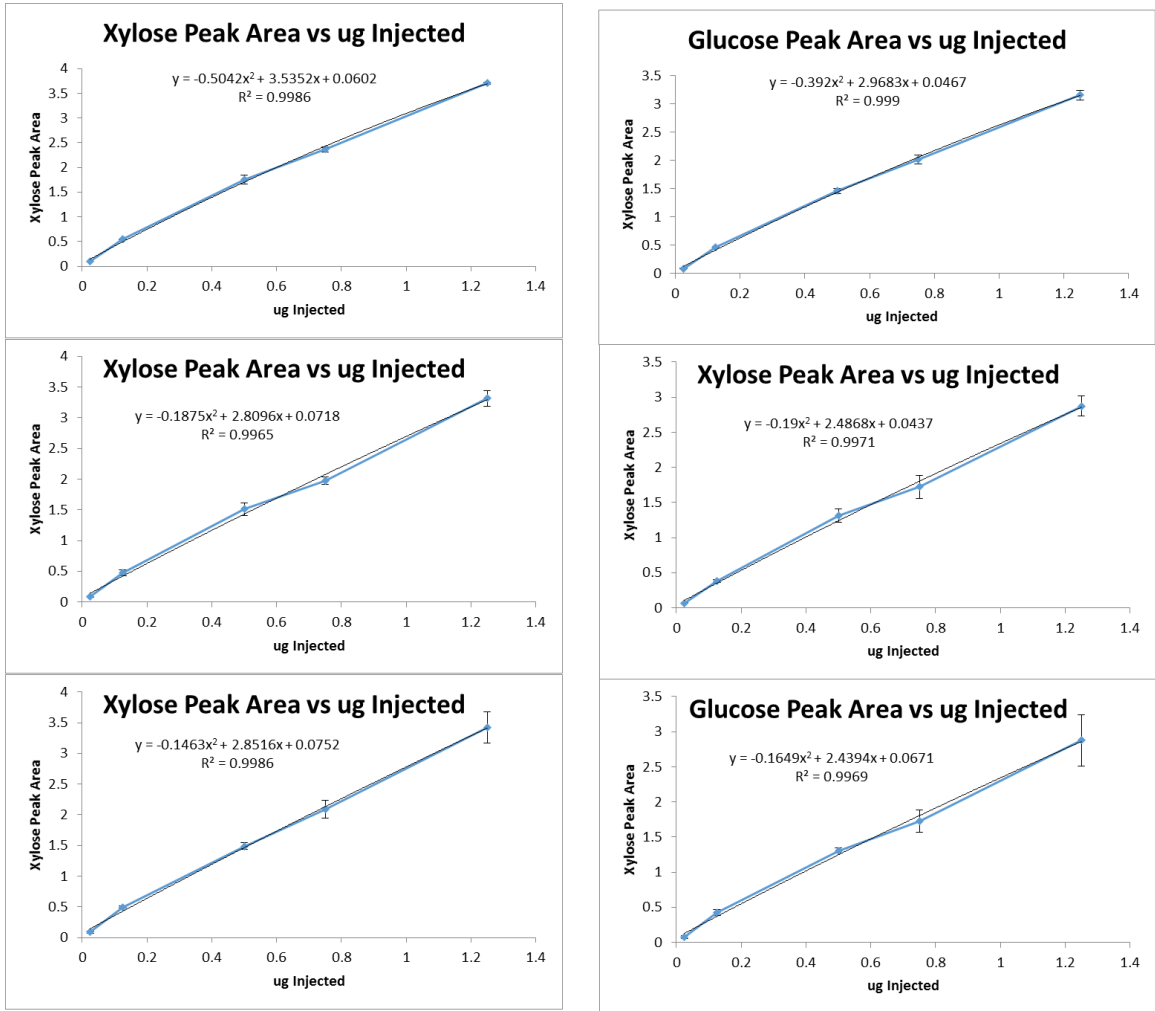


Figure A.6. Xylose and glucose calibration curves for 10092013 data sets.

APPENDIX B:

Mass spectra of switchgrass lignin dissolved in various ionic liquids.

Notes: Lignin was extracted from switchgrass using formic acid at 50°C. Spectra were obtained at 400°C gas temperature in positive mode after subtracting background m/z peaks.

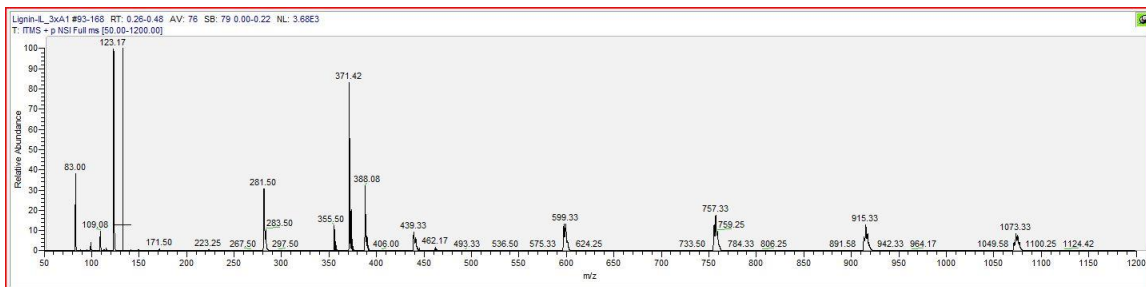


Figure B.1. Mass spectrum of lignin (FA 50 °C) dissolved in 1-allyl-3-methylimidazolium chloride ([AMIM][Cl]).

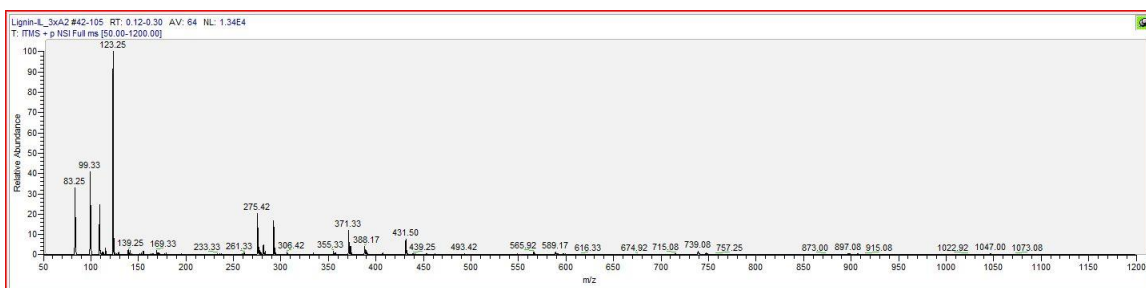


Figure B.2. Mass spectrum of lignin (FA 50 °C) dissolved in 1-allyl-3-methylimidazolium xylene sulfonate ([AMIM][XS]).

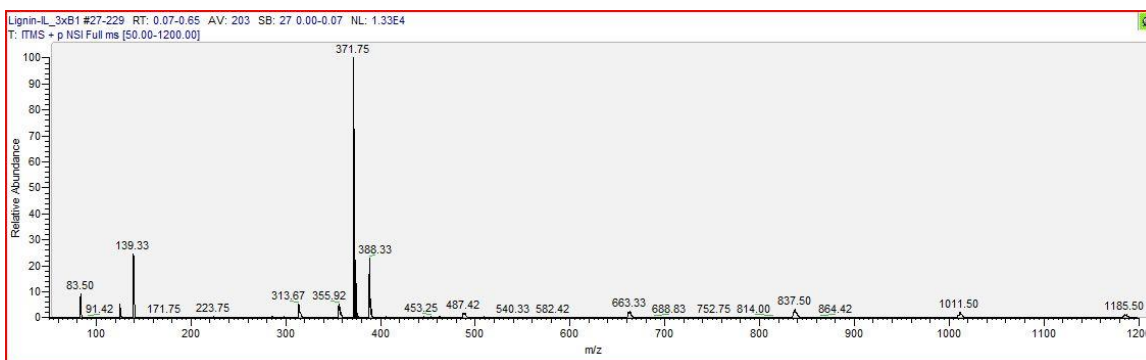


Figure B.3. Mass spectrum of lignin (FA 50 °C) dissolved in 1-butyl-3-methylimidazolium chloride ([BMIM][Cl]).

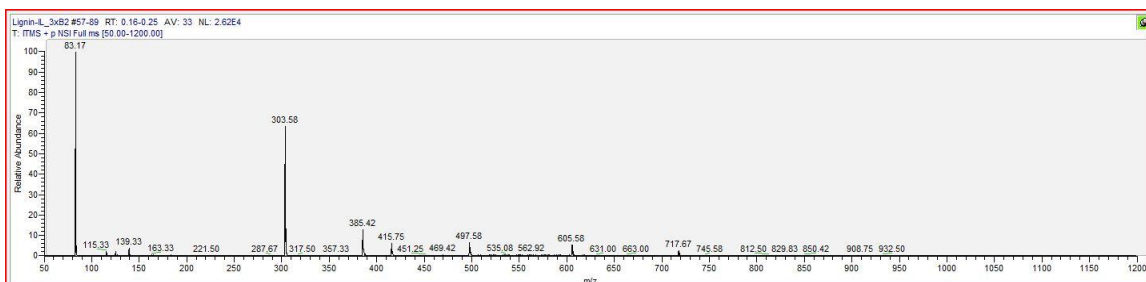


Figure B.4. Mass spectrum of lignin (FA 50 °C) dissolved in 1-butyl-3-methylimidazolium xylene sulfonate ([BMIM][XS]).

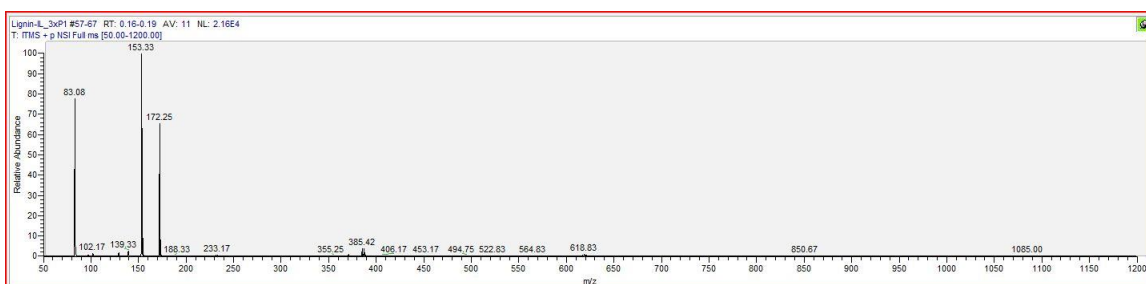


Figure B.5. Mass spectrum of lignin (FA 50 °C) dissolved in 1-pentyl-3-methylimidazolium bromide ([PMIM][Br]).

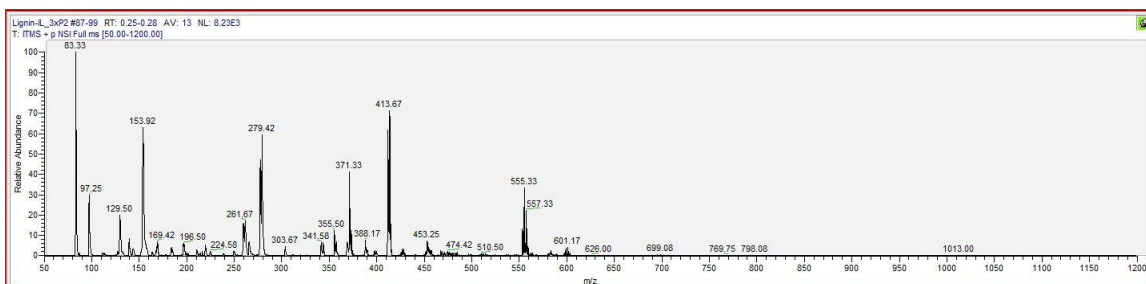


Figure B.6. Mass spectrum of lignin (FA 50 °C) dissolved in 1-pentyl-3-methylimidazolium nitrate ([PMIM][NO₃]).

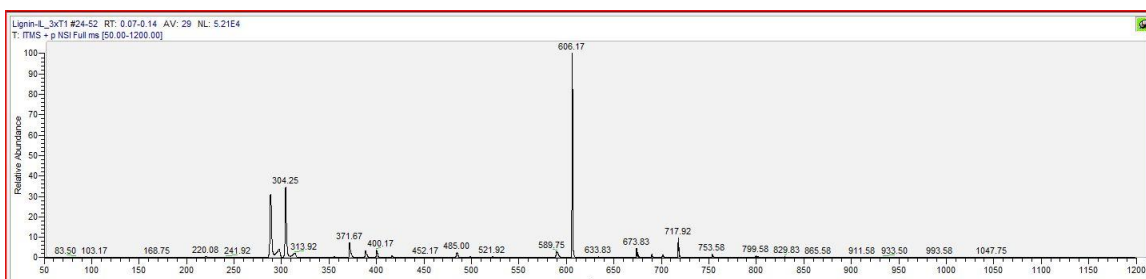


Figure B.7. Mass spectrum of lignin (FA 50 °C) dissolved in trihexyltetradecylphosphonium bromide ([THTDP][Br]).

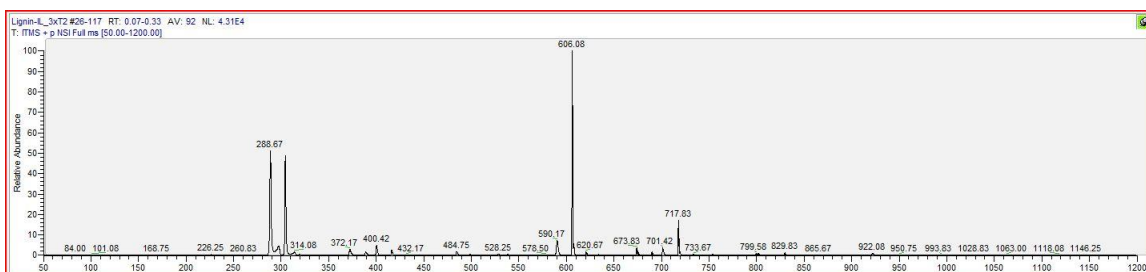


Figure B.8. Mass spectrum of lignin (FA 50 °C) dissolved in trihexyltetradecylphosphonium nitrate ([THTDP][NO₃]).